EVALUATION OF TRAVIS PEAK GAS RESERVOIRS, WEST MARGIN OF THE EAST TEXAS BASIN

A Thesis

by

YAMIN LI

Submitted to the Office of Graduate Studies of
Texas A&M University
in partial fulfillment of the requirements for the degree of

MASTER OF SCIENCE

May 2007

Major Subject: Petroleum Engineering

EVALUATION OF TRAVIS PEAK GAS RESERVOIRS, WEST MARGIN OF THE EAST TEXAS BASIN

A Thesis

by

YAMIN LI

Submitted to the Office of Graduate Studies of
Texas A&M University
in partial fulfillment of the requirements for the degree of

MASTER OF SCIENCE

Approved by:

Chair of Committee,	Walter B. Ayers, Jr.
Committee Members,	Duane A. McVay
	Wayne M. Ahr
Head of Department,	Stephen A. Holditch

May 2007

Major Subject: Petroleum Engineering

ABSTRACT

Evaluation of Travis Peak Gas Reservoirs, West Margin of the East Texas Basin.

(May 2007)

Yamin Li, B.S., University of Petroleum (China)

Chair of Advisory Committee: Dr. Walter B. Ayers, Jr.

Gas production from low-permeability (tight) gas sandstones is increasingly important in the USA as conventional gas reservoirs are being depleted, and its importance will increase worldwide in future decades. Travis Peak tight sandstones have produced gas since the 1940s. In this study, well log, 2D seismic, core, and production data were used to evaluate the geologic setting and reservoir characteristics of the Travis Peak formation. The primary objective was to assess the potential for basinward extension of Travis Peak gas production along the west margin of the East Texas Basin.

Along the west margin of the East Texas Basin, southeast-trending Travis Peak sandstones belts were deposited by the Ancestral Red River fluvial-deltaic system. The sandstones are fine-grained, moderately well sorted, subangular to subrounded, quartz arenites and subarkoses; reservoir quality decreases with depth, primarily due to diagenetic quartz overgrowths. Evaluation of drilling mud densities suggests that strata deeper than 12,500 ft may be overpressured. Assessment of the geothermal gradient (1.6 °F/100 ft) indicates that overpressure may be relict, resulting from hydrocarbon generation by Smackover and Bossier formation potential source rocks.

In the study area, Travis Peak cumulative gas production was 1.43 trillion cubic feet from January 1, 1961, through December 31, 2005. Mean daily gas production from 923 wells was 925,000 cubic ft/well/day, during the best year of production. The number of Travis Peak gas wells in “high-cost” (tight sandstone) fields increased from 18 in the decade 1966-75 to 333 in the decade 1996-2005, when high-cost fields accounted for 33.2% of the Travis Peak gas production. However, 2005 gas production from high cost fields accounted for 63.2% of the Travis Peak total production, indicating that production from high-cost gas wells has increased markedly.

Along the west margin of the East Texas Basin, hydrocarbon occurs in structural, stratigraphic, and combination traps associated with salt deformation. Downdip extension of Travis Peak production will depend on the (1) burial history and diagenesis, (2) reservoir sedimentary facies, and (3) structural setting. Potential Travis Peak hydrocarbon plays include: updip pinch-outs of sandstones; sandstone pinch-outs at margins of salt-withdrawal basins; domal traps above salt structures; and deepwater sands.

ACKNOWLEDGEMENTS

I wish to express my sincere thanks and appreciation to my research advisor, Dr. Walter B. Ayers, for his expert guidance, invaluable influence, and tremendous support throughout my education at Texas A&M University.

Also, I wish to thank Dr. Duane A. McVay for his valuable advice, support, and helpful suggestions during this research and for his contributions while serving on my graduate advisory committee. I would like to thank Dr. Wayne M. Ahr for his valuable advice and suggestions during the course of my study and for his contributions and serving on my graduate advisory committee. I also thank Dr. W. John Lee for his influence in my research and with all the knowledge that he shared with me.

I gratefully acknowledge funding of this project by Burlington Resources (now ConocoPhillips) through the Crisman Institute at Texas A&M University, Petroleum Engineering Department. Special thanks goes to Paul M. Basinski of ConocoPhillips for championing this project. Thanks, also, to M.J. Systems, IHS, and A2D for providing well logs, and to HPDI for making available their production database. SEI allowed ConocoPhillips to release five regional, 2-D seismic lines that were essential for the study.

I wish to express my gratitude to my husband, Weiqiang Li. I could not go through this process without his support and encouragement. I would like to extend my thanks and admiration to my parents, brothers and sister-in-law for their invaluable support.

Many thanks to the teachers of the Harold Vance Department of Petroleum Engineering and to Texas A&M University. Finally, my thanks go to all of my friends and colleagues for sharing both the tough and sweet moments at Texas A&M University.

TABLE OF CONTENTS

Page

Page

LIST OF TABLES

LIST OF FIGURES

Page

INTRODUCTION

The Travis Peak (TP) Formation is well-known as a low-permeability sandstone reservoir in East Texas, Louisiana, Arkansas, and Mississippi, where it produces primarily natural gas. The TP is part of the Lower Cretaceous Trinity Group, which overlies the Cotton Valley Group; it is overlain by the carbonate Pettet Formation along the west margin of the East Texas Basin (ETB) (Fig. 1). The TP formation is a fluvial-deltaic unit. TP

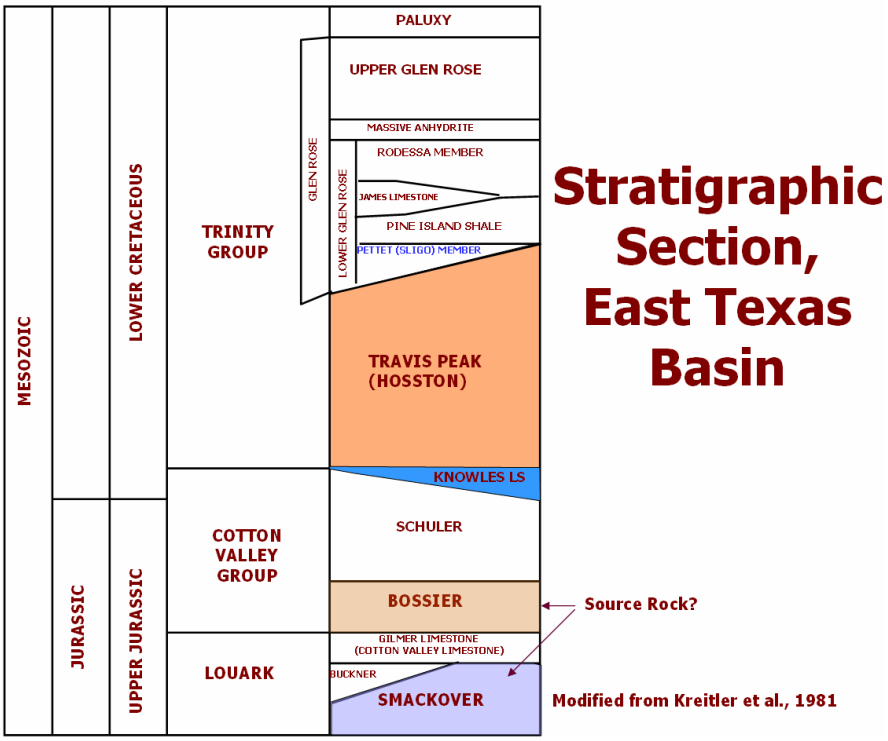

Figure 1. Stratigraphic column of East Texas Basin showing the Travis Peak-Hosston Formation (Modified from Kreitler et al., 1981).

This thesis follows the style and format AAPG Bulletin.

terrigenous clastic influx into terrigenous clastic influx into the Gulf Coast basin was directed along two axes. These were the Ancestral Mississippi River depocenter, where the Hosston Formation was deposited east of the present Sabine Uplift, and the Ancestral Red River Depocenter (Fig. 2) (Saucier, 1985; Salvador, 1987; Worrall and Snelson, 1989). The latter was located along the west margin of the ETB, and it provided sediment to this study area.

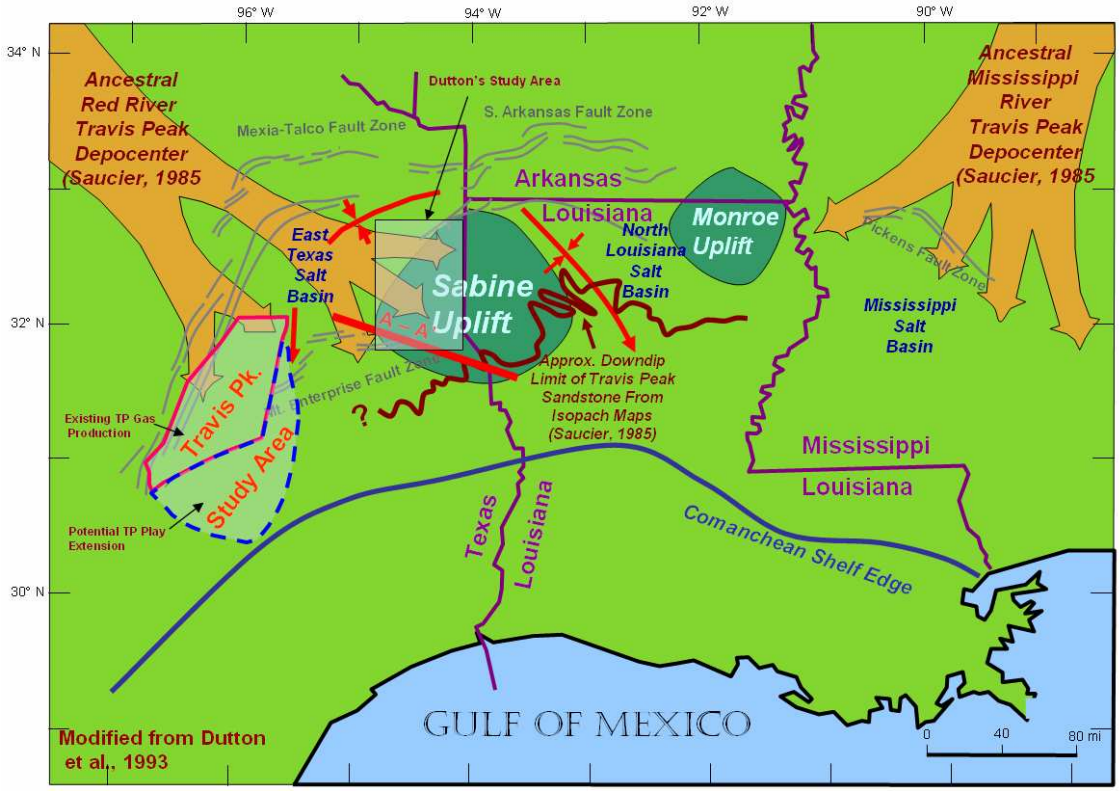

Figure 2. Major axes of Travis Peak-Hosston terrigenous clastic influx and general tectonic setting in East Texas, north Louisiana, and Mississippi (modified from Bartberger et al., 2003; after Dutton et al., 1993).

The TP clastic sediments of the Ancestral Red River thicken basinward, to the south and southeast. During early TP-Hosston time, an alluvial plain environment dominated the north and west parts of study area. Fluvial systems of the Ancestral Red River fed sediments to delta systems to the east and south. During middle to late TP time, eustatic sea level rise resulted in shoreline retrogradation, and by Pettet time, a shallow, an open-shelf environment covered most of the study area (Bushaw 1968).

The TP Formation is composed of interbedded fluvial-deltaic sandstones and associated shale beds (Fig. 3). The upper 300 ft of the TP Formation is the mainly hydrocarbon-bearing interval (Fracasso and others, 1988; Dutton et al., 1991; after Saucier, 1985).

There are few published descriptions of petrography for TP sandstone from the west margin of the ETB. However, in the Sabine Arch area, TP sandstones are fine- to very fine-grained sandstone, silty sandstone, muddy sandstone, and sandy mudstone (Dutton et al., 1991). The sandstones are quartzarenites and subarkoses, with illite, chlorite, and

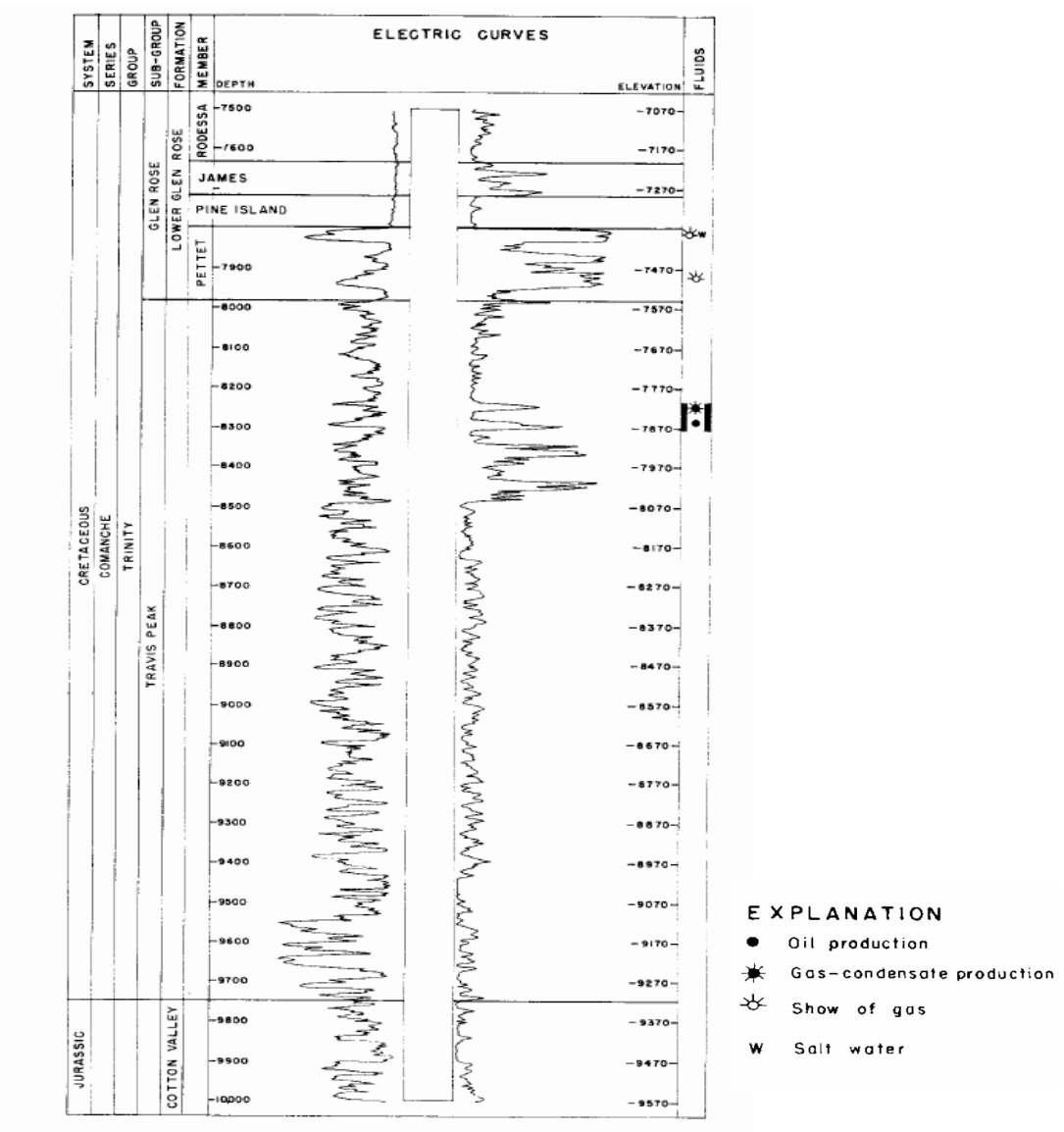

Figure 3. Type well log for Reed field showing interbedded TP sandstones and shales (from Hill, 1951). Zones tested for or producing hydrocarbons are shown in the right-hand column. See Figure 12 for Reed field location.

fine quartz matrix. Average porosity of clean sandstones is approximately 11% (Dutton et al., 1991). TP sandstone porosity and permeability decrease markedly with depth, owing to diagenesis. For clean sandstones in the Sabine Uplift, average permeability decreases from 10 md at 6,000 ft to 0.001 md at 10,000 ft. Among the diagenetic processes affecting reservoir permeability are quartz cementation, decreasing secondary porosity, and overburden pressure (Dutton et al., 1991; Fracasso et al., 1988). Many TP reservoir rocks are low-permeability sandstones, and thus, they generally require hydraulic fracture treatments to produce gas at economic rates.

Most TP hydrocarbon fields occur in combination traps, where both structural setting and stratigraphic pinch-outs play (Fig. 6) dominant roles. Sandbody extent, geometry, and orientation, which are important in determining field extent, are controlled by depositional systems. The structure map of the Cotton Valley Formation top (TP base, Fig. 4) shows the major structural features in the study area. The axis of the East Texas plunges southward through eastern Henderson and Anderson Counties. The regional structural map (Fig. 4) does not show the many salt-related structures that were important to hydrocarbon migration and trapping along the west margin of the basin (Fig. 5). These features include the Mexia-Talco fault zone, salt diapers and pillows, and turtle structures.

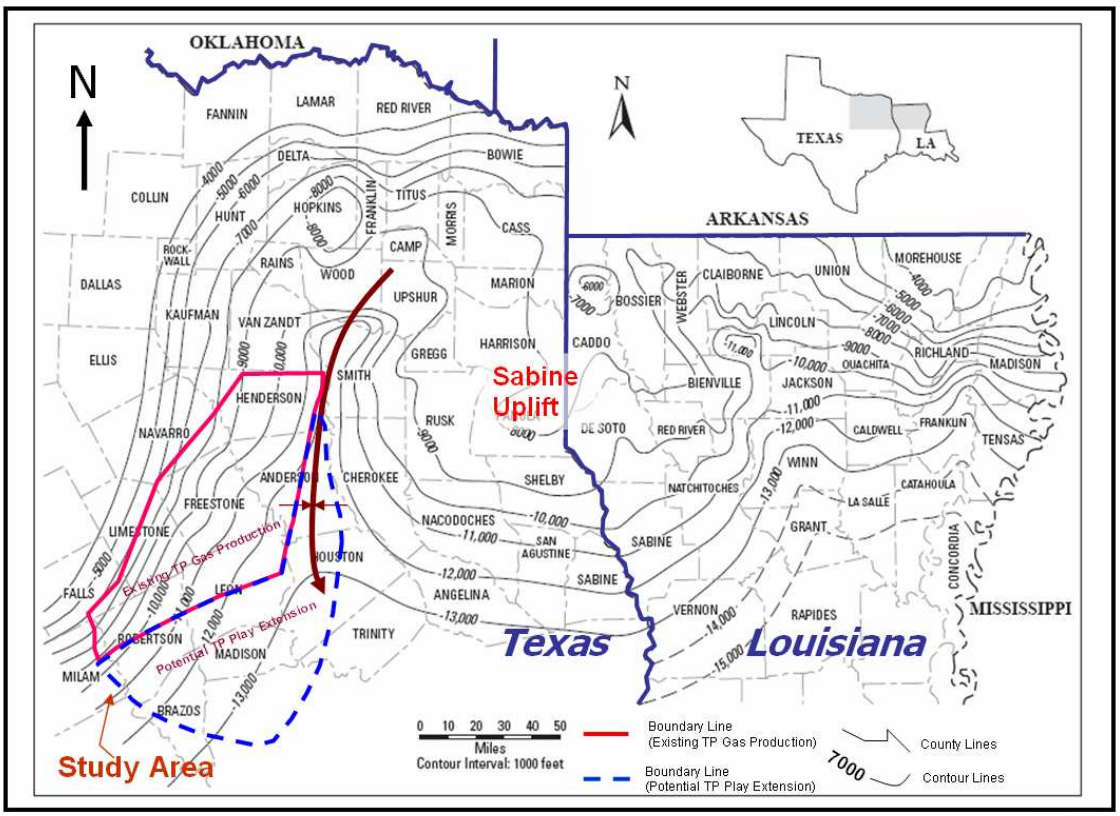

Figure 4. Structure, top of the Cotton Valley Group Sandstone (base of Travis Peak Formation), showing the location of this study (modified from Finley, 1984).

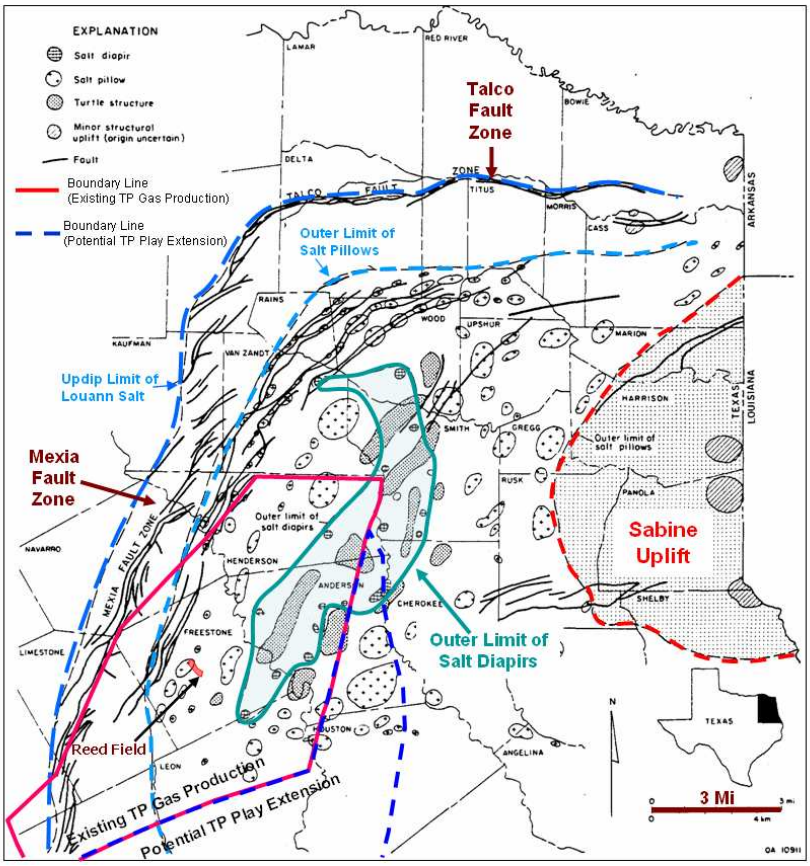

Figure 5. Major tectonic elements in East Texas (modified from Jackson, 1982).

Along the west margin of the ETB, faults and intermediate-amplitude salt structures are of primary importance in forming structural, combination, or stratigraphic traps. Pinch-outs of permeable sandstones into impervious sandstones or shales are important in hydrocarbon trapping (Seni and Kosters, 1989). Although many wells produce from the TP Formation in the updip area, the basinward extent of the formation is not reported in published maps (Bartberger et al., 2003), and the potential for play extension was unknown.

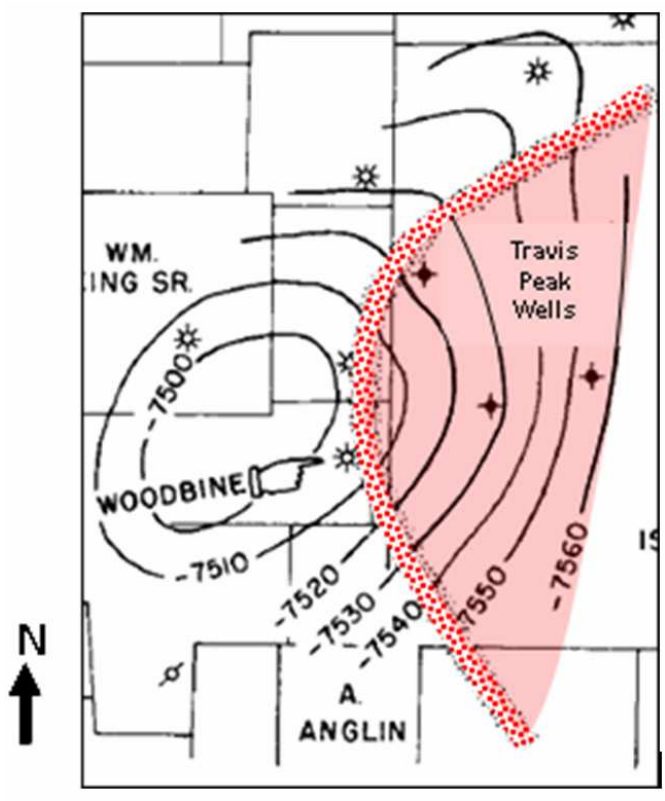

Figure 6. Structure, top of Travis Peak formation in Reed field, showing that productive Travis Peak sandstone (red) pinches out to the west (modified from Hill, 1951). See Figure 3 for type well log and Figure 5 for field location.

Objectives

The objectives of this study were to evaluate the geology and reservoir properties and to review the production history of the TP in an area along the west margin of the East Texas Basin (Fig. 4), to assess the potential for hydrocarbon play extension. To accomplish these objectives, I acquired, evaluated, and integrated diverse geoscience and engineering data.

Methods and Data

Data used in this study were (1) digital and raster well logs provided by M.J. Systems, IHS and A2D, (2) 2-D SEI seismic lines, which they allowed ConocoPhillips to release to for the study, (3) VSP surveys for 2 wells, (4) petrophysical data from one well, (5) x core analysis reports, (6) production data from HPDI, (7) well information from the Texas Railroad Commission, and (8) published literature. Sequence stratigraphic models of the sedimentary fill of basins is best accomplished by a combining seismic, well log, core, petrophysical, and petrographic, and biostratigraphic data. Cores, outcrops, and petrophysical studies provide detailed vertical resolution and calibration of well log and seismic data. Seismic and well log studies provide information concerning the lateral continuity of the sequence stratigraphic framework, and biostratigraphy provides the time constraints. Unfortunately, limited core data were available for this study.

Well Log Data

A total of 860 well logs were acquired for the 11-county area study area along the western margin of East Texas Basin (Fig. 7). These logs were provided by M.J. System, IHS, A2D, and by ConocoPhilips. Data acquired for most wells included a standard suite of resistivity, spontaneous potential, and gamma-ray logs. Some wells have additional logs, such as formation density, neutron density, litho-density, and sonic velocity. Approximately 180 well logs are poor, unusable quality. These poor quality well logs were mainly from the downdip part of study area. Most updip wells, where the top of the

TP was less than 12,000 ft, penetrated the top of the TP, and several wells penetrated the top of the Bossier formation. Unfortunately, few downdip wells (TP top >12,000 ft) penetrate much of the TP, which greatly limited detailed stratigraphic analysis. Formation tops and marker beds were correlated across the west flank of East Texas Basin. The formation names and criteria for identification of formation tops were based on previous regional studies by ConocoPhillips. More than 7 horizons were correlated across the study area and were used for stratigraphic analysis. The most difficult horizon to map in well logs was the TP/Cotton Valley contact, because there is little lithologic contrast between the formations. Only 35 of the total 860 well logs were useable quality digital format logs; the rest were image logs or poor quality digital logs. Moreover, the digital logs were mostly in the updip part of the study area. Therefore, quantitatively mapping of TP properties, such as net sand, net-to-gross, etc., was beyond the scope of this study.

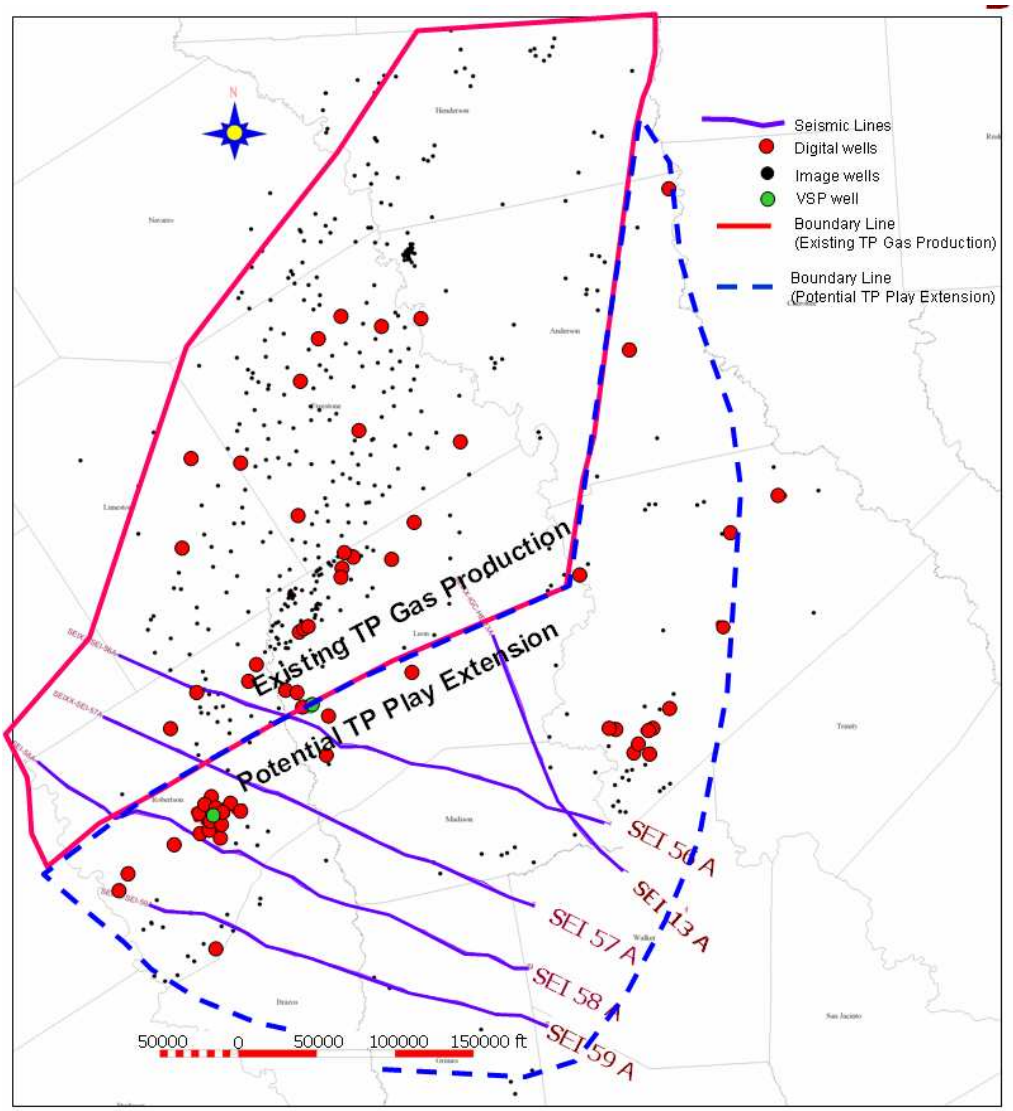

Figure 7. Locations of 2D seismic lines and wells having raster or digital well logs.

Seismic Data

ConocoPhilips made available for this study approximately 200 miles of 2-D seismic line data in five lines from SEI, with SEI approval (Fig. 7). All the seismic lines are dip lines. The quality of seismic is sufficient for regional structural analyses and preliminary stratigraphic analysis.

Integration of Well Log and Seismic Data

Regional structural and stratigraphic analysis required integration of well log and seismic data. Integration of well log and seismic data included the correlation of formation tops in well log with seismic reflections and the conversion of seismic time to depth. To convert seismic time to depth, ConocoPhilips provided VSP (vertical seismic profile) data for two wells, one in Leon County and the other in Robertson County. The well log, VSP, and seismic data were loaded and interpreted in GeoGraphix. The time to depth plot (Fig. 8) shows the function of depth and two way time from the checkshot survey of one VSP. I compared the velocity data from ConocoPhillips (Fig. 8) with Davidoff's (1993) velocity data (Fig. 9) and found good agreement of data in the same county.

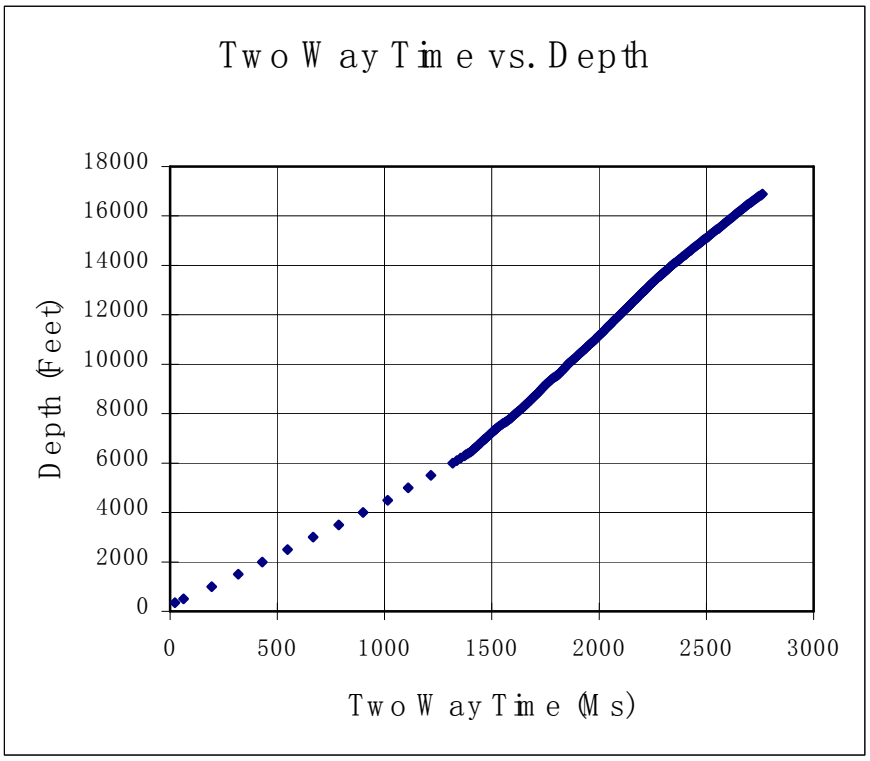

Figure 8. Depth and time relations from a VSP in a Robertson Co. well. (Data from Halliburton Energy Services, 2005).

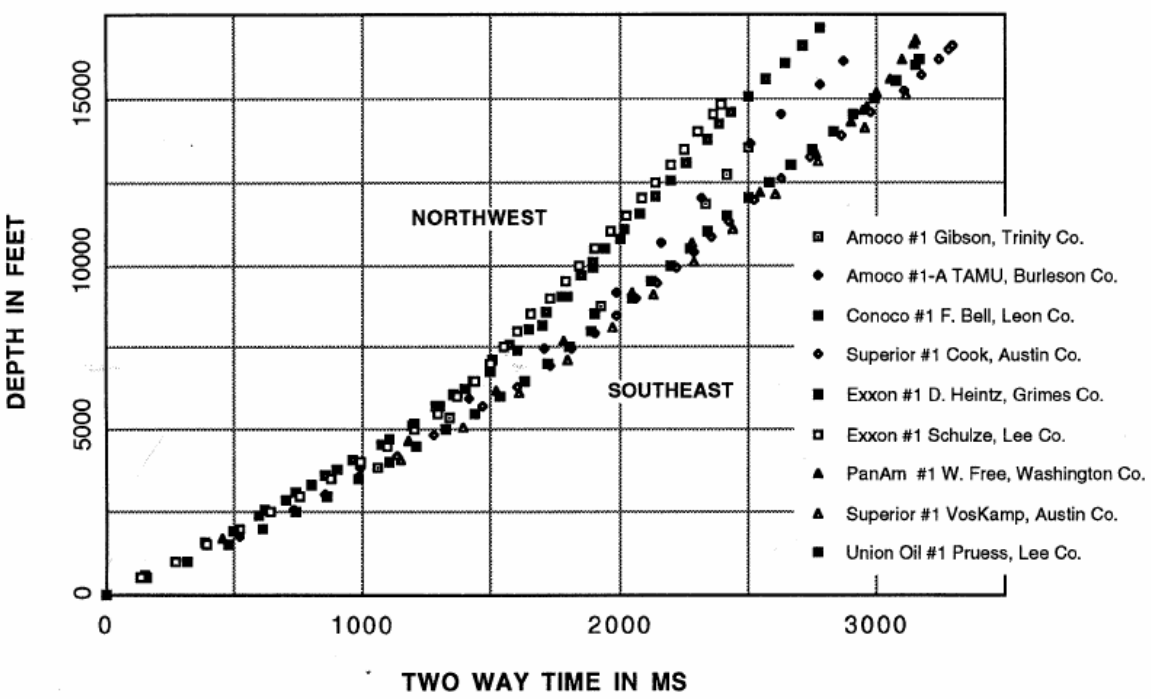

Figure 9. Time–depth data from nine wells (Davidoff, 1993).

Acoustic velocity commonly varies with depth and with location across large regions, such as this study area. Davidoff (1993) presented velocity data for several parts of this study area. To further assess velocity gradient in the study area, I posted 11 wells on seismic line. For those wells, I had picked tops of the Pettet, and Travis Peak formations. I recorded depths of formation tops in the well logs and corresponding times for the same horizons that I had mapped in the seismic lines. Then, I cross plotted the data to determine a velocity equation (Fig. 11 and Table 1).

I used the velocity equation to tie seismic and well log interpretations in GeoGraphix and to make structural maps (Fig. 10). From this analysis, I found that the relationship between depth and two-way travel depth is linear in the thin (~7,300 to 14,000 ft) zone that was investigated. This conclusion differs with that of Davidoff (1993), who

evaluated 9 checkshot surveys from this general area and conclude that the average velocity to a given depth decreases going from the northwest to the southeast (basinward), owing to a southeastward thickening of the Tertiary section.

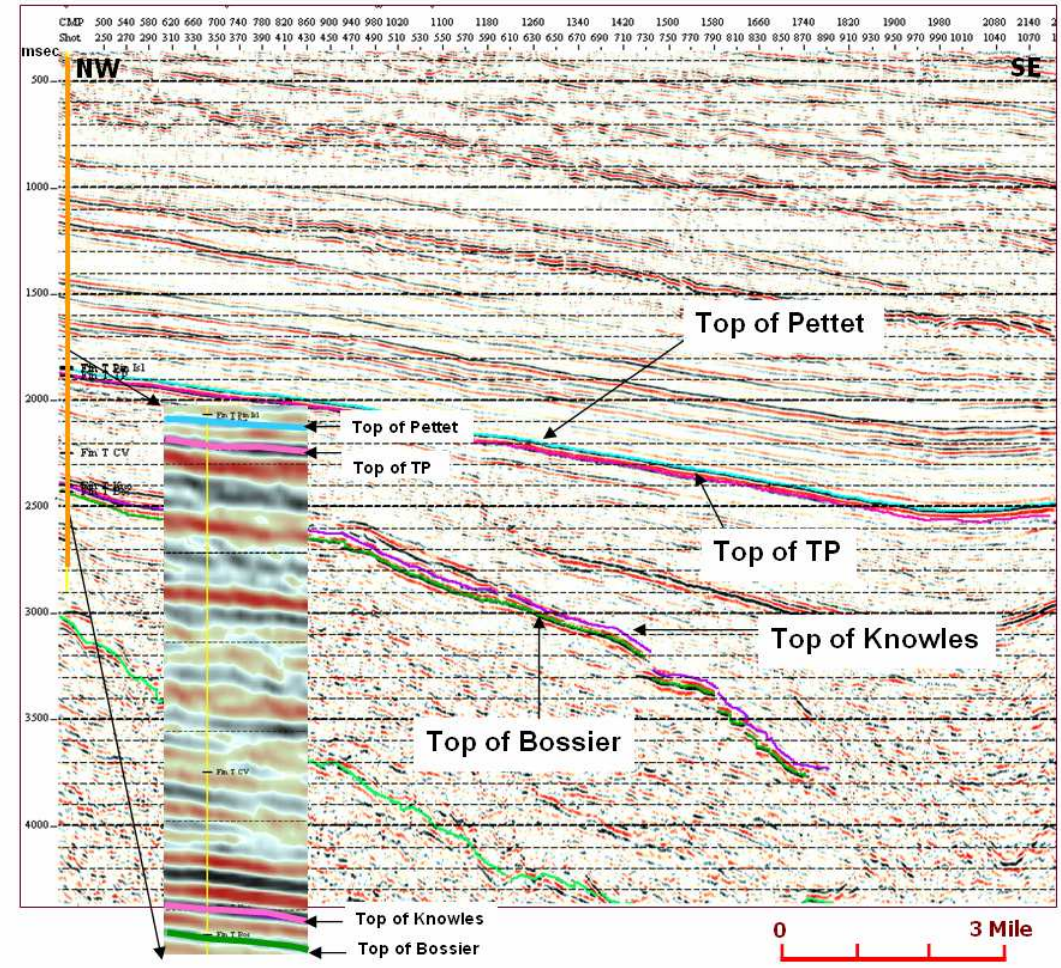

Figure 10. Example of the tie between seismic and well log data.

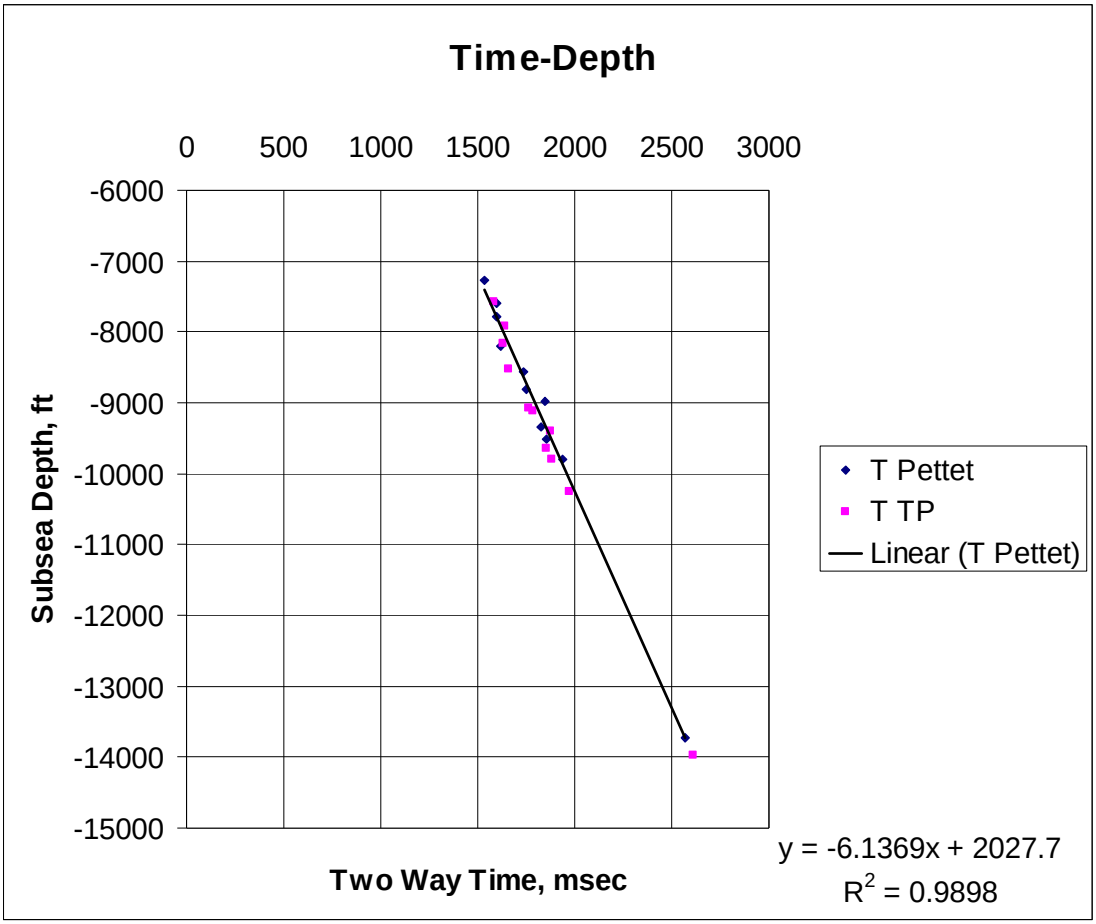

Figure 11. Velocity estimate from plot of subsea depth vs. two-way time for top of the Pettet and Travis Peak formations for 11 wells.

Table 1. Subsea depth from 11 wells and two way time from corresponding horizons in four seismic lines.

Ses Line	T Pet				T TP		
	Well ID	MD, ft	Subsea depth	Time, msec	MD, ft	Subsea depth	Time, msec
56 A	423953027500	7721	-7272	1536	8027	-7577	1581
	423953025500	8028	-7602	1595	8348	-7923	1642
	423953022600	8196	-8196	1620	8533	-8533	1663
	423953045700	8971	-8561	1734	9482	-9072	1766
57 A	423953043100	8228	-7793	1596	8603	-8168	1632
	423953065400	9217	-8806	1752	9528	-9118	1787
58A	423953099100	9351	-9351	1826	9645	-9645	1855
	423953103400	9513	-9513	1851	9794	-9794	1881
	423953093900	9788	-9788	1937	10261	-10261	1969
59 A	423953060300	9249	-8981	1849	9661	-9393	1878
	421853022200	14045	-13730	2567	14298	-13983	2610

Petrophysical Data

Petrophysical data were available for only one well along the west margin of the ETB. These data were in a single report prepared for Burlington Resources by GeoSystems LLP (2003). The report includes laboratory analyses of 5 TP intervals and includes image porosity, calculated permeability, and petrographic description of the TP formation. These petrophysical results were compared with similar TP data from the Sabine Uplift (Dutton and Diggs, 1992) and were integrated with pressure, temperature, and burial history data of this study to infer TP reservoir properties in the downdip regions of the study area.

Mud Weight and Temperature Data

Mud weight and bottomhole temperature data were recorded from 106 well log headers (Fig. 12), which were collected from M.J. System (M.J. System, 2005). These data were used for pressure and temperature analysis. Subsurface temperature analysis is important to assess whether potential source rocks have generated hydrocarbon and to infer the stage of diagenesis in TP potential reservoir rocks, especially where petrographic and petrophysical data are limited. Analysis of drilling mud weights is a useful method for clarifying the pressure regime. Previous Travis Peak studies were focused on the Sabine Uplift area. Thus, I analyzed mud weights from wells along the west flank of the ETB.

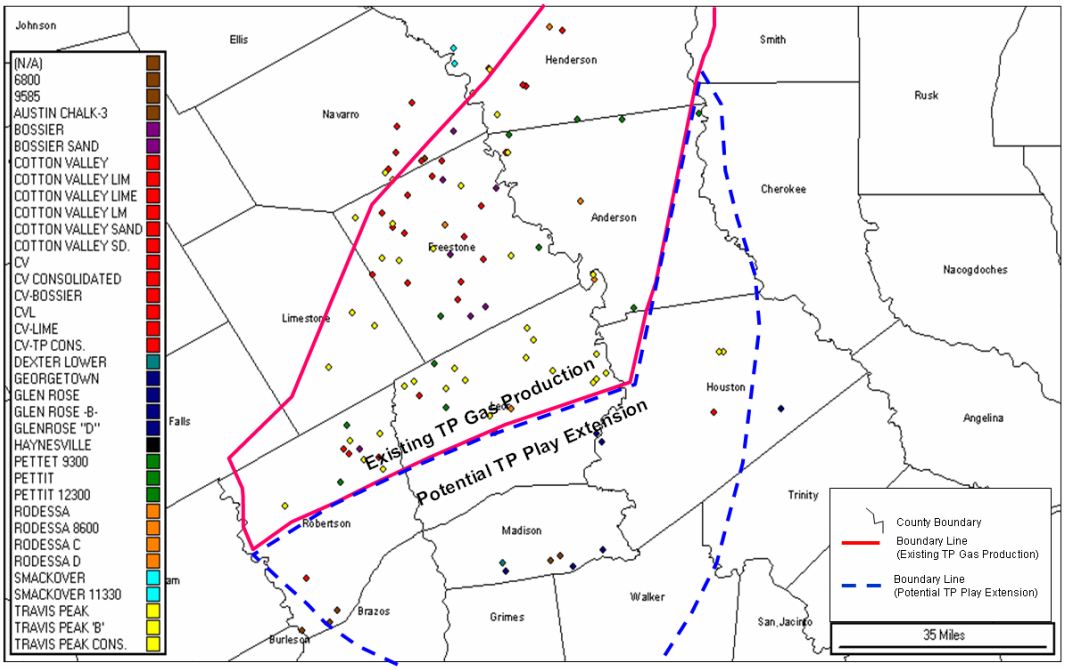

Figure 12. Well locations for temperature and pressure analysis (well logs from M.J. Systems).

Production Data

Travis Peak gas production in the study area began in 1961. Analyzing the production history and production trends provided insight to hydrocarbon trapping mechanisms and regional variability of reservoir quality. To assess production, I collected HPDI gas, oil and water production data from approximate 1,500 wells in 7 counties (Fig. 13). TP sandstone is well as a known tight sand reservoir. However, some TP fields have high porosity and permeability reservoir rocks. The Texas Railroad Commission (RRC) defines cost (essentially tight sand) fields and identifies high cost fields in Texas. I used the RRC definition and calculated the total gas, oil water production in study area from 1961 to 2005. To evaluate gas production, I made production contour and bubble maps and overlaid those maps on structure maps to understand trapping mechanisms. Also, well completion and production data were used to understand the TP development history.

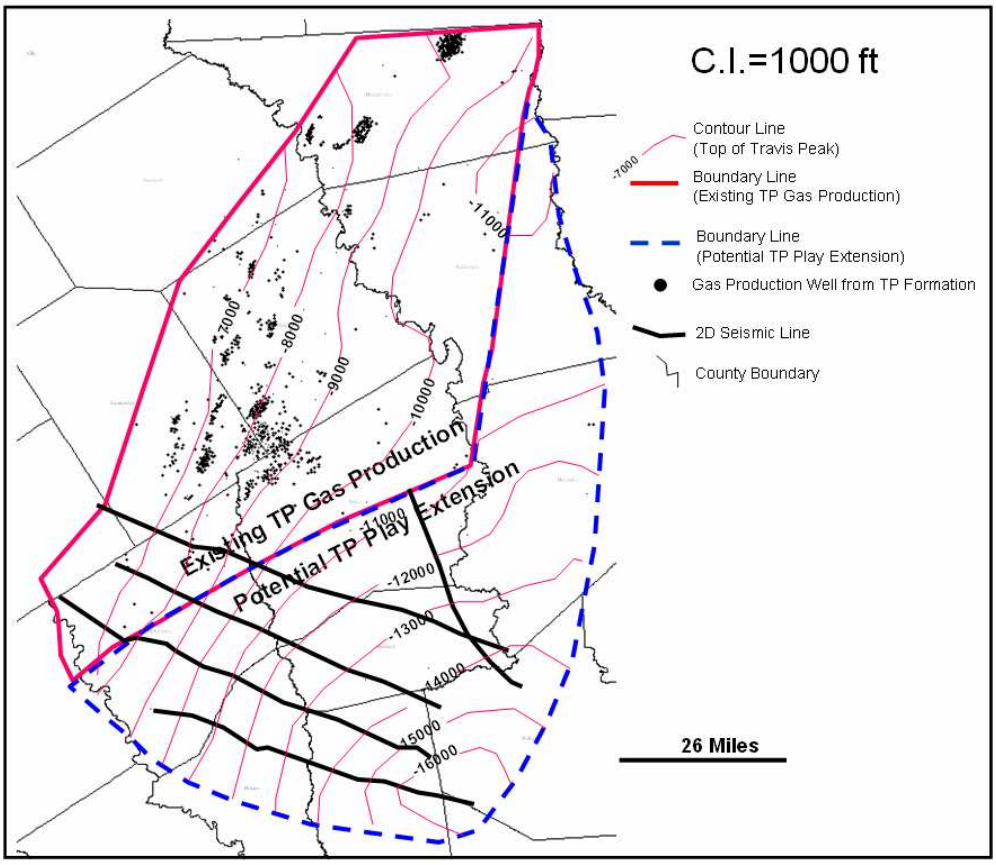

Figure 13. Well locations for production analysis (from Li and Ayers, 2006) (data collected from HPDI, 2005).

REGIONAL STRUCTURAL SETTING

Seni and Kreitler (1981) report that the East Texas Basin originated with early Mesozoic rifting, and that salt tectonics related to the Jurassic Louann Salt greatly affect younger Mesozoic and early Tertiary sedimentation patterns and formation of salt-related features and hydrocarbon traps (Fig. 14). They divided the evolution of East Texas Basin to three stages on the basis of tectonic activity and depositional fill of the basin. During the initial infilling of the ETB (Triassic through Early Cretaceous), the tectonic movement associated with rifting was very active and was followed by salt movement. Crustal rifting, and rapid, fault-controlled subsidence were characteristic of this stage. Very thick Triassic rift-basin fill, Jurassic evaporates, and Lower Cretaceous fluvial-deltaic sediments were deposited in the basin. The Lower Cretaceous Massive Anhydrite Formation signaled the termination of initial step of basin infilling. The middle stage infilling of the ETB included deposition of strata between the Massive Anhydrite and the Upper Cretaceous Navarro Group. These strata are relatively thin fluvial-deltaic deposits that occur around the basin margin. The dominant tectonic activity during the middle stage was salt-related tectonics. During the final stage of the ETB fill, thick Tertiary marine and fluvial-deltaic systems of the Midway, Wilcox, and Claiborne Groups filled the basin and prograded into the Gulf of Mexico. (Seni and Kreitler, 1981).

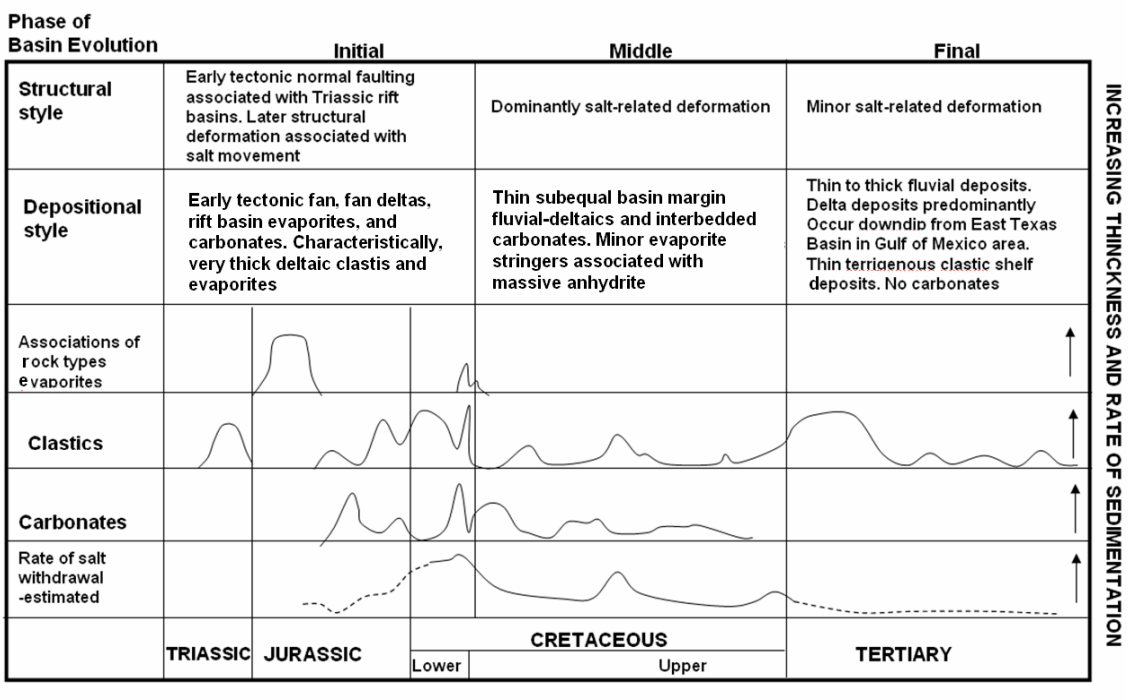

Figure 14. Summary of relations between infilling of the East Texas Basin and structural and depositional styles, rock types, and salt deformation (from Seni and Kreitler, 1981).

REGIONAL STRATIGRAPHY

The Lower Cretaceous TP formation was deposited on earlier Mesozoic strata that were greatly affected by syndepositional and post-depositional deformation of the underlying Jurassic Louann Salt. Therefore, understanding TP depositional and structural characteristics and the potential for TP hydrocarbon play extension along the west margin of the ETB requires analysis of the stratigraphy and structure of these underlying strata, beginning with the Louann Salt.

Louann Salt - Stratigraphic Analysis and Salt Tectonic Significance

Pre-Louann Salt strata and basement-related structural activity had little effect on deformation of post-Louann strata and formation of hydrocarbon traps in the ETB. In contrast, the middle Jurassic Louann Salt played a distinct role in affecting deposition of younger strata and the formation of hydrocarbon traps in those strata. Upper Jurassic, Cretaceous, and Tertiary strata overlying the Louann Salt are at least 18,000 ft (5,500 m) thick. Commonly, these younger strata are folded to form anticlines and synclines, especially in the central part of the basin; folds diminish in amplitude updip toward the Mexia-Talco fault zone (Figs. 5, 15, and 16).

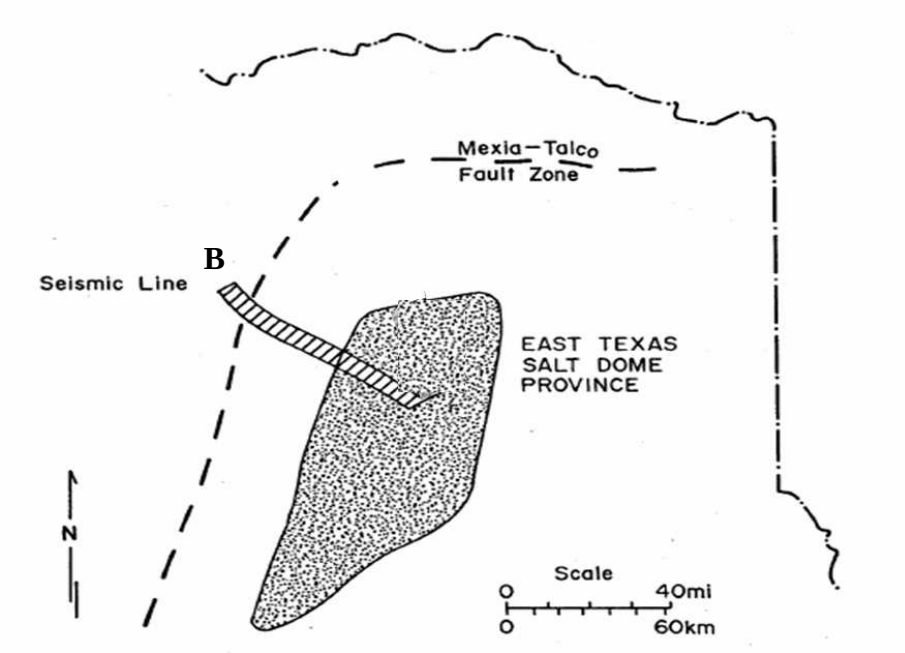

Figure 15. Location map, seismic line, East Texas, showing East Texas Salt Dome Province, Mexia-Talco Fault Zone, and location of seismic line B (Fig. 16) (Modified from Jackson, 1981).

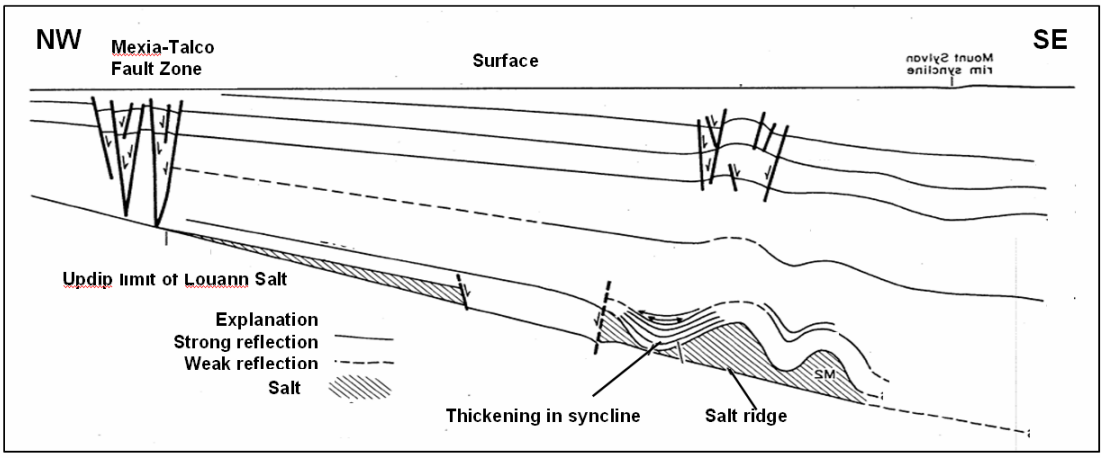

Figure 16. Schematic interpretation of dip-oriented seismic section along line B from Mexia-Talco fault zone to near Mount Sylvan diapir, East Texas Basin (modified from Jackson, 1981). See Figure 15 for location.

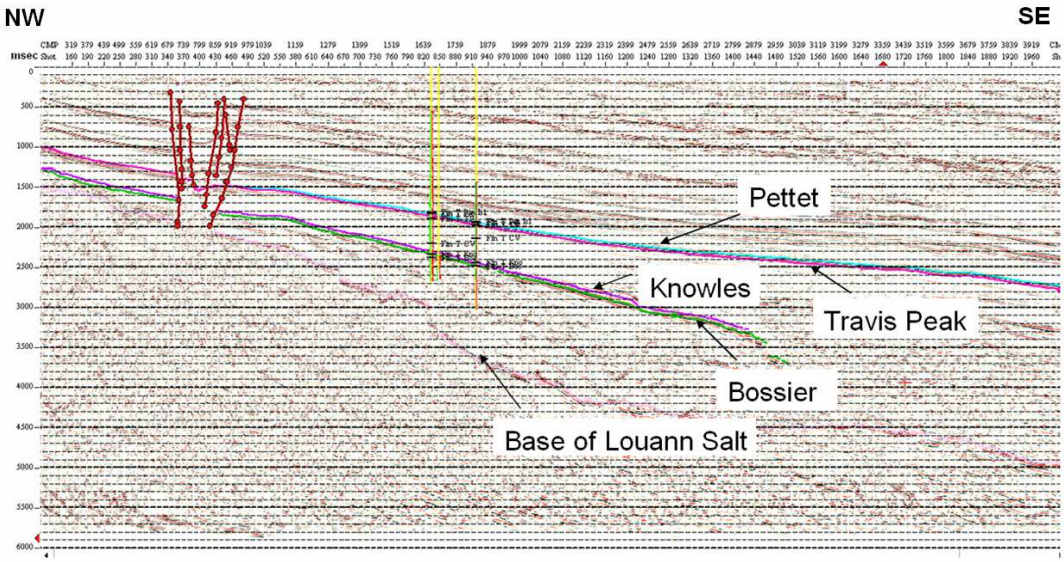

Figure 17. Seismic line 58A from this study (Data from Seismic Exchange Inc.). (See Fig. 7 for location).

The differential loading of overlying sediments forced the salt movement, when the upper stress from overlying sediments big enough. Now image the salt like high density liquid underground. It is easy to understand that salt moved away from areas of maximum loading, because of the stress. After salt move away from maximum loading place, that place will become a syncline (Fig. 16). Sediments will continue to deposit in that withdrawal synclines until all the salt was squeezed from beneath the depocenter. Bossier sands and shales, Cotton Valley, and Travis Peak Formations, the first major post-Louann clastic deposits, probably initiated salt movement in most parts of the basin. During Cotton Valley- Travis Peak time, salt structures may have been characterized by discontinuous salt anticlines separated by withdrawal synclines depositional basins (Wood, 1981).

Salt diapirs, salt anticline, and turtle-structure are salt structure in East Texas Basin. In study area, salt diapirs are uncommon and are rarely seen in 2D seismic lines (Figs. 17 and 18). Salt diapirs usually developed in the center of the Basin and relatively small (Fig. 5). Primarily vertical rather than lateral salt movement generated the salt diapirs. Turtle-structure always developed close to salt diapirs.

Salt anticlines occur mainly around the outer edges basin (Fig. 5).Salt anticline is very common in study area, which is interpreted from 2D seismic reflector in study area (Fig. 18). Salt anticlines are indicated by thinning of overlying sediments. Salt anticlines may deform great thicknesses of overburden; Extensional faults are common at the crests of the anticlines. For example, the cross section. The generation mechanism of salt anticline is different with salt diapirs. For salt anticline, the salt was pushed laterally into ridges that were subdivided by loading and further segment into anticline.

Interpretation of five dip-oriented seismic profiles provides information on the timing and nature of salt mobilization near the western margin of the basin. Structural and stratigraphic disconformities along some of these reflections delineate Louann Salt (Figs. 17 and 18). Seismic sequence Louann Salt is characterized by prominent boundary reflections and a lack of internal reflections. The top of salt is placed between coherent reflectors associated with the overlying sediments.

The low-amplitude folds of Salt happened at the region of the basin margin (Fig. 18). The profile shows the Louann Salt thinning to a pinch out going northwest, toward the Mexia fault zone. The Mexia fault zone appears as a large flower fault. The position of the fault appears to be related solely to the updip pinch out of the Louann Salt. Louann

Salt shows noticeable thinning in synclines and thickening with internal reflections in anticlines. Upper Jurassic strata folding above the salt.

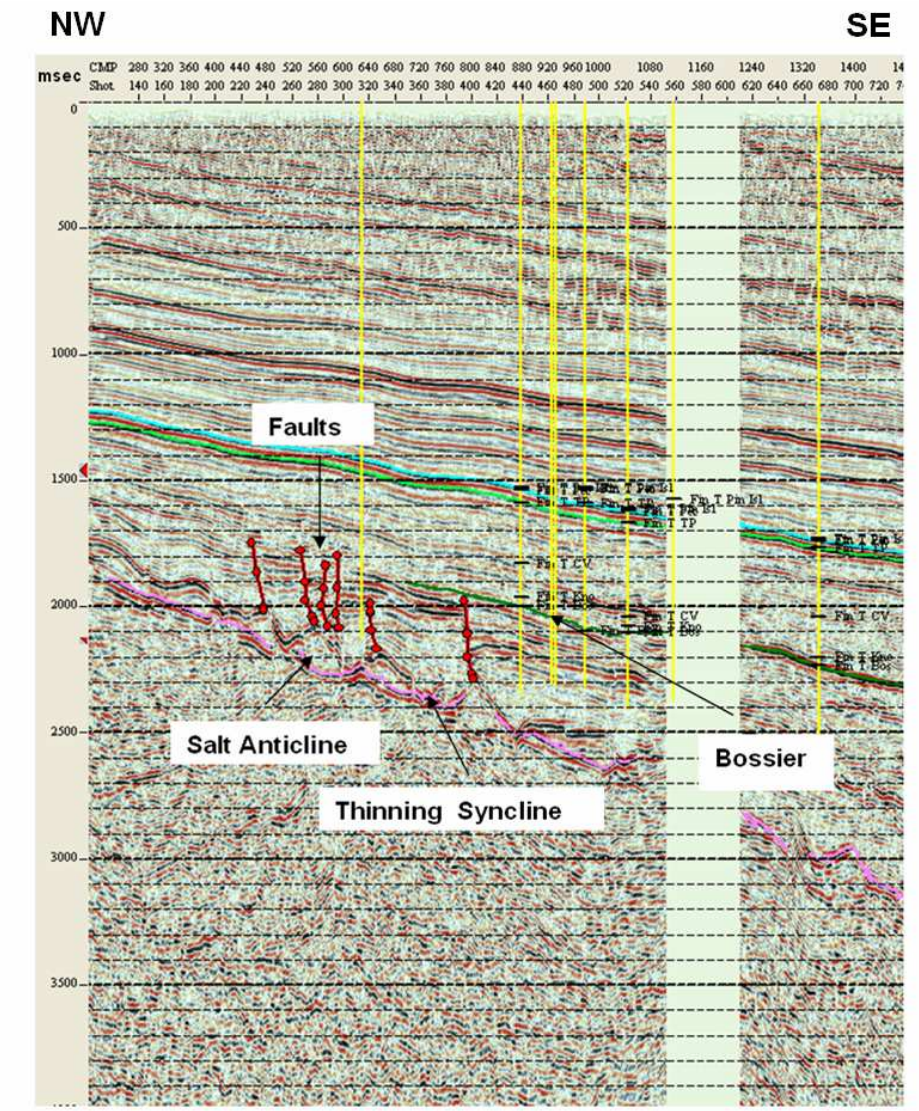

Figure 18 . Line drawing of the interpretation of seismic line 56A in the study area (Data from Seismic Exchange Inc.). See Figure 7 for location.

Smackover Formation

In East Texas, the Smackover was deposited in a carbonate slope environment (Sassen and Moore1978). The depositional environment for Smackover was anoxic and

hypersaline, which allowed the algal kerogen to be preserved. Smackover carbonate mudstones may be the source rock for Travis Peak hydrocarbon (Dutton, 1987).

Bossier Formation

Throughout most of the study area the Bossier sequence is interpreted as marine shale. However, along the south part of the west flank, well-developed sandstone bodies are interbedded with the marine shale. Cross section A-A' (Figs. 19 and 20) is a cross from Navarro to Freestone County, showing the Bossier formation.

In study area, few well are deep enough to penetrate the Bossier, especially in the southeast downdip region. Structural maps made using only well log data (Fig. 21) or only seismic data (Fig. 22) are less reliable than structural maps made by combining the two types of data. Therefore, I integrated well logs and 2D seismic data to build a structure map for top of Bossier formation (Fig. 23).

The subsea structure of the Bossier is generally characterized by monoclinal dip to the southeast (Fig. 23). The top of Bossier is approximately (-)19,000 ft in the deep, downdip part of part the area (Fig. 23). Unfortunately, there is only one well in this area. In the study area, the top of the Bossier is shallowest ((-)8,000 ft) near the basin margin, along the Mexia Fault Zone. Structural relief of the Bossier top is approximately 11,000 ft in the area. Generally, the Bossier seismic reflector is strong near Mexia fault (Fig. 17), but basinward, the Bossier reflector is weak and difficult to identify. Basinward deterioration of the Bossier reflector may be attributed to data quality changes in rock properties.

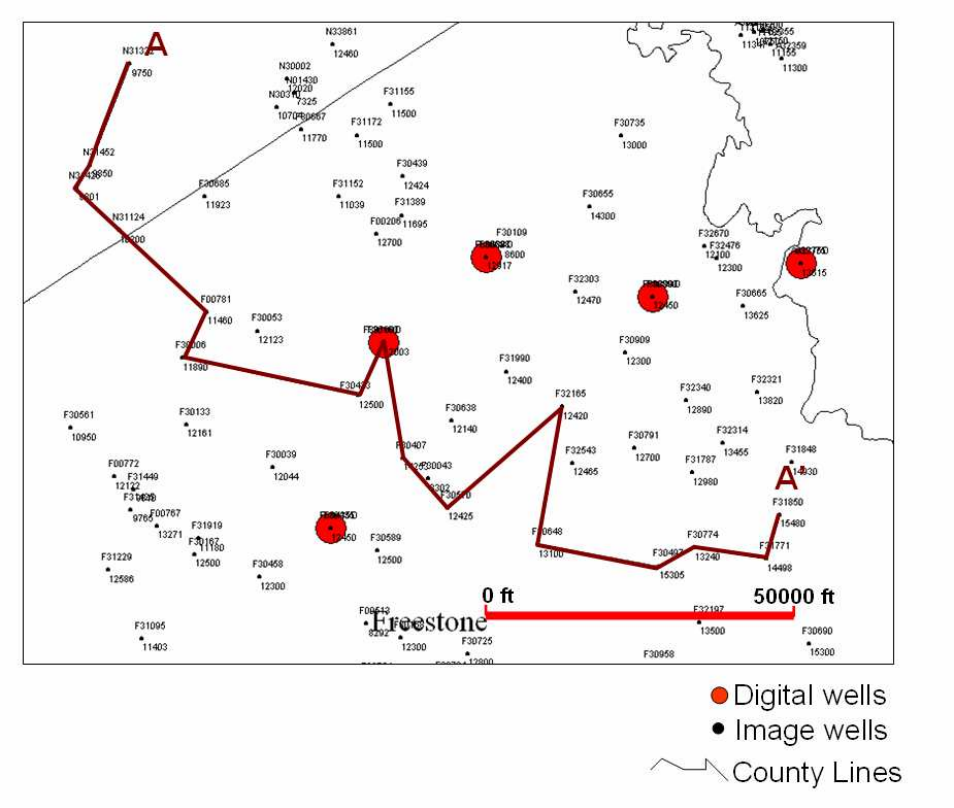

Figure 19. Location of structural cross section A-A', Freestone County, East Texas Basin.

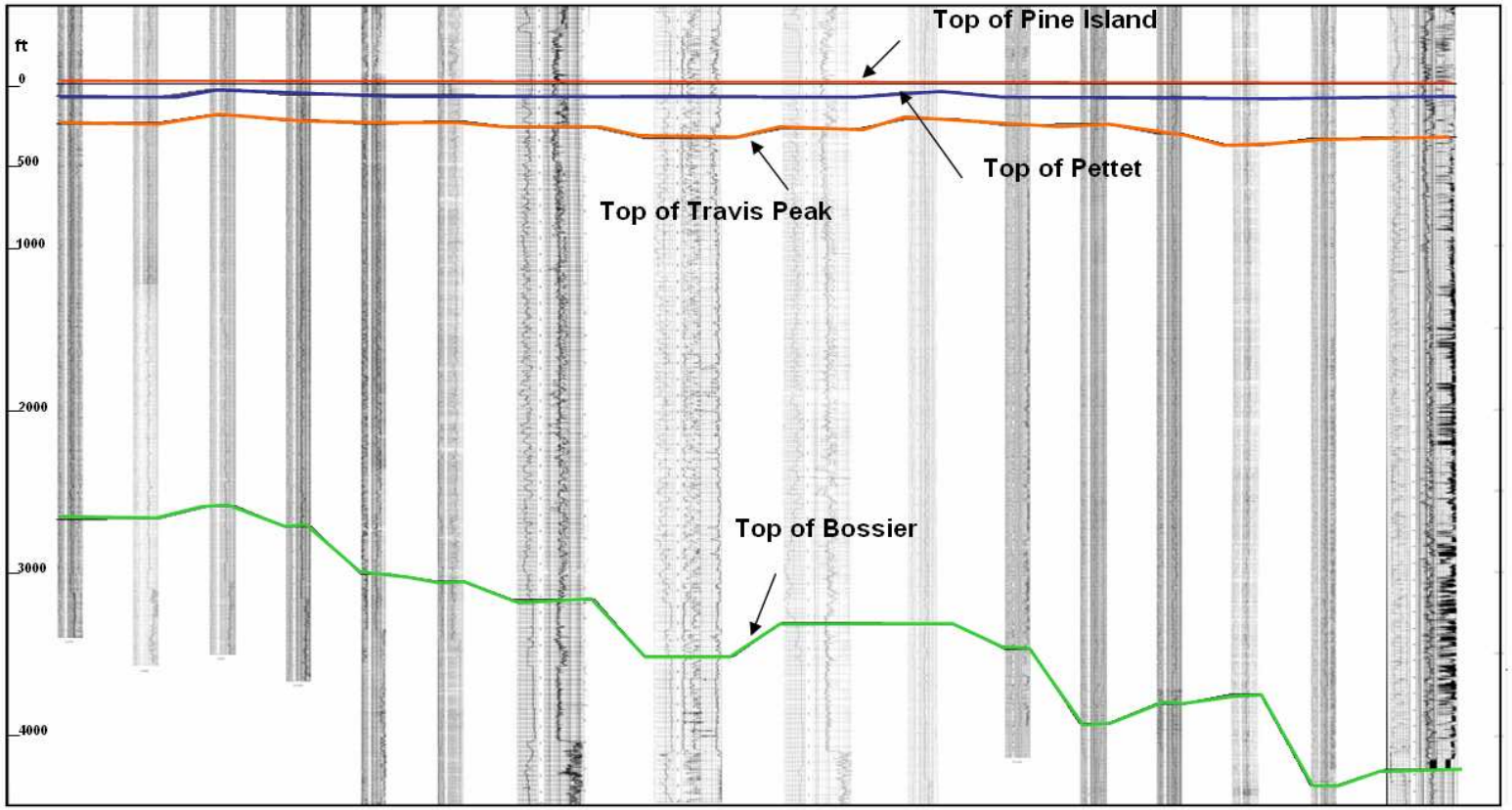

Figure 20. Cross section A-A', Freestone and Navarro Counties (Datum is Top of Pine Island; equal spacing between wells). See Figure 19 for location

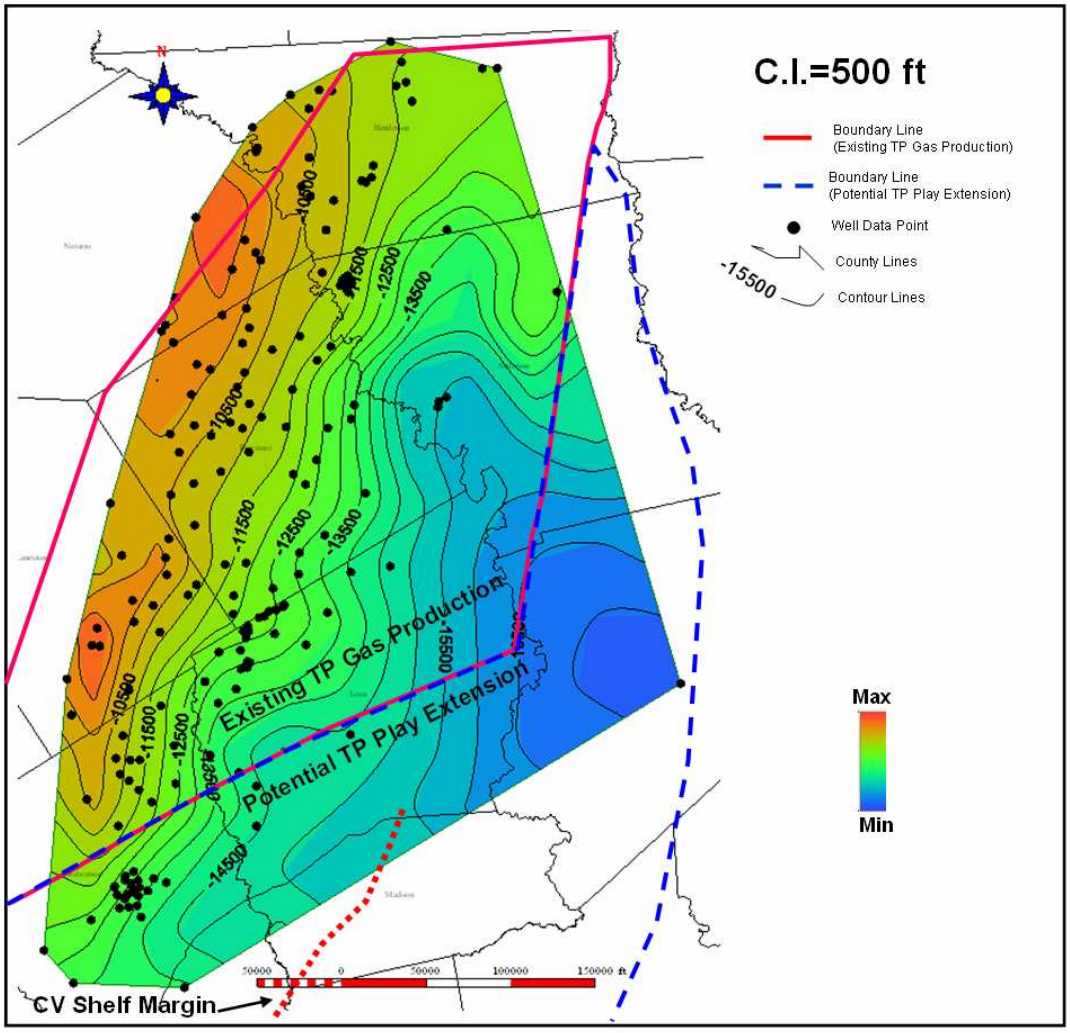

Figure 21. Structure, top of Bossier formation, from well logs (S.L. datum).

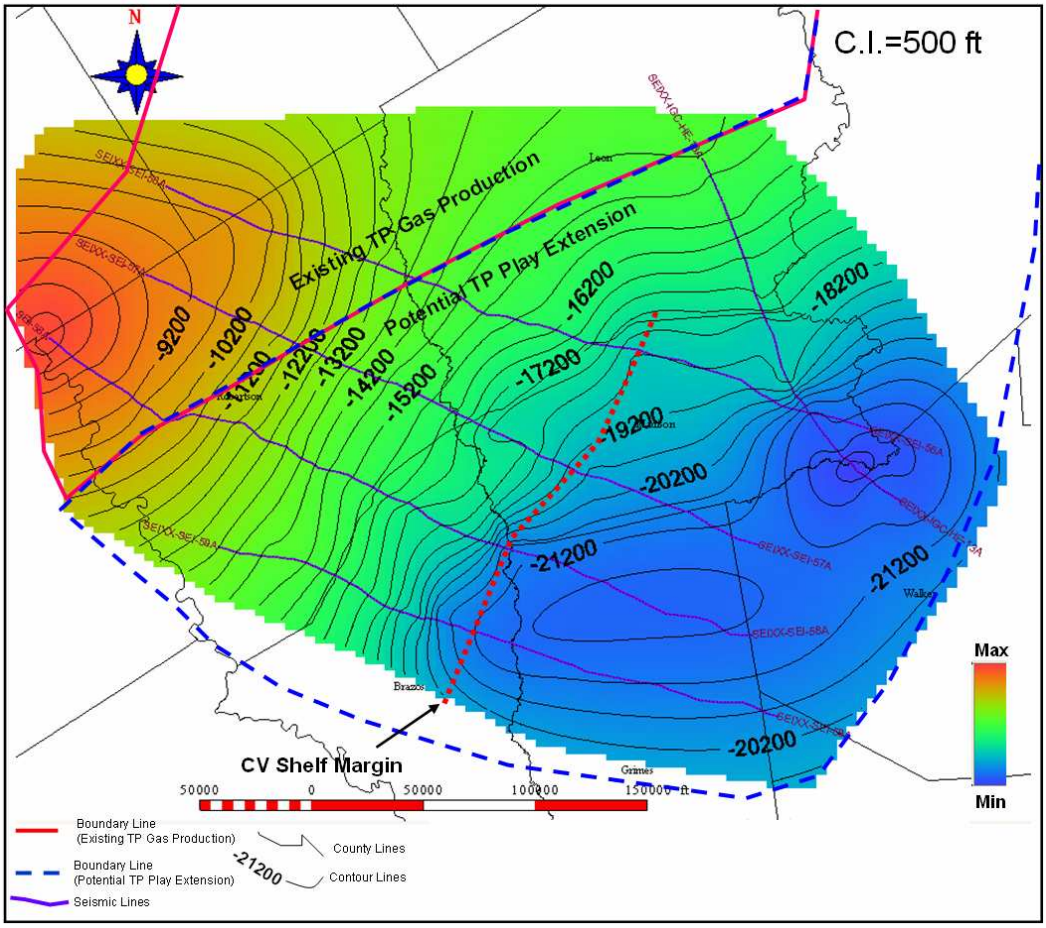

Figure 22. Structure, top of Bossier formation from five 2-D seismic lines (S.L. datum).

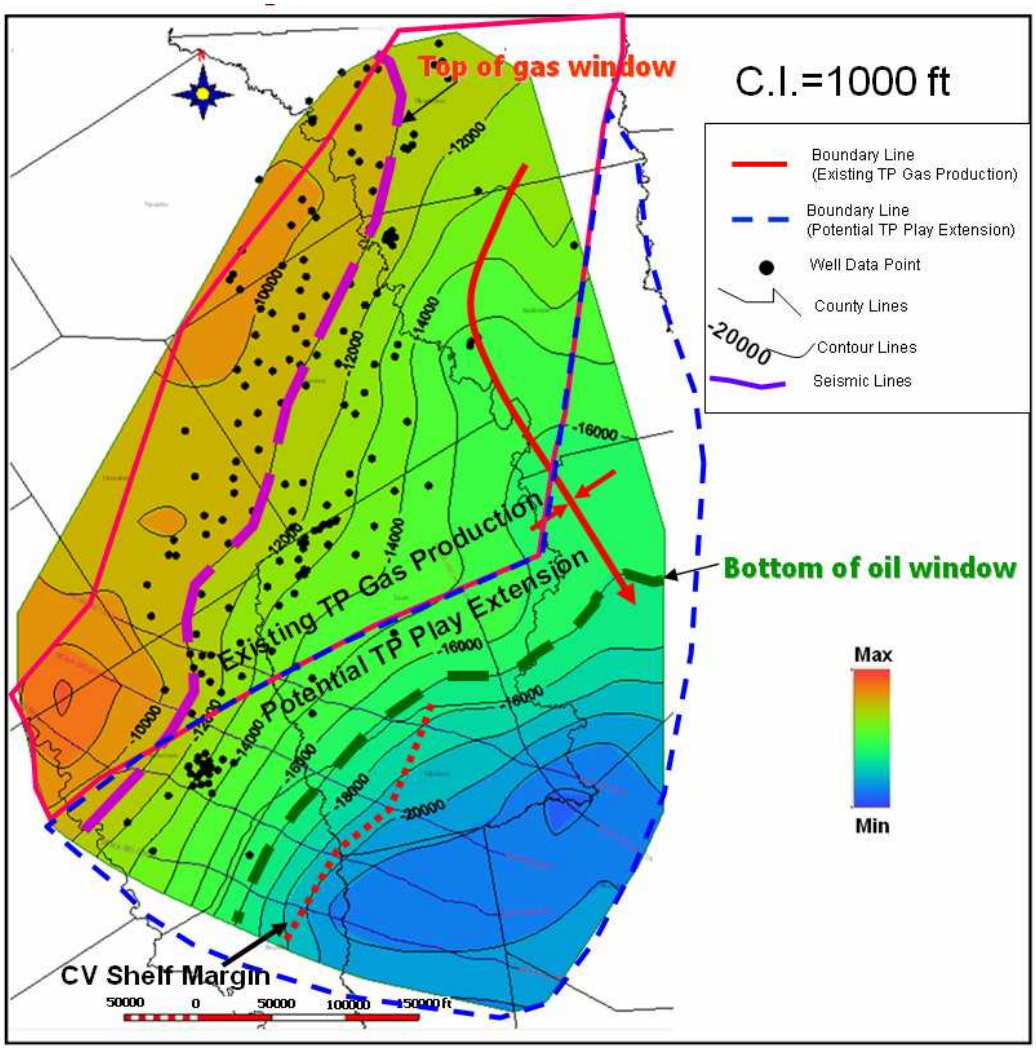

Figure 23. Structure, top of Bossier formation from integrated seismic and well log data (S.L. datum).

Cotton Valley Group

The Cotton Valley Group is an Upper Jurassic to Lower Cretaceous sequence of sandstone, shale, and limestone. In the study area, the top of the Cotton Valley ranges from 4,000 ft below sea level in the updip zero region to more than 13,000 ft below sea level are the downdip margin.

The Cotton Valley Group and overlying Travis Peak (Hosston) Formation represent the first major influx of terrigenous clastic sediments into the Gulf of Mexico Basin (Salvador, 1987; Worrall and Snelson, 1989). Prodelta, delta-front, and braided-stream facies have been identified in the Cotton Valley Group in the northwestern part of the East Texas basin (McGowen and Harris, 1984). The prodelta facies contains minor amounts of very fine-grained sandstone and siltstone. Cotton Valley delta-front deposits typically consist of interbedded sandstone and mudstone with a few thin beds of sandy limestone, and commonly, they are overlain by a thick wedge of braided-stream sediments (McGowen and Harris, 1984).

In parts of East Texas, the Travis Peak / Cotton Valley boundary is marked by a regional transgressive deposit, the Knowles Limestone (Fig. 24). However, the Knowles Limestone does not extend throughout the East Texas basin (Saucier, 1985), and where it is absent, Travis Peak sandstones directly overlies Cotton Valley sandstones (Finley, 1984), making correlation of the boundary difficult to impossible, especially where well log data are limited in the downdip region. Therefore, separate isopach maps were not made for the two intervals, but rather, the Peak sandstone and Cotton Valley were mapped together.

In the study area, approximate 190 wells penetrated the entire Cotton Valley section. An isopach map from the top of the Travis Peak to the top of Bossier shows that the interval thickness ranges from less than 3,000 ft in the updip region to more than 5,000 ft in the downdip area (Fig. 25). The thickest strata occur along the basin axis (compare

Figs. 4 and 25), in the same position that Finley (1984) mapped thickest Cotton Valley strata.

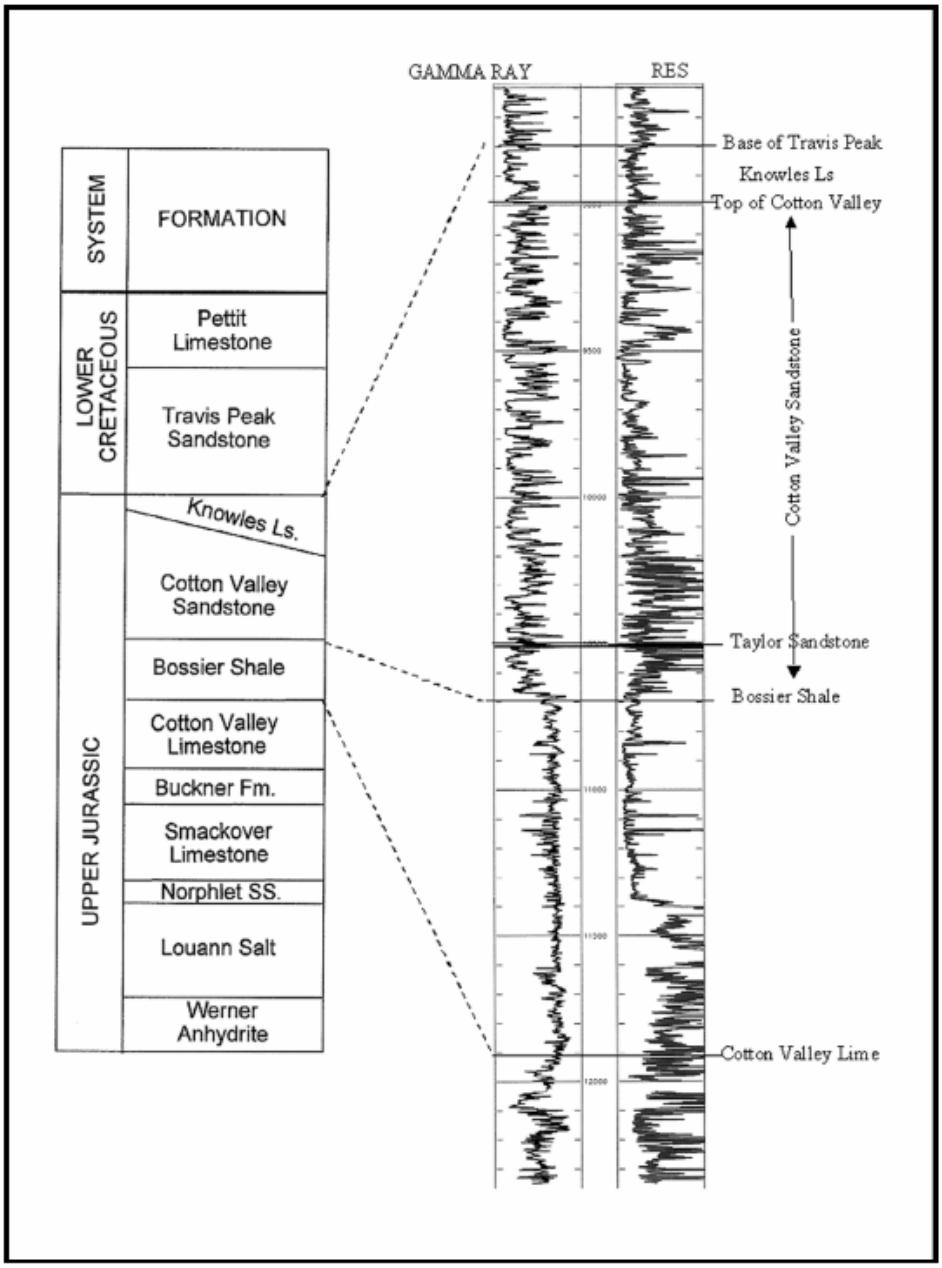

Figure 24. Stratigraphic column of Upper Jurassic and Lower Cretaceous units in the East Texas Basin, with a gamma ray type log of Cotton Valley/Bossier interval showing the Knowles Limestone (from Kosters et al., 1989 and Wescott, 1985).

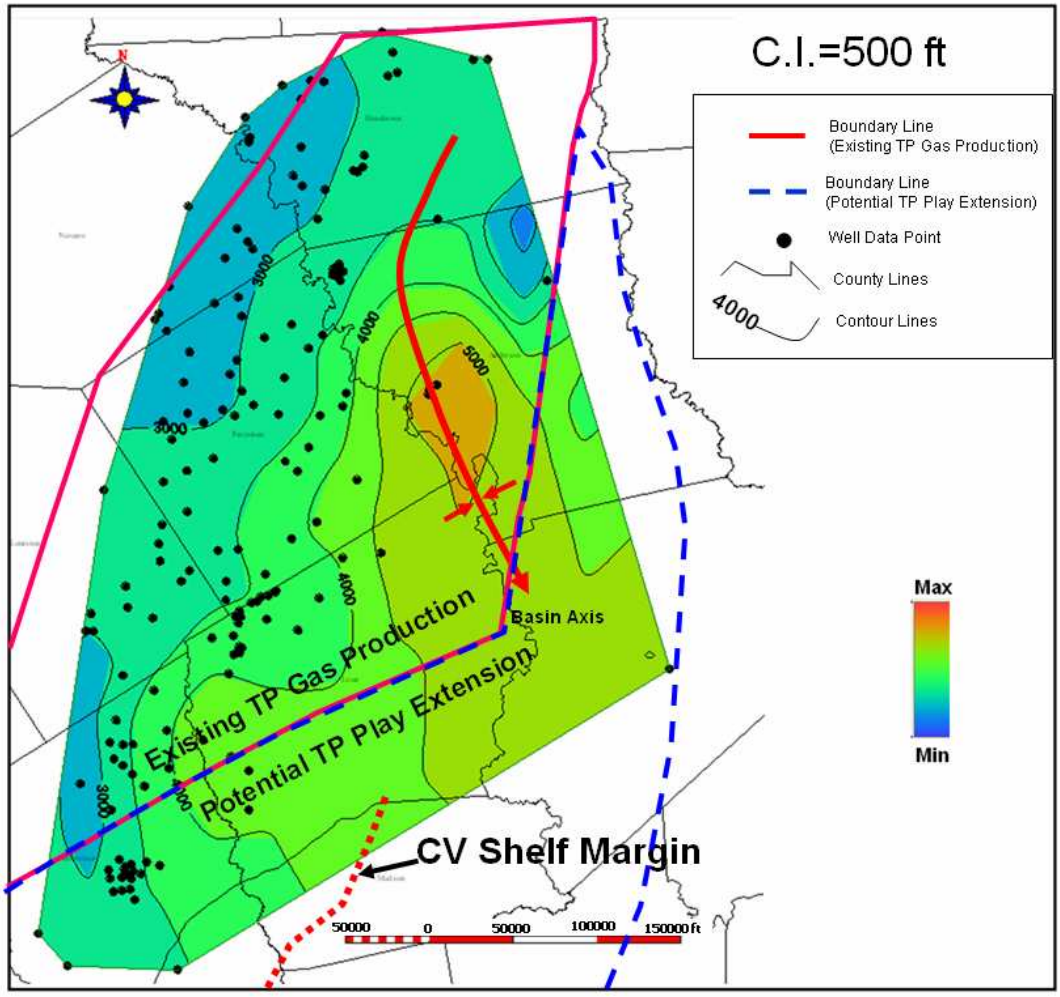

Figure 25. Isopach map, top of Travis Peak to top of Bossier Formation.

Travis Peak – Hosston Formation

The top of the Travis Peak Formation is transitional and is characterized by marine-reworked clastic sediments that grade upward to Pettet formation carbonates. Owing to this transitional contact, the top of Travis Peak formation can be difficult to pick. The SP is similar to that of shale, but the resistivity is high. It is hard to say that zone is the rework Travis Peak strata or carbonate sediments of the overlying marine unit. Therefore, I made a density / neutron crossplot to analyze the lithology in that zone

(Fig. 26). From the crossplot, I found the lithology of the questionable zone is predominately carbonate, which was supported by laboratory analysis. Thus I placed this questionable zone in Pettet formation.

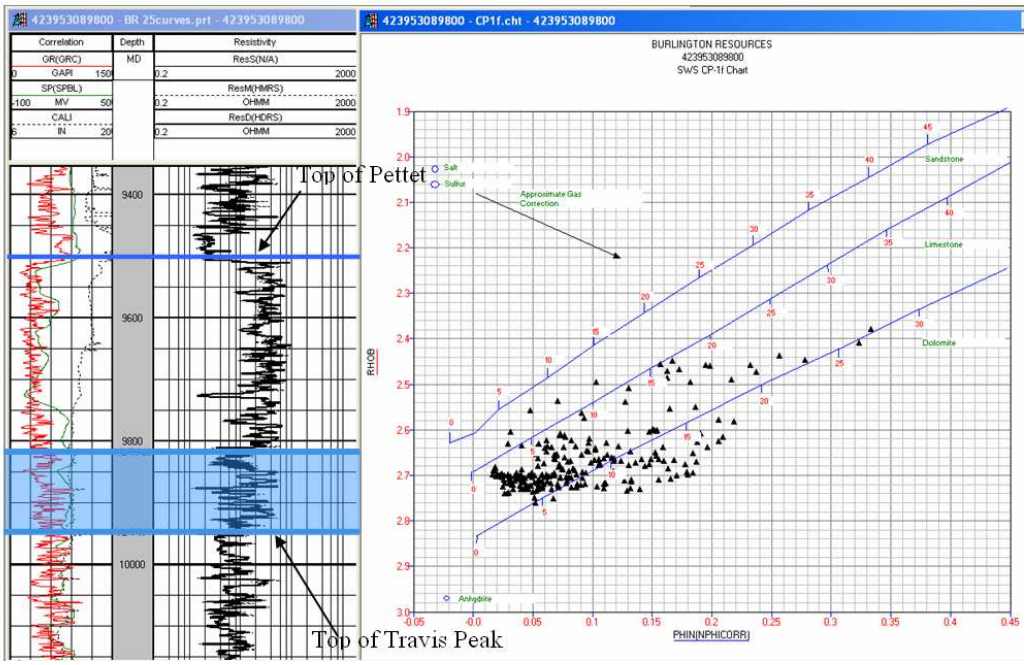

Figure 26. Density-neutron crossplot for lithologic analysis of the transitional, medium resistivity zone between the Travis Peak and Pettet formations,

Depositional Systems

Bushaw (1968) published paleogeographic maps for the Travis Peak and Pettet formations on the basis of interpretation of 100 well cores in the ETB. During early Travis Peak time, alluvial plain and shoreline environments dominated the study area (Fig. 27). The coastal plain-shoreline transition was characterized by fine sediments and the seaward termination of red bed deposits. Fluvial systems of the Ancestral Red River fed sediments to delta systems to the east and south. Continental and delta plain

sediments were deposited in a very narrow band. During Middle Travis Peak-Pettet time, eustatic sea level continued to rise rapidly, but environments shifted little relative to the early Travis Peak-Pettet time. During late Travis Peak-Pettet time, however, dramatic landward shift of depositional environments accompanied eustatic sea level rise that resulted in marine sedimentation over the present study area. In summary, from early to late TP-Hosston time, eustatic sea level rise resulted in shoreline retrogradation. By Pettet time, a shallow, open-shelf environment covered most of the study area.

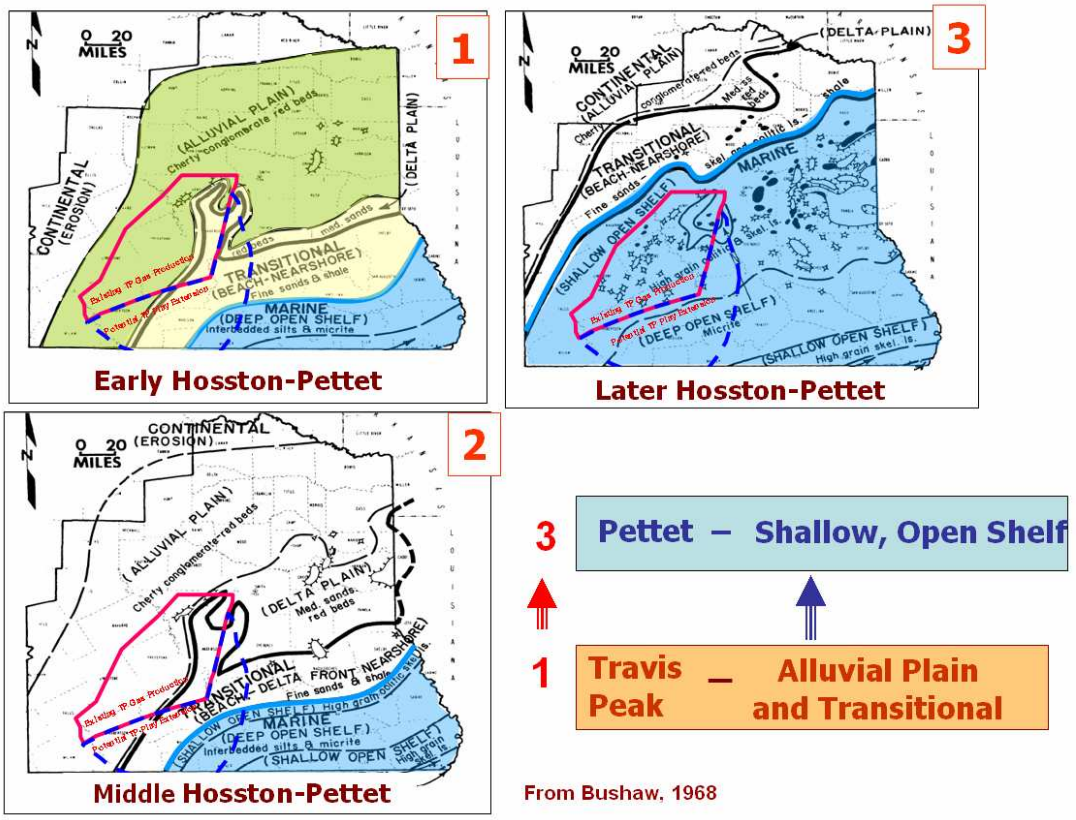

Figure 27. Paleogeographic setting, Travis Peak and Pettet formations, East Texas Basin (modified from Bushaw, 1968).

The lower TP formation is composed predominately of thick fluvial channel-fill sandstones deposited by straight channels (low sinuosity), braided streams (Figs. 28-30) (Bushaw, 1968; Davies, Williams, and Vessel, 1991). Fluvial deposits are enveloped in thinner deltaic, paludal, and paralic deposits. The middle and upper TP sandstones are braid-to-meandering (high sinuosity), channel-fill deposits that are interbedded with deltaic deposits (Tye, 1989). The fundamental difference between high and low sinuosity channel can be recognized on the basis of the difference in the sinuosity, width, and depth of channels (Fig. 30) and on the basis of primary sedimentary structures recognized in cores and at outcrop. However in the subsurface, evidence of channel style geological record is distinguished primarily from the vertical succession of sandstones and shales, sedimentary structures in cores, and lithologic descriptions, and mapped geometries.

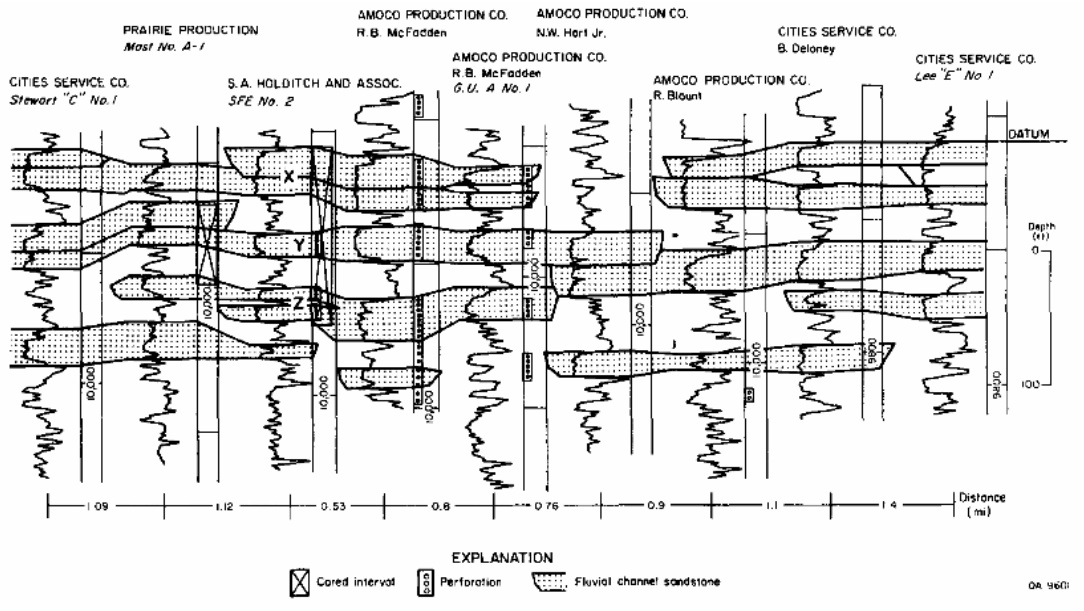

Figure 28. Stratigraphic cross section illustrating the occurrence and geometry of channelbelt sandstones in the lower Travis Peak (from Dutton et al., 1991).

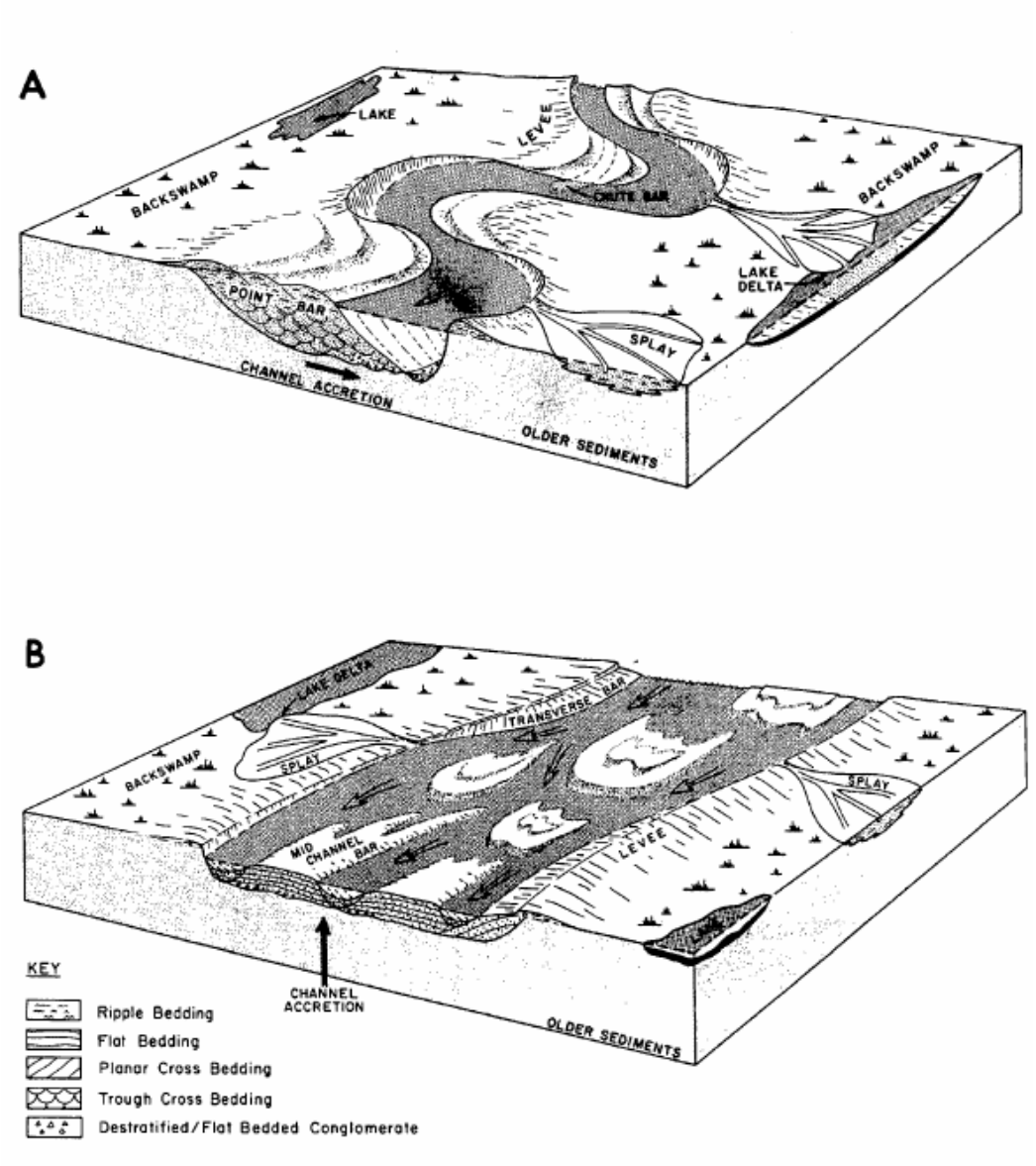

ure 4. Schematic block diagrams illustrating differences between single channel, fluvial systems characterized by different channe
e. A) High sinuosity (meandering) system, B) Low sinuosity (straight) system.

Figure 29. Schematic block diagrams illustrating differences between single channel fluvial systems characterized by different channel styles. (A) High sinuosity (meandering) system. (B) Low sinuosity (straight) channel system (Davies et al., 1991).

High-sinuosity channel deposits consist of sand-rich, point bar deposits that are interbedded with flood basin deposits consisting of shales and thin sandstones (Fig. 27)

(Davies et al., 1991). Low-sinuosity channel-fill sands are fine-grained and well sorted, and they contain very little interbedded, floodplain shale (Fig. 27). They originate from vertical accretion of braid bars. These multistory sandstones commonly consist of 2 to 5 stacked channels-fill sand deposits (Davies et al., 1991).

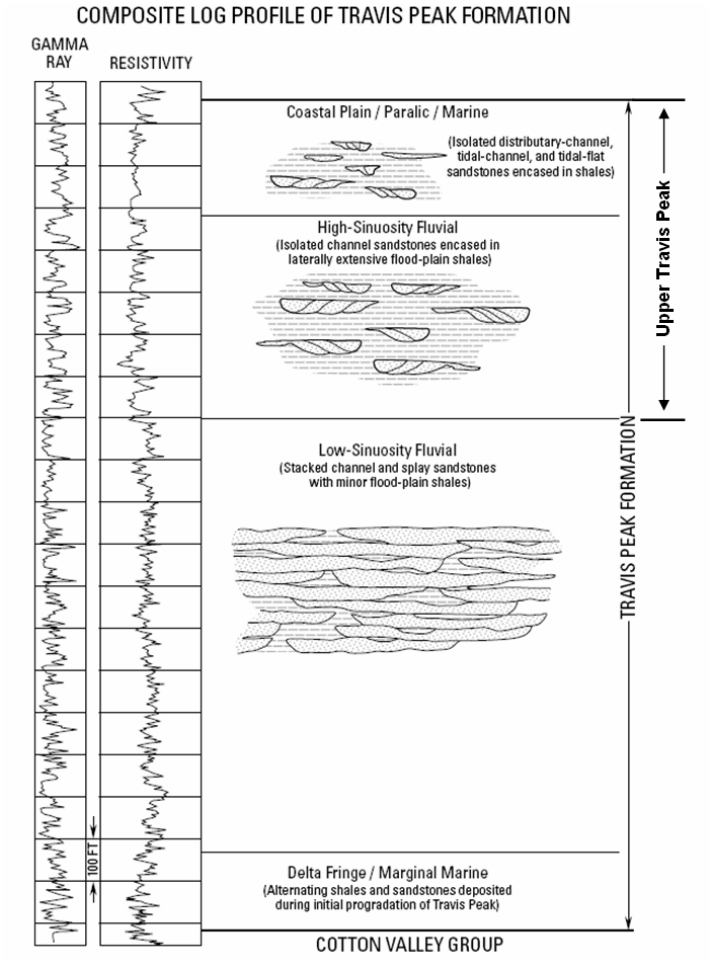

Figure 30. Composite wireline log showing gamma-ray and resistivity responses through complete section of Travis Peak Formation in East Texas (modified from Davies and others, 1991).

Regional depositional systems were evaluated to assess the potential for hydrocarbon play extension in TP sandstones. Data used for depositional systems analysis were 35 digital well logs, 22 image well logs, and five 2D seismic lines.

To assess depositional systems, I mapped net sand thickness for the upper 300 ft of the TP formation, and for the interval from 300 to 1,000 ft below the TP top. These intervals were selected because (1) the upper 300 ft (approximately) of the TP is comprised of sandstones that are thinner and shalier than those of the lower TP interval, and (2) using the existing well log database, I could not correlate the boundary between the TP and the underlying Cotton Valley Group. Therefore, I decide to map intervals or "slices" of the TP that were thick enough to capture the essence of the depositional systems but, in the lower interval, did not cross into the Cotton Valley Group.

Net sand thicknesses were calculated from gamma ray (GR) and spontaneous potential (SP) log responses. The shale baseline and clean sandstone baseline for the GR were selected using all the digital well data (Fig. 31). For some image wells, net sand thickness was calculated from SP log response. I used 4 wells to test the establish the relation between net sand thickness calculated from GR versus SP logs and generate an equation for converting between those two methods of net sand thickness determination (Figs. 32 and 33). Net sand thicknesses calculate from GR was consistently greater than net sand thickness calculate from GR.

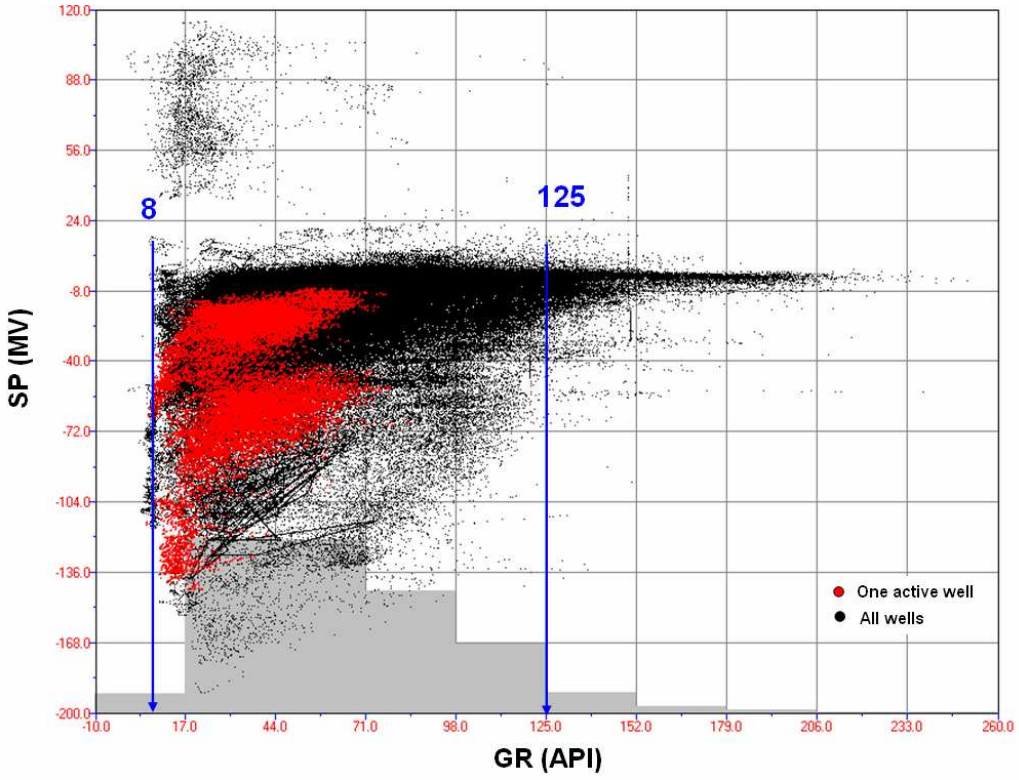

Figure 31. GR vs. SP plot for one (red) and all (black) digital wells, showing the GR baselines selected for net sandstone calculations. The shale baseline is 125 API and the clean sandstone baseline is 8 API.

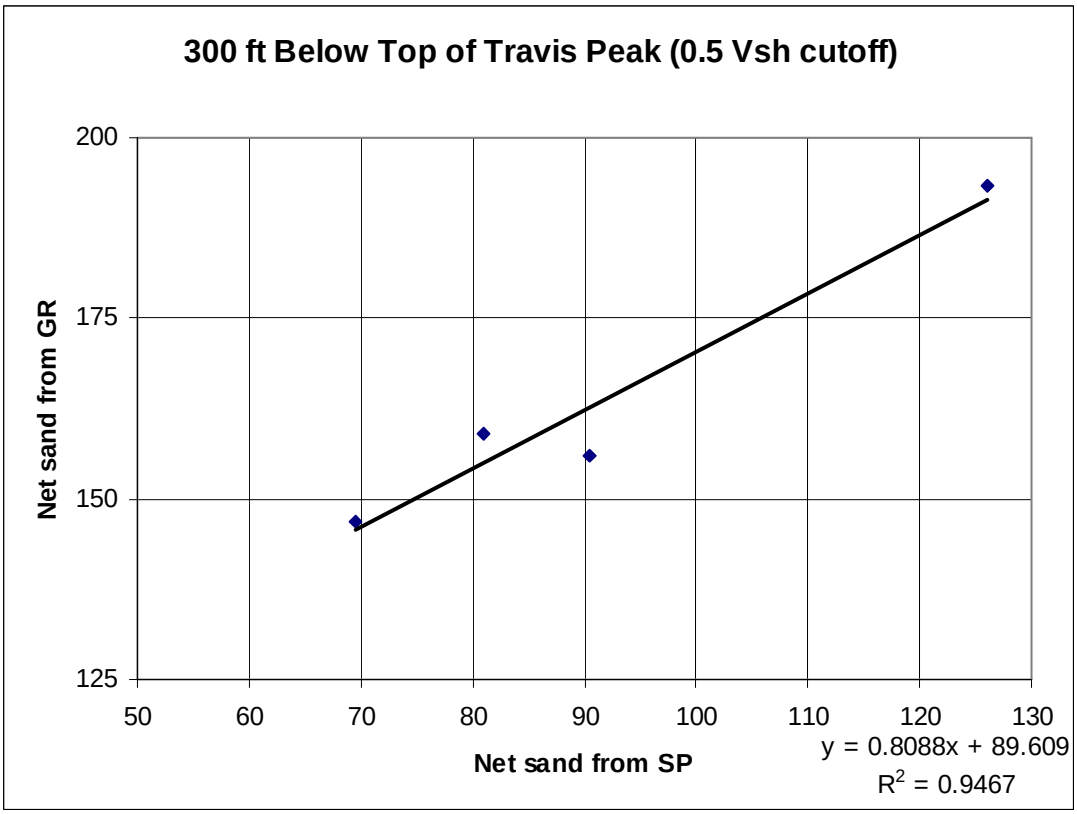

Figure 32. Relationship between net sandstone thicknesses calculated from SP and from GR in the upper 300 ft of the Travis Peak formation (0.5 V_{sh} cutoff).

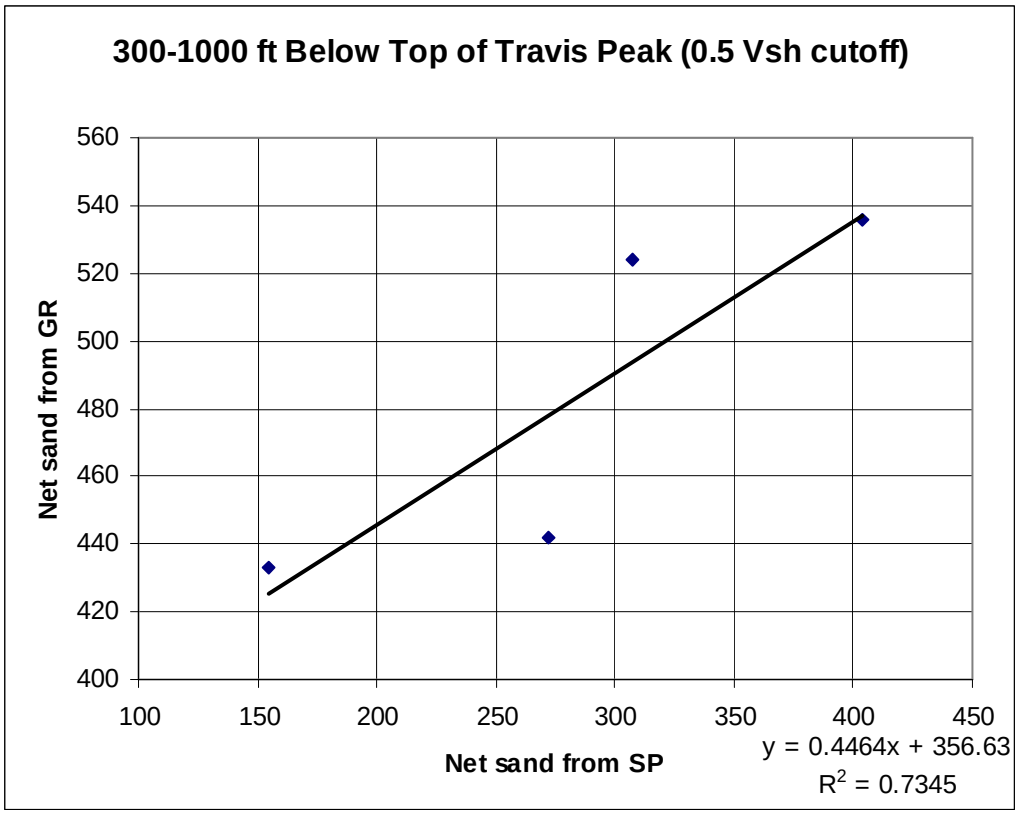

Figure 33. Relationship between net sandstone thickness calculated from SP and from GR the interval 300 to 1,000 ft below the Travis Peak (0.5 V_{sh} cutoff).

Using the net sandstone thicknesses determination from 57 digital and image well logs, I mapped net sand thickness in 300-ft interval below top of Travis Peak and in the 300 to 1,000-ft interval below the top of the Travis Peak (Figs. 34 and 35, respectively). A limitation on the reliability of these maps was the paucity of well control; in the southeast half of the study, only 6 wells penetrated the mapped TP intervals. In 300 ft interval below top of Travis Peak, the mean value of net sand thickness is 169.7ft (56.5%) (Fig. 34), whereas, in the interval 300 ft to 1,000 ft below top of Travis Peak, the mean value of net sand thickness is 488 ft (69.7%) (Fig. 35).

TP sandstones along the west margin of the ETB occur in belts that are dip-elongate (Figs. 34 and 35); they trend southeastward, orthogonal to the TP-Bossier isopach contours (Fig. 25), as well as the shelf margin trends identified in 2D seismic lines (next section). These sandbody geometries and trends are consistent with basinward transport of sediment by the Ancestral Red River fluvial deltaic system of described by Saucier (1985) (Fig. 2). Interpretation of 2D seismic data (next section) suggests that, in the study area, TP strata are predominantly fluvial deposits. I infer that these TP fluvial systems supplied sediment to deltas and submarine fans further basinward, in Grimes, Walker, and Houston Counties.

Well Log Response Characteristics

Well log discrimination of low- and high-sinuosity channel-fill sandstones is difficult. High sinuosity channels tend to be characterized by an upwards-fining profile that is serrate in gamma ray and spontaneous potential (SP) curves (Fig. 30). Low-sinuosity,

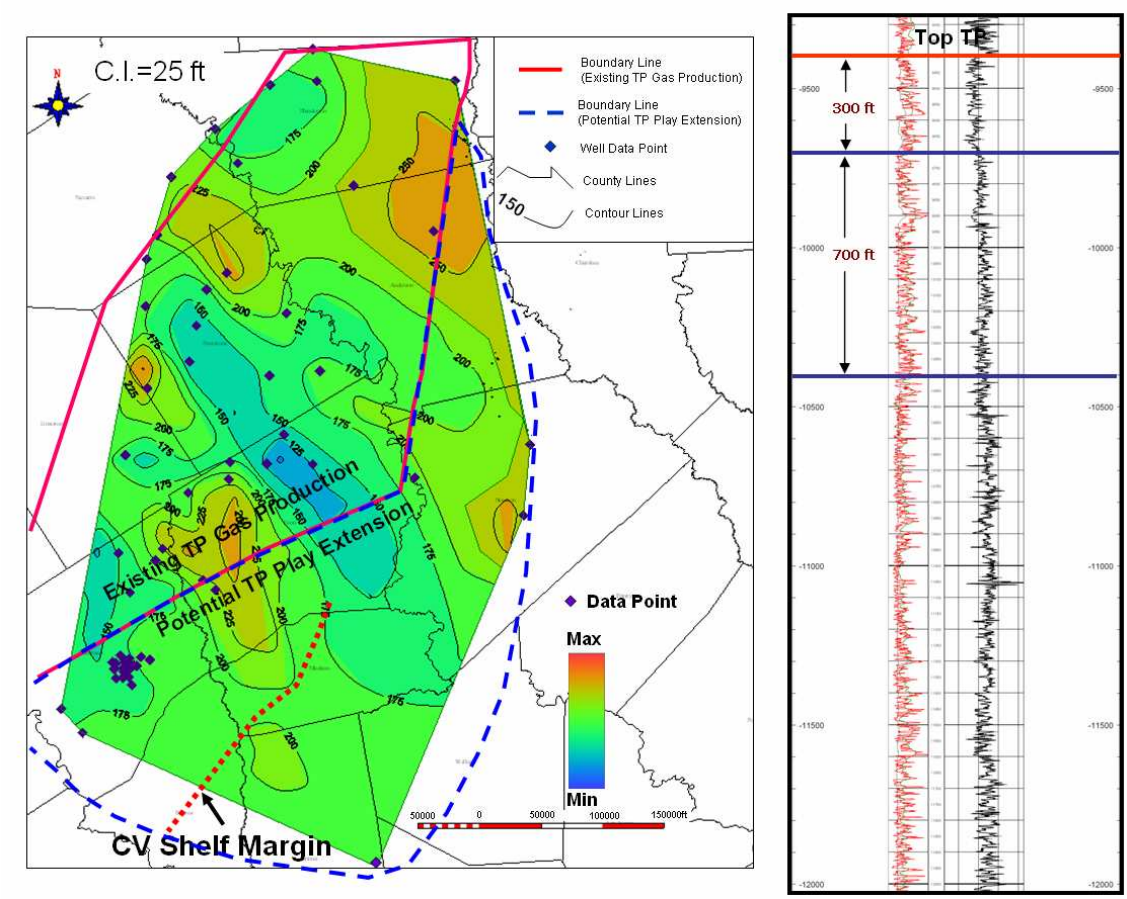

Figure 34. Net sandstone thickness (0.5 V_{sh} cutoff) of the upper 300 ft of the Travis Peak formation. Sandbodies trend northwest-southeastward, orthogonal to the paleoslope.

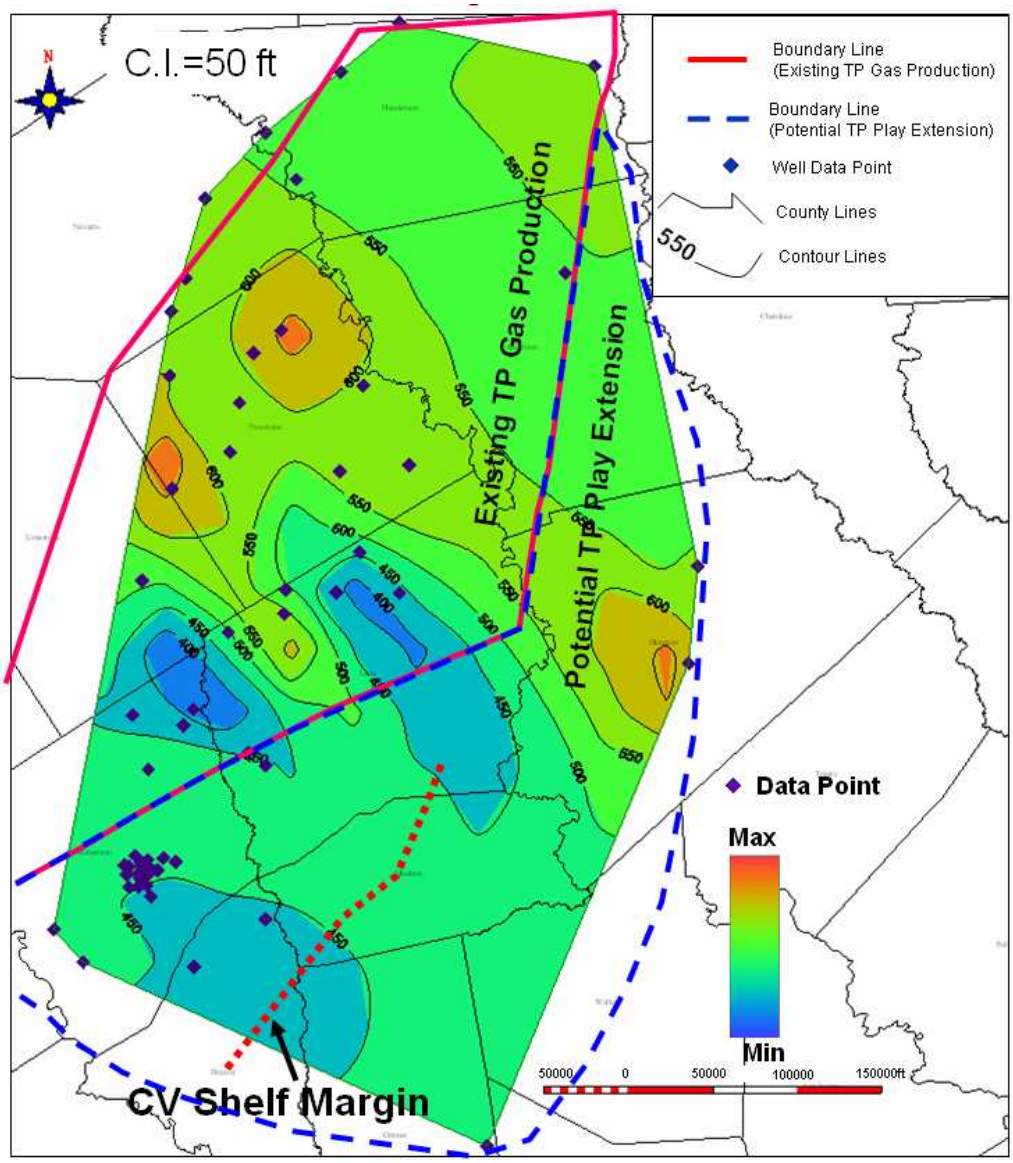

Figure 35. Net sandstone thickness (0.5 V_{sh} cutoff) of the interval from 300 ft to 1,000 ft below the top of the Travis Peak formation. Sandbodies trend northwestward-southeastward, orthogonal to the paleoslope.

stacked, channel-fill sandstones commonly have a blocky well log profile that also may be strongly serrate (Davies ,et al., 1991). Well log responses in channel-fill sandstones may be complicated by the presence of shale-clast conglomerates, which result in an increase in gamma ray response and a decrease in SP.

Structural Features

Within the study area, 244 wells penetrated the top of Travis Peak formation. Well logs were integrated with seismic data to map the top of Travis Peak formation across the study area. The subsea depth to top of TP ranges from (-)5000 ft to (-)17,000 ft and is characterized by monoclinal dip to the southeast (Fig. 36). Structure contours in southern Anderson County suggest that there may a structural nose in that area.

From the velocity graph (Fig. 11), the time and depth for top of Travis Peak have good relationship. A subsea structure map is contoured on the TP reflector from seismic line (Fig. 37). The Travis Peak reflector is indicated by the second strong, continuous reflector below the Pettet (Fig. 10). Depth to Top of TP ranges from higher than -5300 to an estimated -17300 feet, and is generally characterized by monoclinal dip to the southeast (Fig. 37). I combine structure contour map made from well logs with structure contour map made from seismic lines to generator the Subsea structure contour of Top of Travis Peak (Fig. 38). The map is very same with the map made from well logs. But the control area is bigger.

Map Sand isopach maps from the top of Travis Peak to the top of the Lower Travis Peak (Fig. 39), based on well log correlations, reveal that upper Travis Peak depocenter

is characterized to the northwest. The map shows a distinct sediment thickening associated with the basin. Maximum sediment thickness for the mapped interval across the study area is between 1200 and 400 feet.

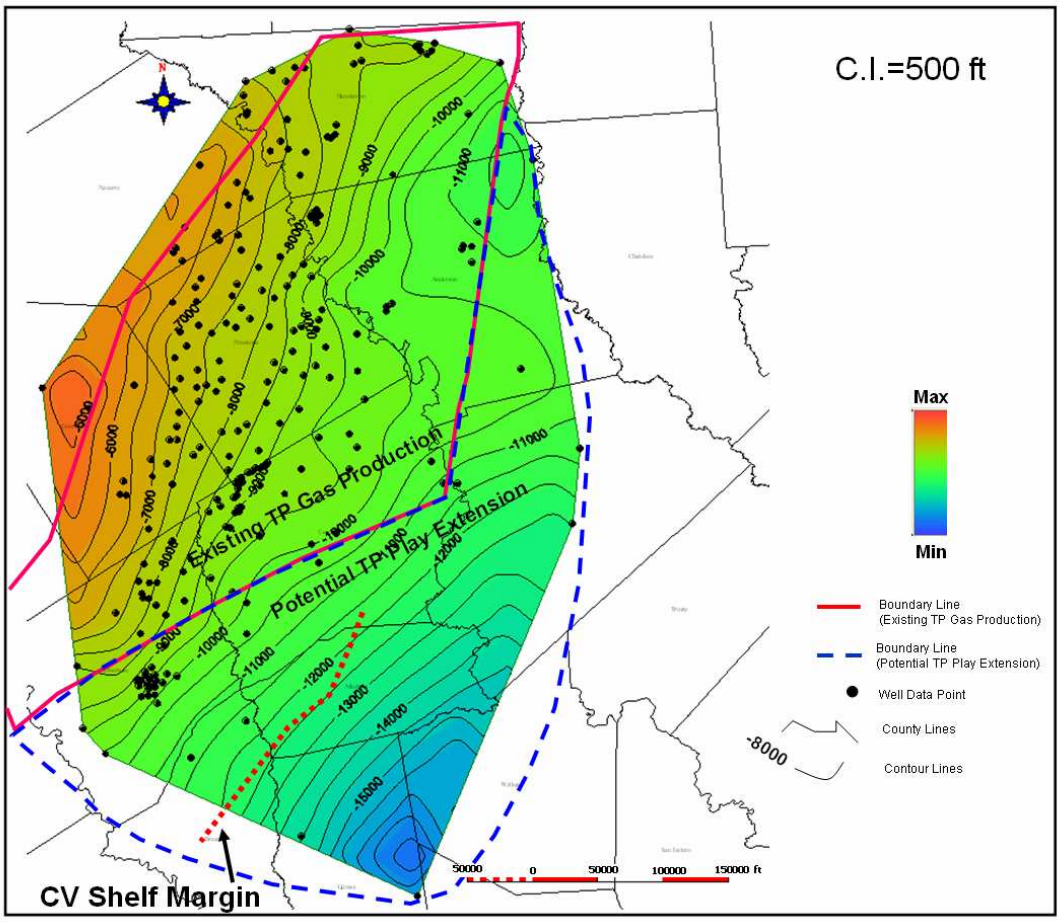

Figure 36. Structure, top of Travis Peak, made with well log data (S.L. datum).

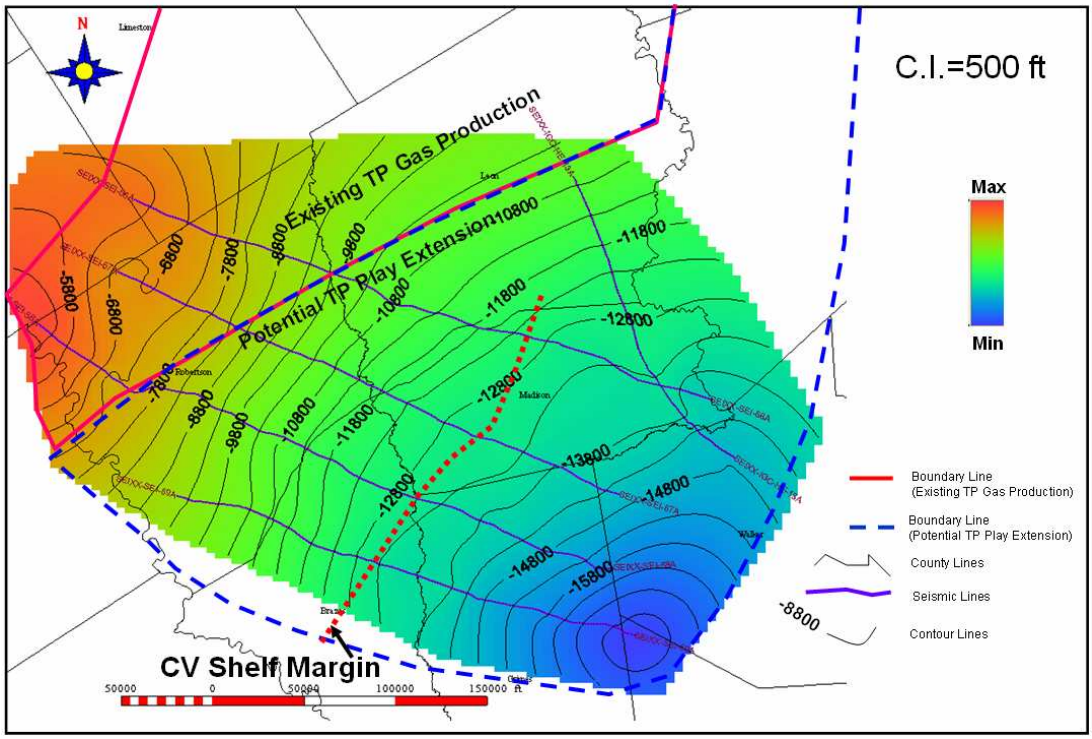

Figure 37. Structure, Top of Travis Peak, made with seismic data (S.L. datum).

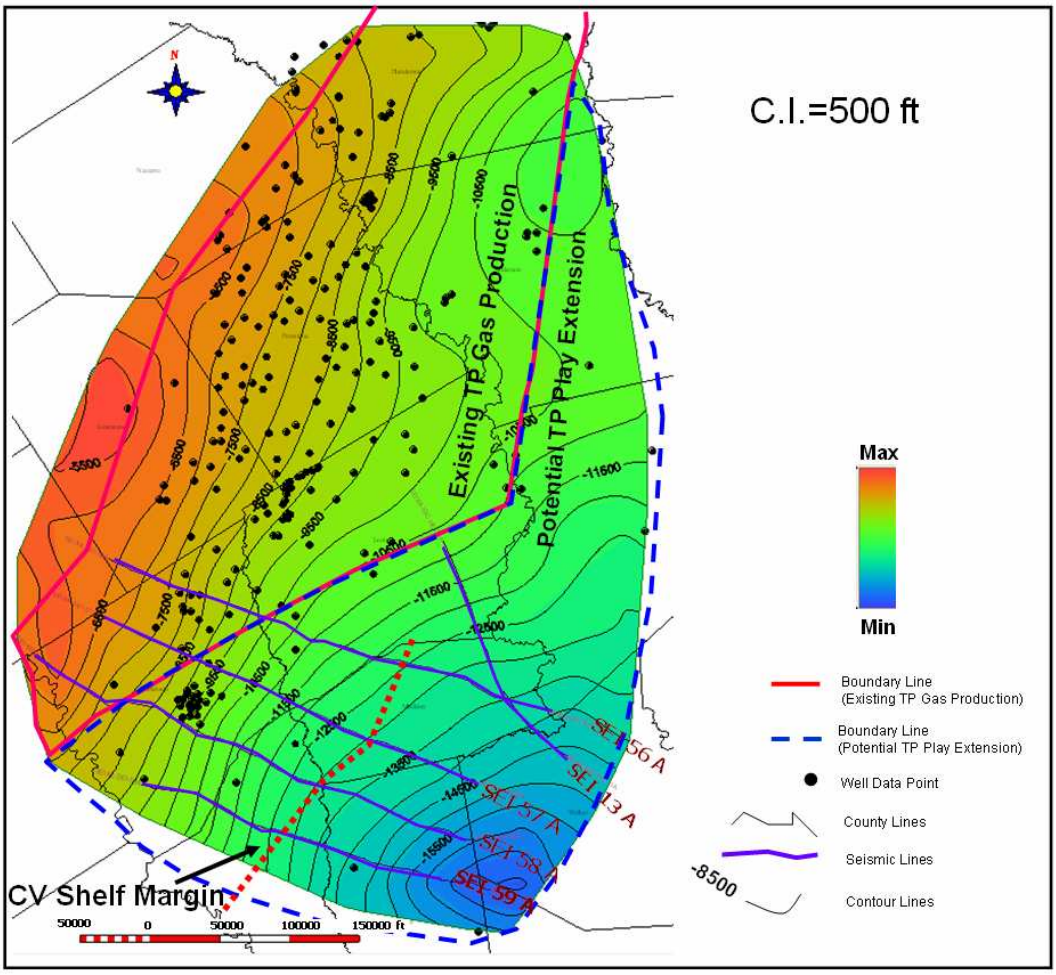

Figure 38. Structure, top of Travis Peak, made from seismic and well log data (S.L. datum).

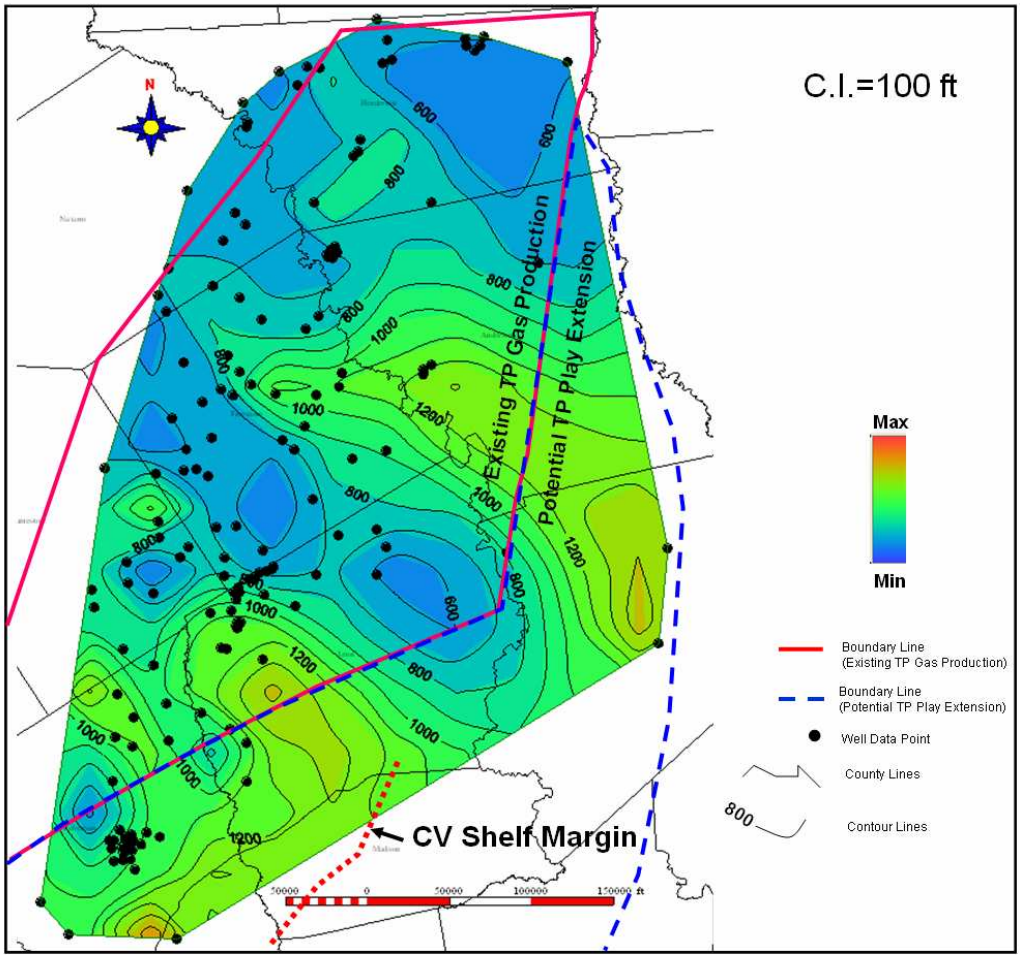

Figure 39. Isopach map, upper Travis Peak. See Figure 27 for "upper" Travis Peak definition.

Pettet and Pine Island Formations

The structure map of the top of the Pettet formation (Fig. 1) shows that the unit dips basinward (Fig. 40). The Pettet isopach map indicates that the formation also thickens basinward (southward) from Limestone to Houston and Madison Counties, where the Pettet thickness exceeds 550 ft (Fig. 41).

The Pettet is composed shallow, open shelf oolitic and skeletal limestones deposited during a slow eustatic sea level rise that began during late Travis Peak time (Bushaw,

1968). Continued eustatic sea level rise during Pine Island time led to deposition of extensive, open-shelf shales and micrites with abundant planktonic organisms. These sediments provide an excellent seal for underlying Pettet carbonate reservoirs.

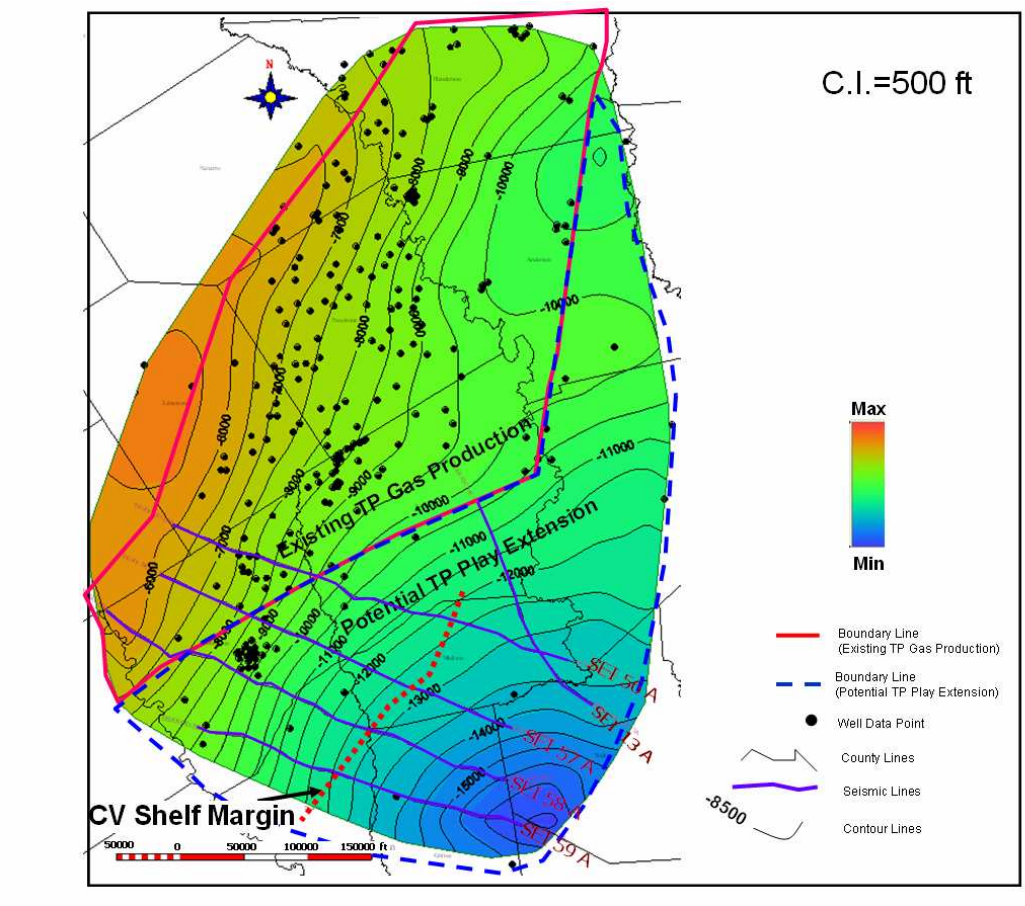

Figure 40. Structure, top of the Pettet formation (S.L. datum). The Pettet formation dips southward. An anticlinal nose plunges eastward in southern Anderson County.

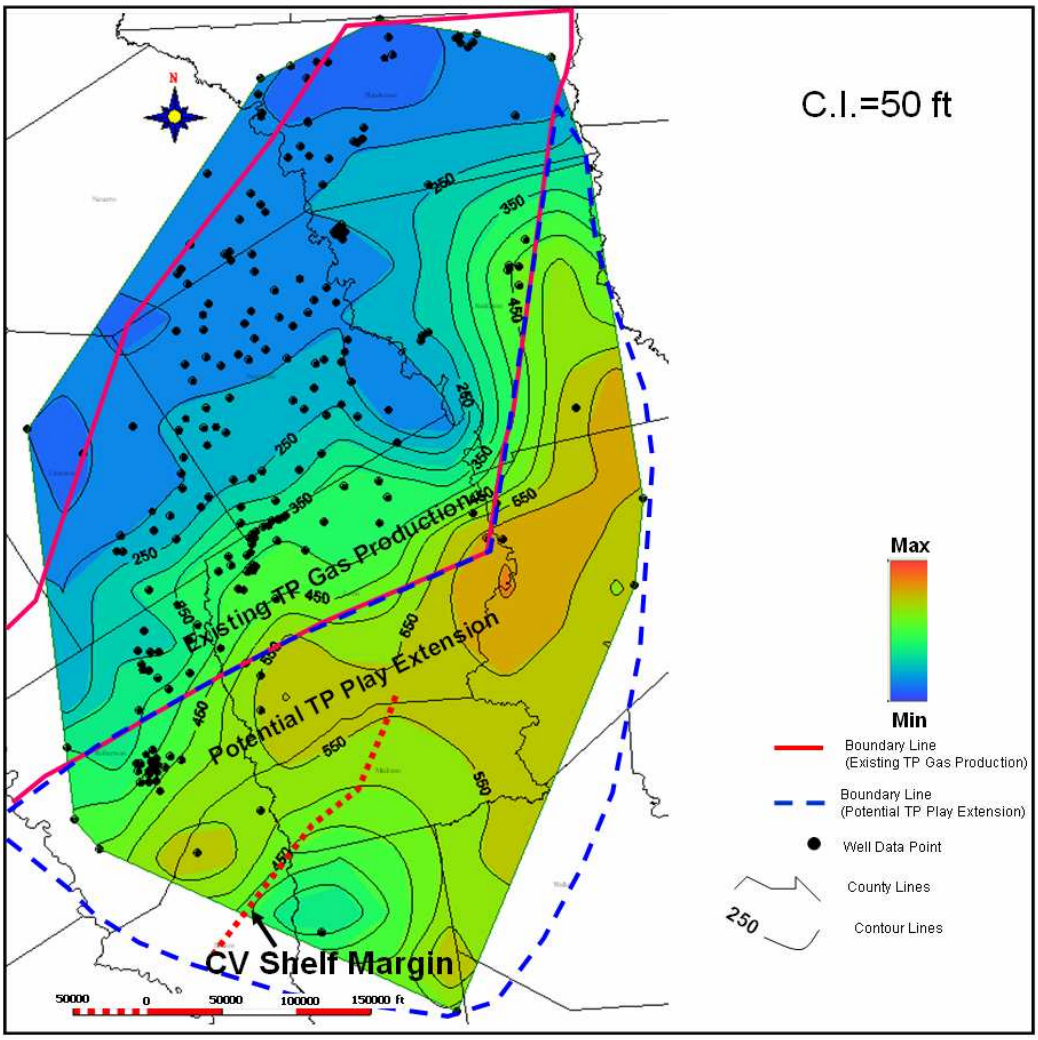

Figure 41. Pettet formation isopach map. The Pettet thickens from approximately 150 ft in Limestone County to more than 600 ft in Houston County.

Seismic Stratigraphic Analysis

Five 2D seismic lines from SEI were available for structural and stratigraphic analysis (Fig. 7). With permission of SEI, ConocoPhillips, provided these seismic lines along with their preliminary picks of the base of Louann Salt, Knowles Limestone, and Travis Peak and Pettet tops. I reinterpreted these horizon picks and evaluated stratigraphy of the

Louann Salt to TP interval. The limited seismic coverage for the area restricted use of these data for stratigraphic analysis, but they provided important insights, especially where well log data were sparse. For this discussion, I used Line SEI-58 A (Fig. 42) to describe the major structural and stratigraphic features in the study area.

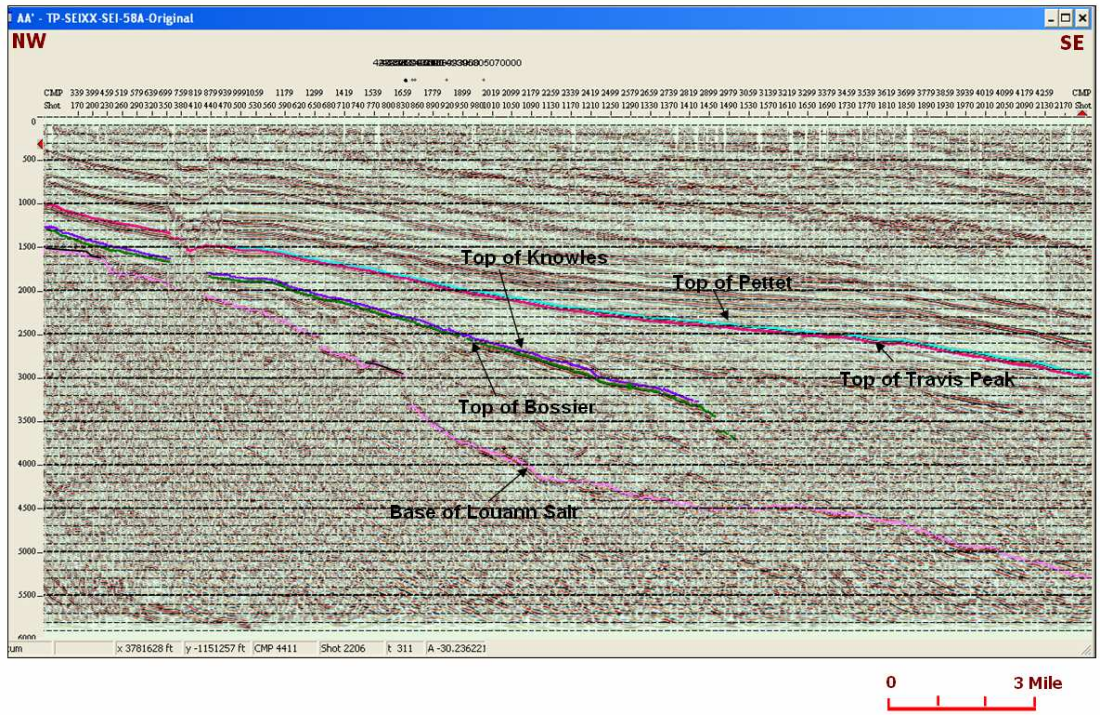

Figure 42. Seismic line SEI-58A, showing base of Louann salt and Bossier, Knowles Limestone, Pettet, and Travis Peak formation tops. See Figure 7 for location.

For this study, I characterized regional and local structural features and stratigraphy of units underlying the TP, because they affected TP depositional systems and hydrocarbon traps. Three depositional packages were identified in the seismic lines. These are the CV/ Bossier/Smackover, Cotton Valley/TP, and Travis Peak/Cotton Valley, undifferentiated (Fig. 44).

The CV/Bossier/Smackover interval is a thick package of clastic and carbonate sediments deposited above Louann Salt. Weight of these and overlying sediments mobilized the salt, which led to deformation of the overlying sediments. A well defined upper Bossier shelf margin is present at the top of this unit (Fig. 44). Internally the Bossier/Smackover trend is highly deformed, owing to salt movement. There is less deformation the updip than in the downdip region, where stratigraphic analysis is impossible due to extreme deformation and indistinct reflectors.

The lower Cotton Valley records onlap that includes buildup of the Knowles Limestone. Davidoff (1993) (Fig. 43) mapped the Knowles as an extensive lower Cotton Valley reef deposit as much as 1,200 ft thick in the in this area. Following Knowles deposition Cotton Valley fluvial-deltaic systems prograded basinward, depositing a thick sequence of clastic deltaic, shelf, slope and basin deposits (Fig. 45, Package 2). Deltaic clinoforms of this package are sequentially offset basinward, and updip, they seismic reflectors become indistinct at the fluvial-deltaic interface.

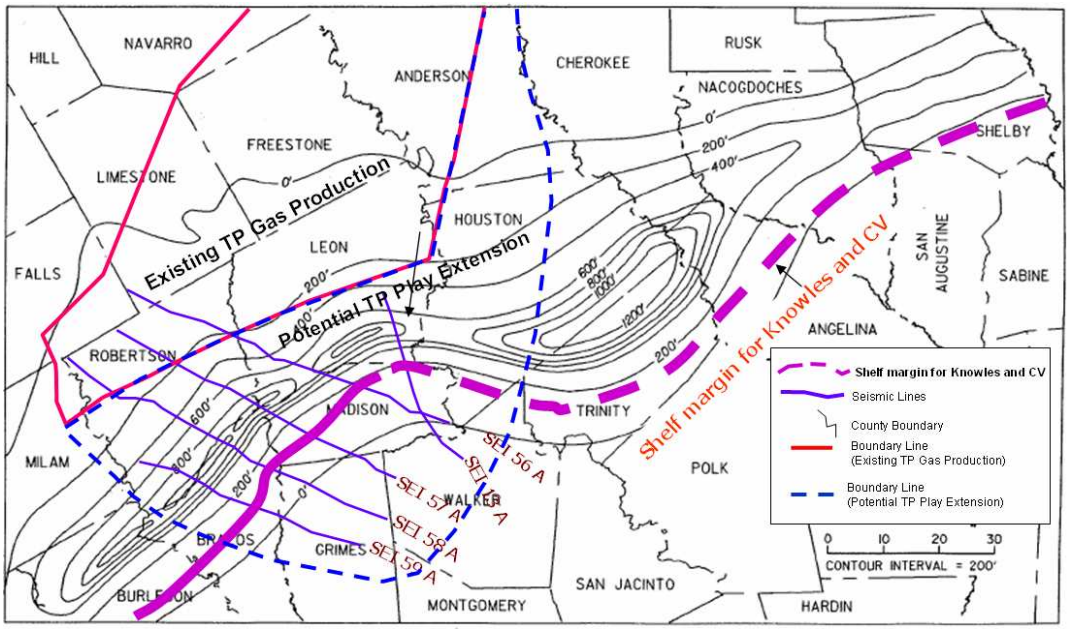

Figure 43. Isopach map showing distribution for the Knowles Limestone (from Davidoff, 1993).

The uppermost package (Fig. 45, Package 3) is comprised of upper Cotton Valley and TP fluvial sediments. This interval is sand rich and generally lacks continuous or thick shales. As a result, there is little acoustic impedance contrast, and seismic reflectors are weak and discontinuous. However, a weak but continuous reflector near the top of this interval may be the boundary between the upper and lower TP slices mapped above. Because there are few well logs for the downdip part of the study area and because no seismic reflectors mark the TP/Cotton Valley boundary, I could not recognize this boundary. However, weak reflectors in Package 3 in the downdip area are parallel to the TP top with no indication of clinoforms that suggestive of deltaic deposition. Therefore, I infer that the upper part of Package 3 represents TP deposits of a

fluvial system that supplied sediments to deltas further to the southeast in Grimes, Walker, and Houston Counties.

Louann salt deformation caused several structural features that may provide hydrocarbon traps. These include the Mexia Fault Zone, folds associated with salt pillows or domes, and minor faults that extend from Package 1 and 2 and which may be hydrocarbon migration pathways (Fig. 44).

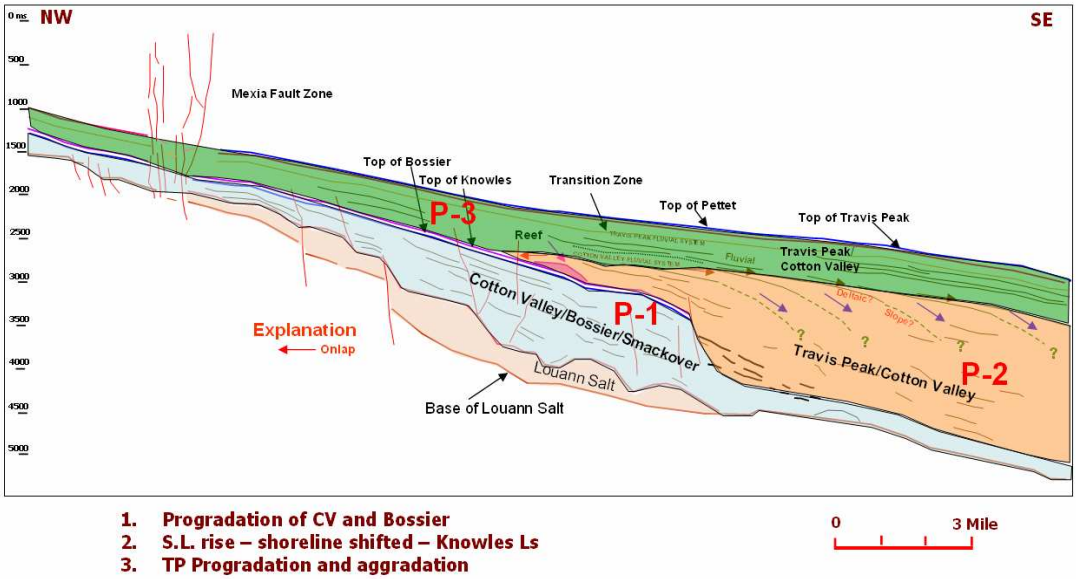

Figure 44. Three major stratigraphic packages were interpreted in line SEI-58A (Figure 42). These are the Bossier/Smackover, Cotton Valley, and Travis Peak/Cotton Valley packages.

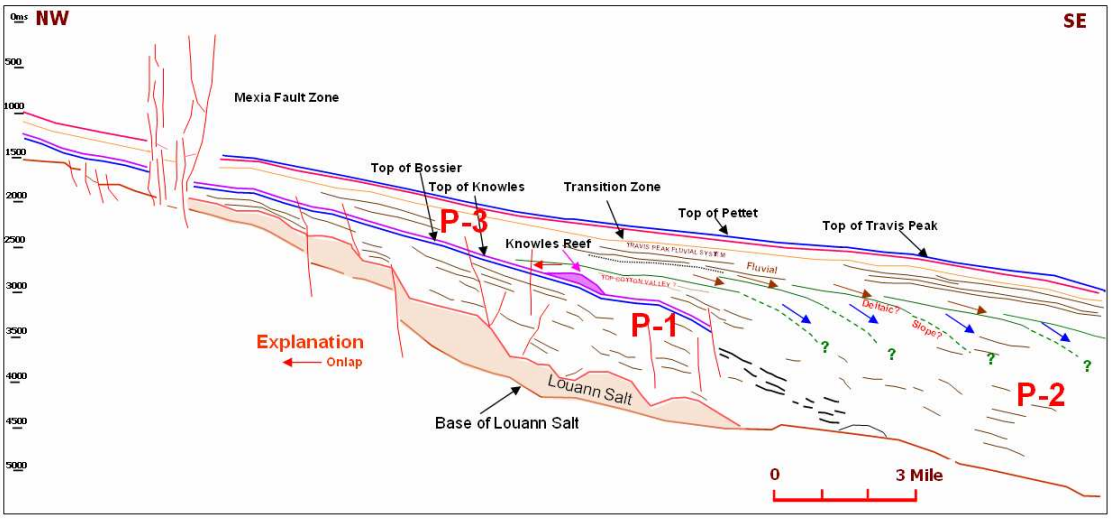

Figure 45. Detailed Interpretation of line SEI-58A (Figure 7).

PRESSURE AND TEMPERATURE ANALYSIS

Pressure Analysis

Commonly, formation pressure gradients are calculated using initial shut-in pressures. Fluid-pressure gradient (FPG) in pounds per square inch/foot (psi/ft) is usually used to evaluate the pore pressure or reservoir pressure. In freshwater reservoirs, 0.43 psi/ft is the normal FPG. For very saline water reservoirs, the FPG will be higher – approximately 0.50 psi/ft. If the FPG exceeds 0.50 psi/ft in a fresh to moderately saline water reservoir, the reservoir is considered to be significantly overpressured. Very saline waters reservoirs are considered to be significantly overpressured if FPG exceed 0.55 psi/ft (Spencer, 1987). In the ETB, TP water salinity is approximately 170,000 parts per million (ppm) total dissolved solids (TDS) (Dutton and others, 1993). Thus, reservoir water salinity is considered to be high, and if the FPGs exceed 0.55 psi/ft, these reservoirs should be considered to be significantly overpressured.

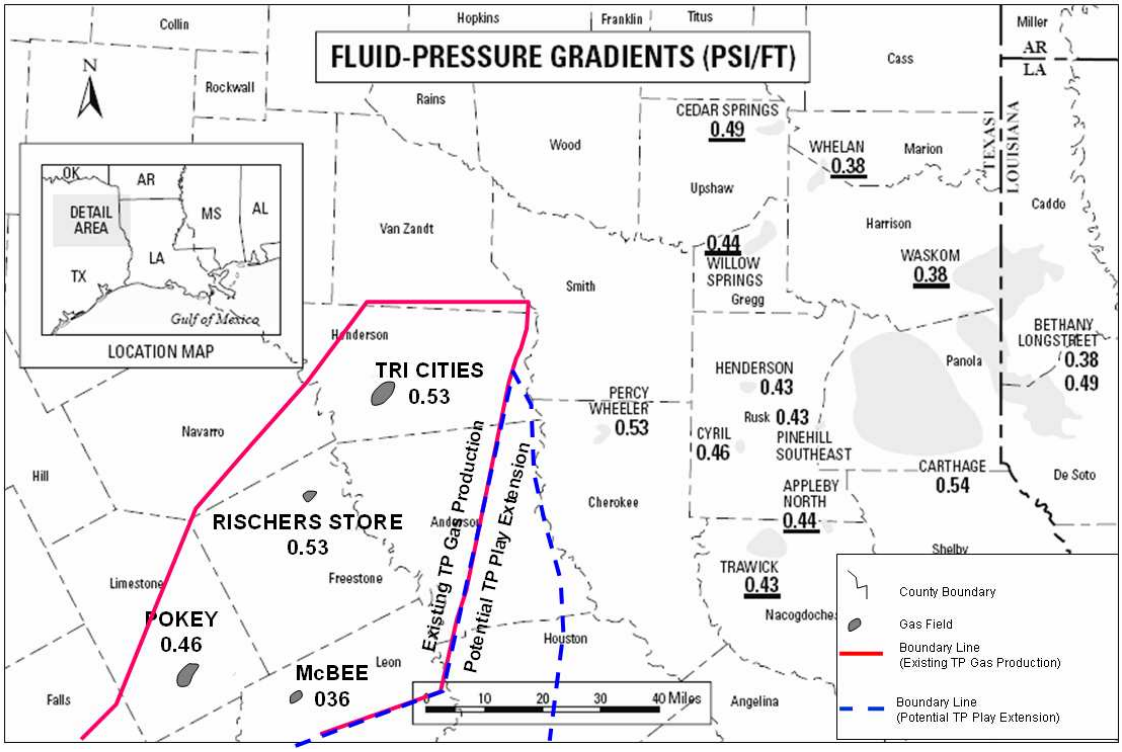

Figure 46. Fluid-pressure gradients in the East Texas Basin. (Modified from Herald, 1951; Shreveport Geological Society Reference Reports, 1946, 1947, 1951, 1953, 1958, 1963, 1987; Kosters and others, 1989; Shoemaker, 1989; and Bebout and others, 1992)

Previous workers assessed TP formation pressures for in Tri-Cities, Rischers Store, Pokey and McBee fields along the west flank of the ETB (Fig. 46) (In Herald (1951), Shreveport Geological Society Reference Reports (1946, 1947, 1951, 1953, 1958, 1963, 1987), Kosters and others (1989), Shoemaker (1989), and Bebout and others (1992). These data were collected by the Bartberger (2003), who calculated FPGs from initial shut-in pressures. Based on the fluid-pressure-gradient cutoff value of 0.55 psi/f, all TP sandstone reservoirs in west flank of East Texas Basin are normally pressured (Fig. 46). Tri-Cities TP field has a slightly elevated FPG of 0.53 psi/ft. Rischers Store and Pokey fields are normal pressure (~40 psi/ft), and McBee field has a subnormal FPG of 0.36

psi/ft. Thus, limited data along the west margin of the ETB indicate that TP reservoirs are mostly normally pressured (Bartberger, et al., 2003). However, Bartberger, et al. (2003) indicated most pressure data available for his study are from sandstones within the upper 300 ft of the formation. Initial shut-in pressures were not available for the middle and lower TP Formation along the west flank of East Texas Basin. However, drilling mud densities can be used to evaluate reservoir pressure in survey studies (Shaker, 2003). To assess TP regional formation pressures along the west margin of the ETB, I recorded the mud density values from headers of 106 wells (Fig. 12, Appendix 1), regardless of completion formation. Mud density is reported as pounds per gallon (ppg); 1ppg = 0.0519 psi/ft pressure gradient (Laudon, 1996 chapter 6).

Some wells headers have mud density values recorded from several runs. In these cases, the deepest run data were used. I converted the mud weight unit from ppg to psi/ft and graphed mud density vs. depth (Fig. 47). Then, I calculated the pressure caused by the drilling mud. In the study area, mud density increases gradually to a depth of 12,500 ft. The pressure gradient above 12,500 is less than 0.549 psi/ft, which suggests normal formation pressure. Strata deeper than 12,500 ft were drilled with much higher mud density (greater than 0.549 psi/ft), which suggests the presence of overpressure. The structure map of the top of Cotton Valley Group (base of TP) (Finley, 1984; Fig. 4) indicates that most of TP formation is shallower than 12,500 ft in the study area,

Therefore, based on Finley's subsea base of Travis Peak structure map, I concluded that, in study area, the entire TP should be normally pressured. When mud densities bubble map (Fig. 48) is overlaid on the tectonic elements map (Fig. 5), it appears that

higher mud densities occur in the deeper part of the basin, and there is no apparent association of formation pressures with faults or salts structures.

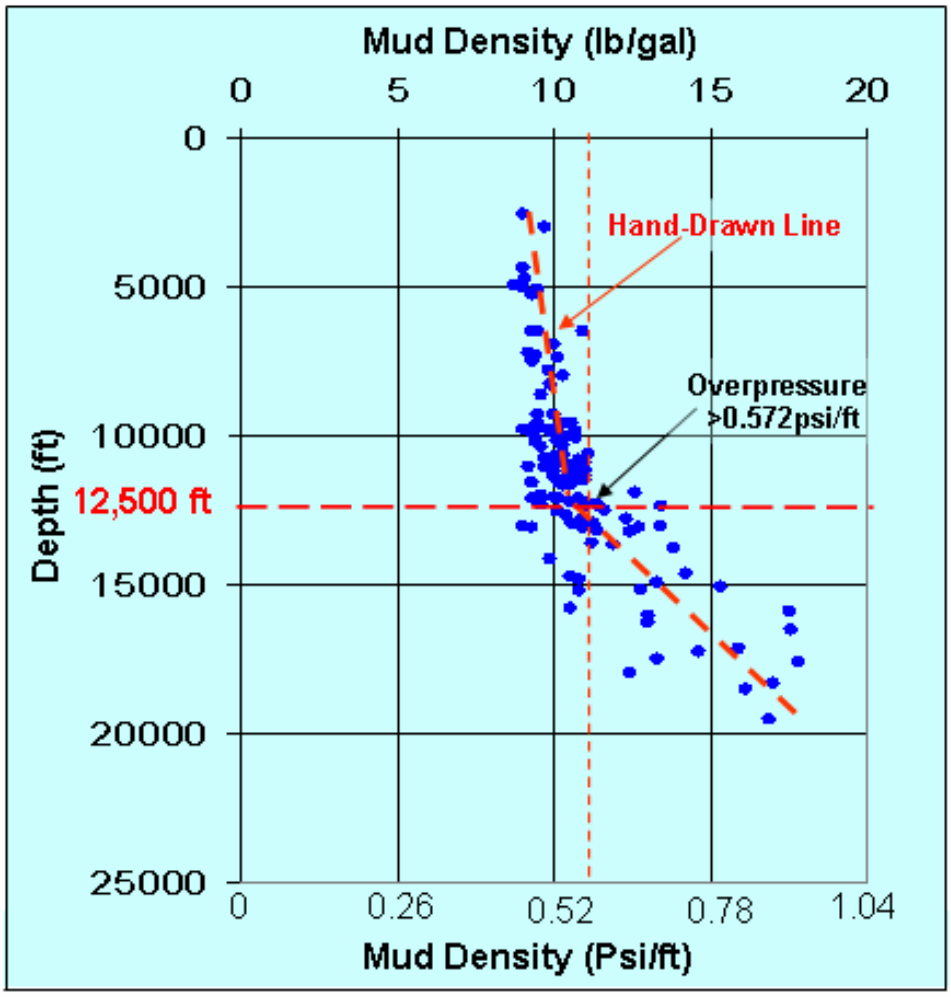

Figure 47. Mud density vs. Measure depth (Data from M.J. System 2005).

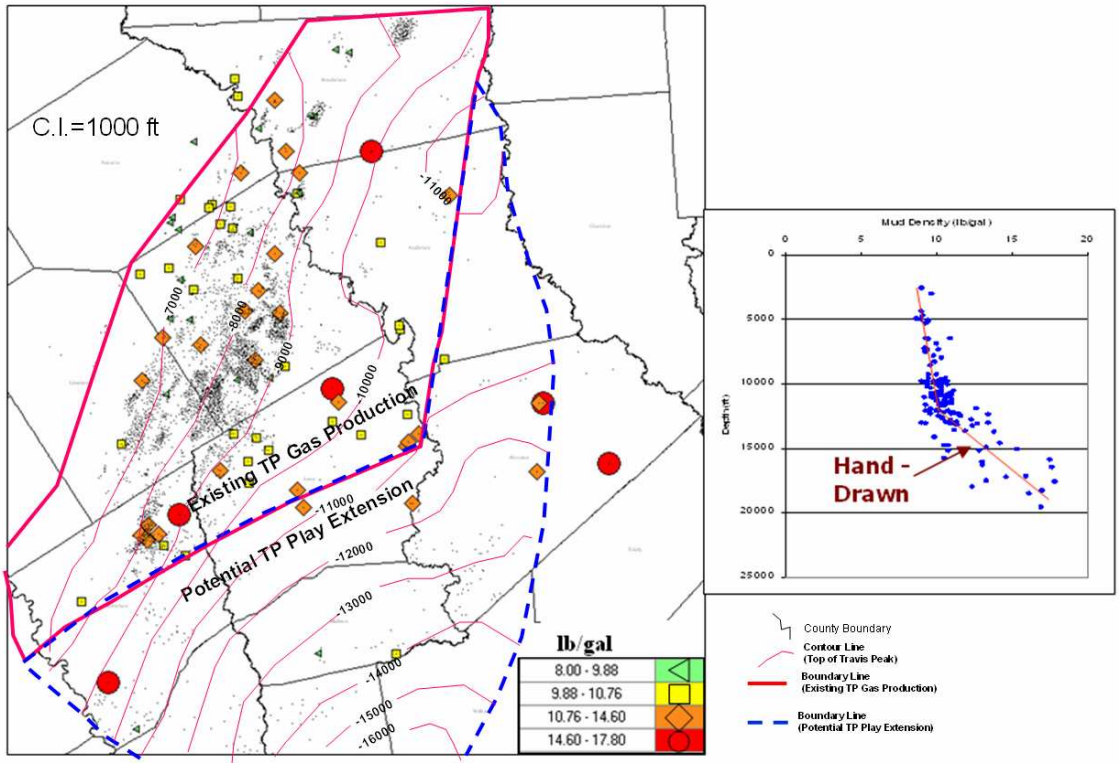

Figure 48. Mapped values and statistical analysis of mud weights, regardless of completion interval, west margin of the East Texas Basin; data are from headers of 106 well logs (Data from M.J. System 2005).

Temperature Analysis

To evaluate TP formation temperatures, I recorded bottomhole temperature (BHT) data from headers of 106 well logs (Appendix 1). If a well had several runs, I picked the deepest run to calculate the temperature gradient. The equation I used to calculate temperature gradient from bottomhole temperature was the Halliburton, GEN-2b Equation:

$$g_G = 100\left[\frac{T_{d2} - T_{d1}}{d2 - d1}\right]$$

g_G …… geothermal gradient

T_d …… temperature at depth d
d …… depth
I use the surface temperautre=66 ^{o}F

Using the calculated geothermal gradients for the 106 wells (Appendix 1), I plotted BHT vs. depth for the 106 wells and determined that the geothermal gradient is 1.55 °F/100 ft (Fig.49). This gradient is slightly less than that reported for the same general area by Davidoff (1993; 1.8 °F/100 ft), and it is considerable less than the temperature gradient reported for the Sabine Uplift area (2.1 °F/100 ft; Dutton, 1985).

The temperature gradient calculated for this area suggest that strata below 5,000 ft are mature for oil generation, and strata below 12,500 ft are well within the gas generation window, which means they are overmature for oil (Fig. 49). The pressure gradient analysis above indicated that strata deeper than 12,500 ft were drilled overbalanced (mud density greater than 0.549 psi/ft), which suggests presence of overpressure.

Upon combining mud density vs. depth plot and bottomhole temperature vs. depth plots (Fig. 49), it appears that 12,500 ft is a depth boundary between normal/overpressure strata, and it is the top of the gas generation window. It is probable that source rocks below 12,500 ft are in the gas generation window, which has resulted in hydrocarbon generation overpressure in the deeper strata, including the Bossier Shale and Smackover formation.

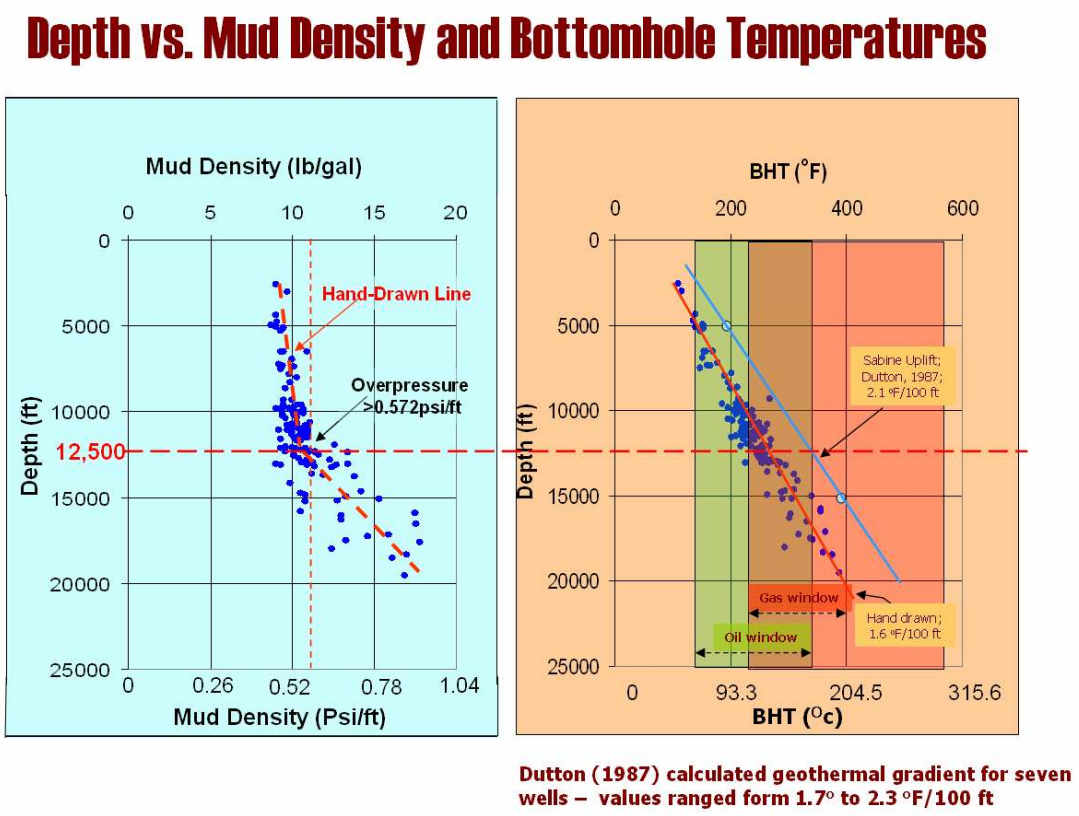

Figure 49. Depth vs. pressure gradient and bottomhole temperatures. Strata below 12,500 ft appear to be overpressured and in the gas generation window.

Overlaying the geothermal gradient bubble map (Fig. 50) on the regional structure map (Fig. 4) suggests that the geothermal gradient is higher near the Mexia Fault Zone than along the axis of the ETB.

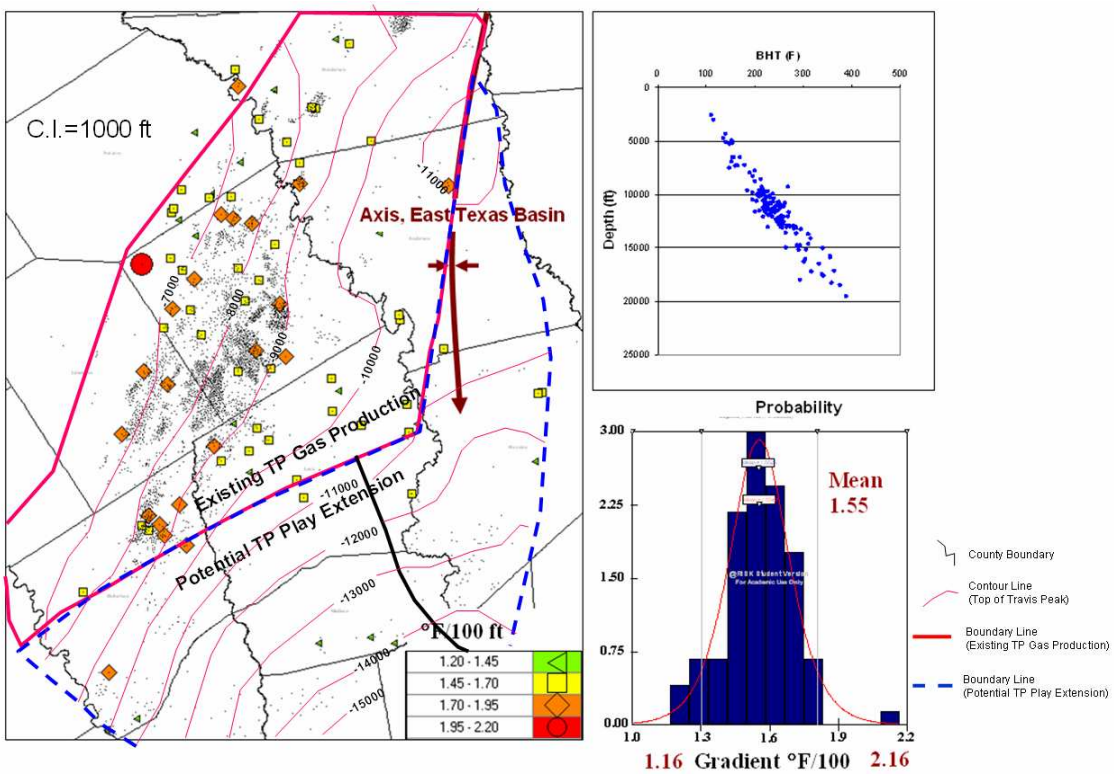

Figure 50. Mapped values and statistical analysis of geothermal gradients, regardless of completion interval or stratigraphic unit present at total depth; based on data recorded from headers of 106 wells. The maximum value of 2.16°F/100 ft is an outlier.

Temperature Gradient Uncertainty

In my study area, BHT values increase consistently with depth. The geothermal gradient ranged from 1.16 °F/100 ft to 2.16°F/100 ft, and the mean value is 1.55°F/100 ft (Fig. 50). As stated above, this gradient is considerably lower than that reported for 7 wells in the Sabine Uplift area, where the range was 1.7°F/100 ft to 2.3°F/100, and the mean was 2.1°F/100 ft (Dutton, 1987). One explanation for the difference may be higher heat flow in the Sabine Uplift. Another possible cause is that I did not filter or abandon well

header data that may have been incorrect or poor quality. A third reason for the difference may be the fact that Dutton (1987) corrected nonequilibration of borehole temperatures using the method of DeFord et al. (1976). However, Dutton (1987) did not explain the exact procedure used for nonequilibration corrections. But they stated that, after non-equilibrium correction for borehole temperatures, the geothermal gradient values were higher than before correction.

Ridgley et al. (2006) studied the geothermal gradient of the southwest part of the ETB. They evaluated several wells in the producing fields and applied correction factors for BHTs using the algorithms of Bebout et al. (1978) and Waples et al. (2004) to get a range of corrected geothermal gradients and BHTs. The range of corrections for BHTs was 33 to 38 ^{o}F. Their corrected temperature gradient for the TP formation is 2.5-2.6 ^{o}F/100 ft, which much higher than the geothermal gradient mean (2.1 ^{o}F/100 ft) in the Dutton (1987) study of the Sabine Uplift and my result (1.6 ^{o}F/100 ft) for the ETB.

It appears that the Bebout et al. (1978) method involved approximating thermal equilibrium using an empirical relation developed by Kehle (1971) to correct BHTs of the Wilcox Group:

$$T_E = T_L - 8.819\times10^{-12} D^3 - 2.143\times10^{-8} D^2 + 4.375\times10^{-3} D - 1.018$$

T_E …… equilibrium temperature, ^{o}F
T_L …… bottom-hole temperature from well logs, ^{o}F
D …… depth, ft

Ridgley et al. (2006) corrected log-derived temperatures in deep wells using

equations modified slightly from those of Waples and Ramly (2001). The correction method depends strongly on time lapsed since the end of mud circulation (*TSC*) and on drilling depth. In this method, the true subsurface temperature (Celsius) is given by:

$$T_{ture} = T_{surf} + f.(T_{meas} - T_{surf}) - 0.001391(Z - 4498)$$

f ..... $1.32866^{-0.005289TSC}$

T_{surf} ..... the seafloor or land-surface temperature (^{o}C)

T_{meas} ..... the measured log temperature (^{o}C)

TSC…… in hour's time since end of mud circulation

Z…… depth below seafloor in meters

Ridgley et al. (2006) did not state the process they used to determine lapsed time since mud circulation. However, they mentioned that the BHTs corrections of 33 to 38 ^{o}F resulted in increased temperature gradients of 0.2 to 0.3 ^{o}F/100 ft.

In summary, previous studies indicate that bottomhole temperatures should be higher than reported on well log headers. Because data were not available to correct BHTs, my geothermal gradient calculated from BHTs may be lower than the true value. If I apply the correction reported by Ridgely et al. (2006; 0.2 to 0.3 ^{o}F/100 ft), the geothermal gradient in the study area is 1.75- 1.85 ^{o}F/100 ft, similar to that reported for this general area by Davidoff (1993; 1.8 °F/100 ft).

TRAVIS PEAK PETROPHYSICAL ANALYSIS

Depositional systems govern sediment size, sorting, and packing, and thus, the original porosity and permeability of sandstone reservoirs. Reservoir characteristics of low-permeability gas reservoirs may result from depositional systems or from diagenetic modification of the original rock properties. Diagenetic alteration is strongly related to sediment composition, burial depth, and age of the reservoir.

Tight gas sandstone can be divided into the three types on the basis of pore geometry. These are sandstones with: (1) open, intergranular pores and with authigenic clay minerals plugging the pore throats; (2) quartz and calcite authigenic cements that occlude intergranular pores and which have large secondary pores that are connected by narrow slots; and (3) largely microporosity, because sandstone intergranular volume is plugged by detrital clay matrix. Generally, Type 2 sandstones are the most common tight gas reservoirs (Spencer, C. W, 1989; Soeder, D. J. and Chowdian, 1990). Type 1 sandstones are rare, and Type 3 sandstones are poor reservoirs because they have low porosity and permeability and typically have no visible macroporosity. (Dutton et al., 1993).

There are few published descriptions of TP reservoirs for the west margin of the ETB. For this study, ConocoPhillips provided a core report that included analyses of Travis Peak (Fig. 51), Cotton Valley, and Bossier, as well as younger strata, from a Robertson County well along the west margin of the ETB (GeoSystems LLP, 2003).

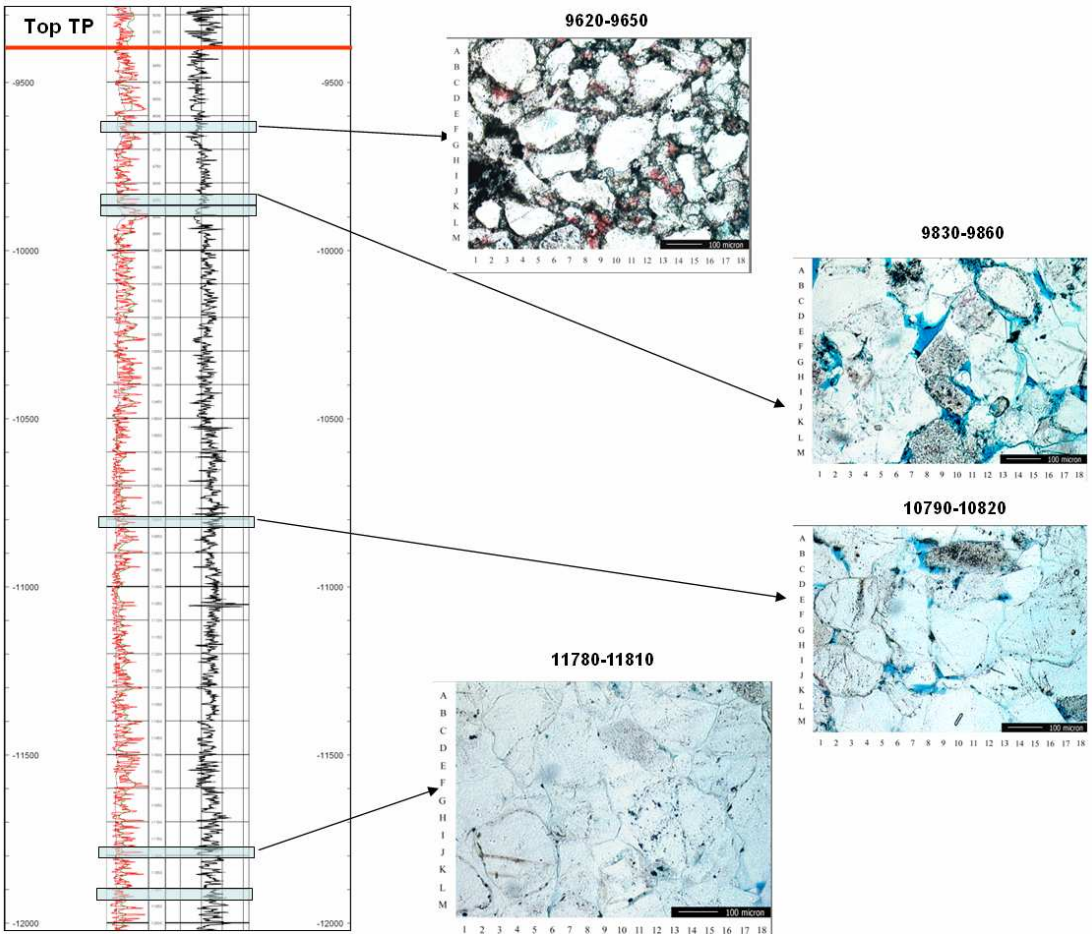

Figure 51. Six sets of drill cuttings samples were analyzed from the TP formation at depths of 9,620-9,650 ft, 9,830-9,890 ft; 9,860-9890 ft, 10,790-10,820 ft, 11,780-11,810 ft, and 11,900-11,930 in Robertson Co. Well name and location are proprietary.

Six cores reported on by GeoSystems (2003) were from TP sandstones. TP sandstones are fine-grained (0.14 to 0.21 mm), moderately well sorted, subangular to subrounded, quartz arenites and subarkoses (Figs. 52 and 53). Monocrystalline quartz is the most abundant framework component; minor framework components are polycrystalline quartz, chert (1-2%), and feldspars. Feldspars are dominantly plagioclase with lesser amounts of potassium feldspars. Lithic framework grains are shale, volcanic rock fragments, and minor schist rock fragments; ductile grains have some compactional

deformation.

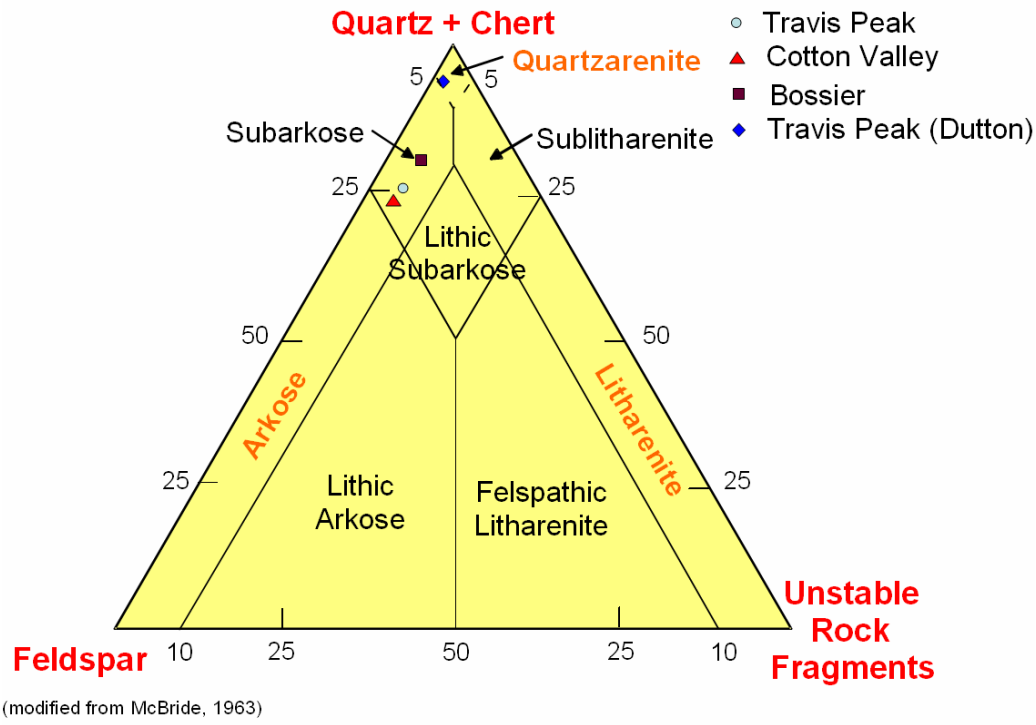

Figure 52. Travis Peak, Cotton Valley, and Bossier framework grain composition, one Robertson County well (GeoSystems LLP, 2003), west margin of the ETB, and Travis Peak average value for the Sabine Uplift area (Dutton and Diggs,1992).

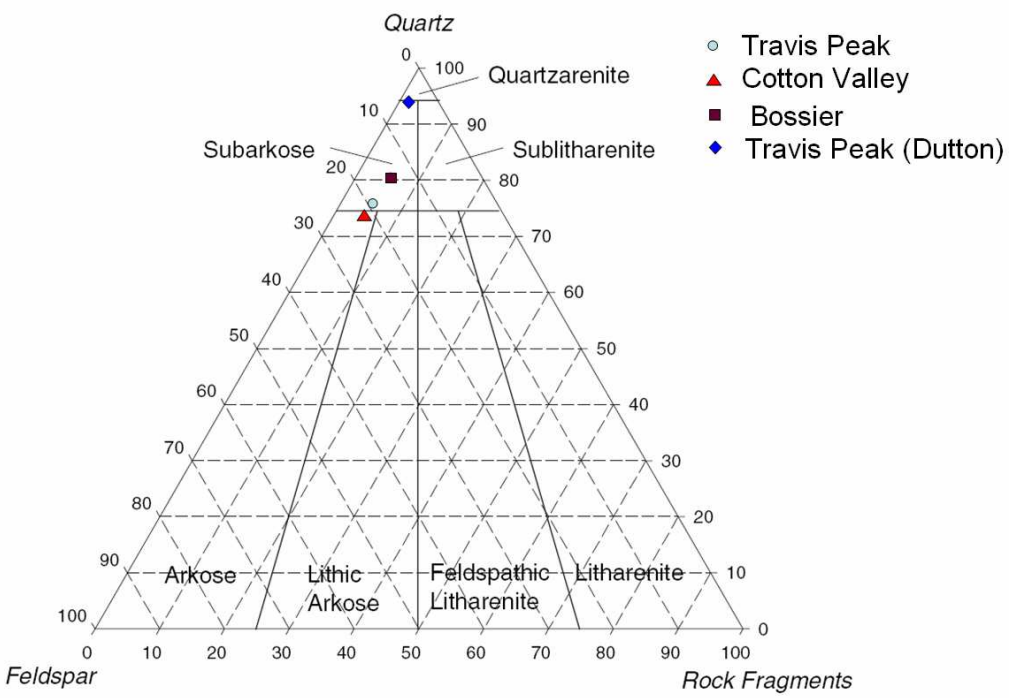

Figure 53. Average sandstone composition of x Travis Peak, Cotton Valley, and Bossier samples from one well in Robertson County (GeoSystems LLP, 2003).

There is incipient secondary porosity generation in form of partial feldspar dissolution. Cementation and other diagenesis events vary with depth, as noted in the following descriptions (Fig. 51).

In the interval from 9,620 – 9,650 (30 ft) euhedral dolomite totally replaced micritic lime mud that filled intergranular pores, resulting in reservoir image porosity of 2.7% and calculated permeability of 0.001 md (GeoSystems LLP, 2003).

TP sandstones in the: 9,830-9,860 ft; 9,860-9,890 ft; and 10,790-10,820 ft intervals have good reservoir quality. They are porous (12.4-13.5% image porosity) and moderately permeable (0.19-0.55 md calculated permeability). Pores are large, intergranular macropores with some smaller intergranular pores. There are some

dissolution pores in leached grains, and there is microporosity associated with clay cements (GeoSystems LLP, 2003).

TP sandstones Intervals from 11,780-11,810 ft and 11,900-11930 ft in these intervals are highly compacted and extensively quartz-cemented; clay cements are less abundant than silica. Clay is pore-lining chlorite that was insufficient to inhibit quartz overgrowths, and silica cement “mushroomed” over clay cements forming interlocking, euhedral quartz overgrowths that largely fill pores and pore throats. These sandstones have poor reservoir quality. Image porosity is low (5.2 – 6.7 md), and calculated permeability is 0.009 – 0.012 md. Porosity occurs as microporosity and as small dissolution pores; intergranular porosity is poorly developed. (GeoSystems LLP, 2003).

TP sandstones from the above Robertson County well along the west margin of the ETB are compositionally very similar to TP sandstones in the Sabine Uplift area In the Sabine uplift area. This suggests that the sandstones are from the same provenance and depositional system (Ancestral Red River), and it is possible that TP knowledge learned from Sabine Uplift studies can be used for make preliminary assumptions concerning diagenesis and reservoir quality of TP sandstones along the west margin of the ETB.

TP strata in the Sabine Uplift are fine-grained to very fine-grained sandstone, silty sandstone, muddy sandstone, and sandy mudstone (Dutton et al., 1991). The sandstones are quartzarenites and subarkoses. The average composition is approximate 95% quartz, 4% feldspar, and 1% rock fragments (Fig. 52). Travis Peak sandstones in the Sabine Uplift contain many authigenic minerals, but quartz is the most abundant porosity occluding cement.

Porosity and Permeability

With increasing burial depth, the volume of quartz cement and compaction increase, and secondary porosity decreases (Dutton, and Diggs, 1992). Clean Travis Peak sandstones average porosity decreases from 16.6 percent at 6,000 ft to 5.0 percent at 10,000 ft. For all Travis Peak sandstones (clean and shaly), average porosity decreases from 10.6 percent at 6,000 ft to 4.4 percent at 10,000 ft (Fig. 54). Average stressed permeability of clean Travis Peak sandstones decreases from 10 md at 6,000 ft to 0.001 md at 10,000 ft. For all sandstones, average stressed permeability decreases from 0.8 md at 6,000 ft to 0.0004 md at 10,000 ft (Fig. 55) (Dutton and Diggs 1992). As a result, many deep TP reservoir rocks are classified as low-permeability sandstones.

I compared the image analysis porosity and calculated permeability values for the Robertson Co. well report (GeoSystems LLP, 2003) with porosimeter porosity and stressed permeability results from Dutton et al. (1991) (Figs. 54 and 55). For the Robertson County TP samples, porosity and permeability variations with depth parallel but are higher than those of TP sandstones from the Sabine Uplift. Most likely, the higher values of the Roberson County analyses result from the different methods of determination. Sabine Uplift samples were analyzed under stress, whereas Robertson County sandstone porosity was determined by image analysis, and permeability was calculated. The anomalously low Robertson County samples were from the 9,620-9,650-ft interval, which has low effective porosity and permeability, owing to dolomite replacement of micritic matrix (Figs. 54 and 55).

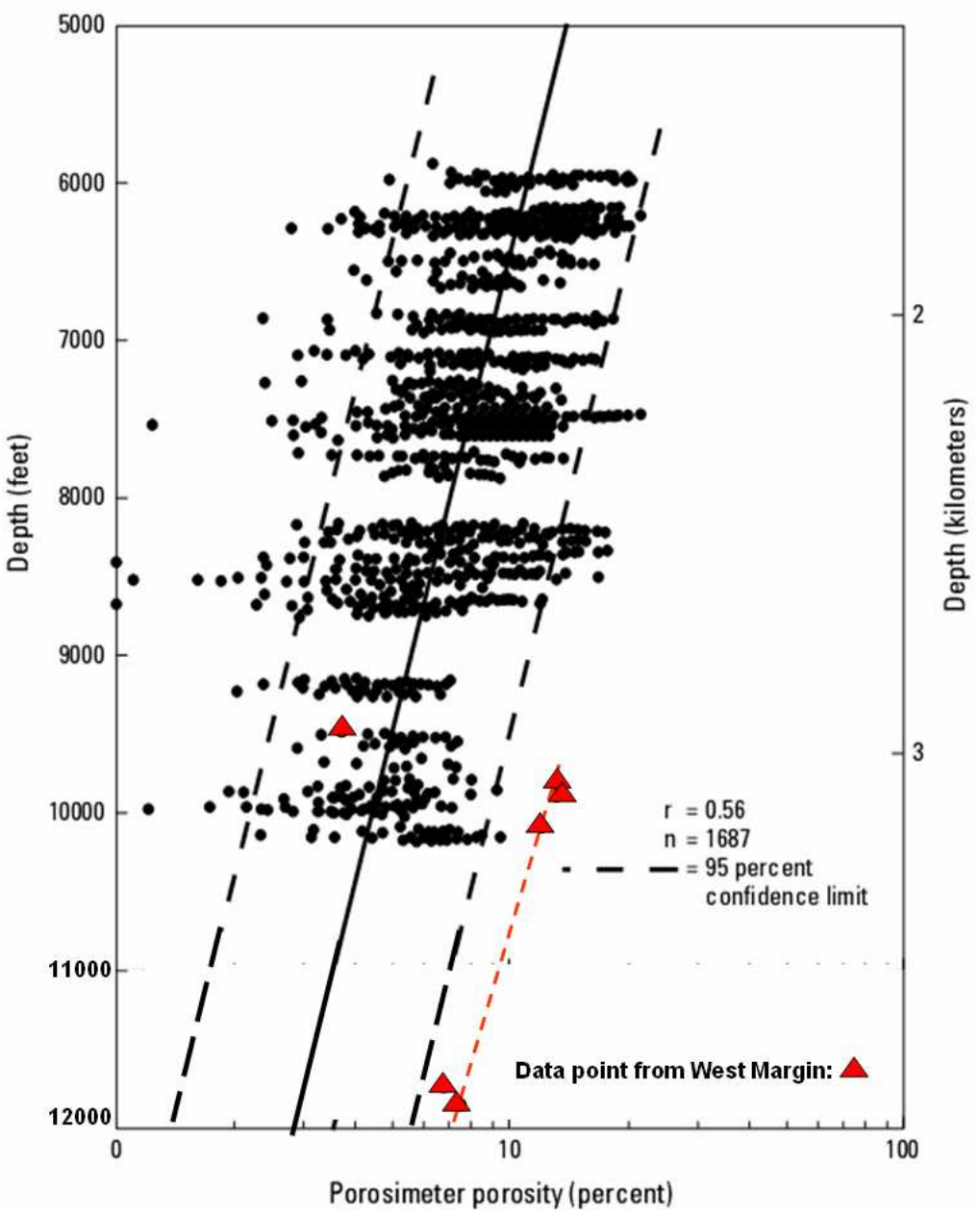

Figure 54. Semi-log plot of porosimeter porosity versus depth for 1,687 Travis Peak Formation sandstone samples, primarily from wells in the Sabine Uplift area (Fig. 2?), with superposed values of 6 samples from one well located in Robertson Co. (GeoSystems LLP, 2003), along the southern part of the west margin of the ETB (modified from Dutton et al., 1991). The Robertson Co. samples reported "image" porosity, which may explain the why porosity of those sample is approximately 3 times the mean value of Dutton et al. (1991) samples at similar depths.

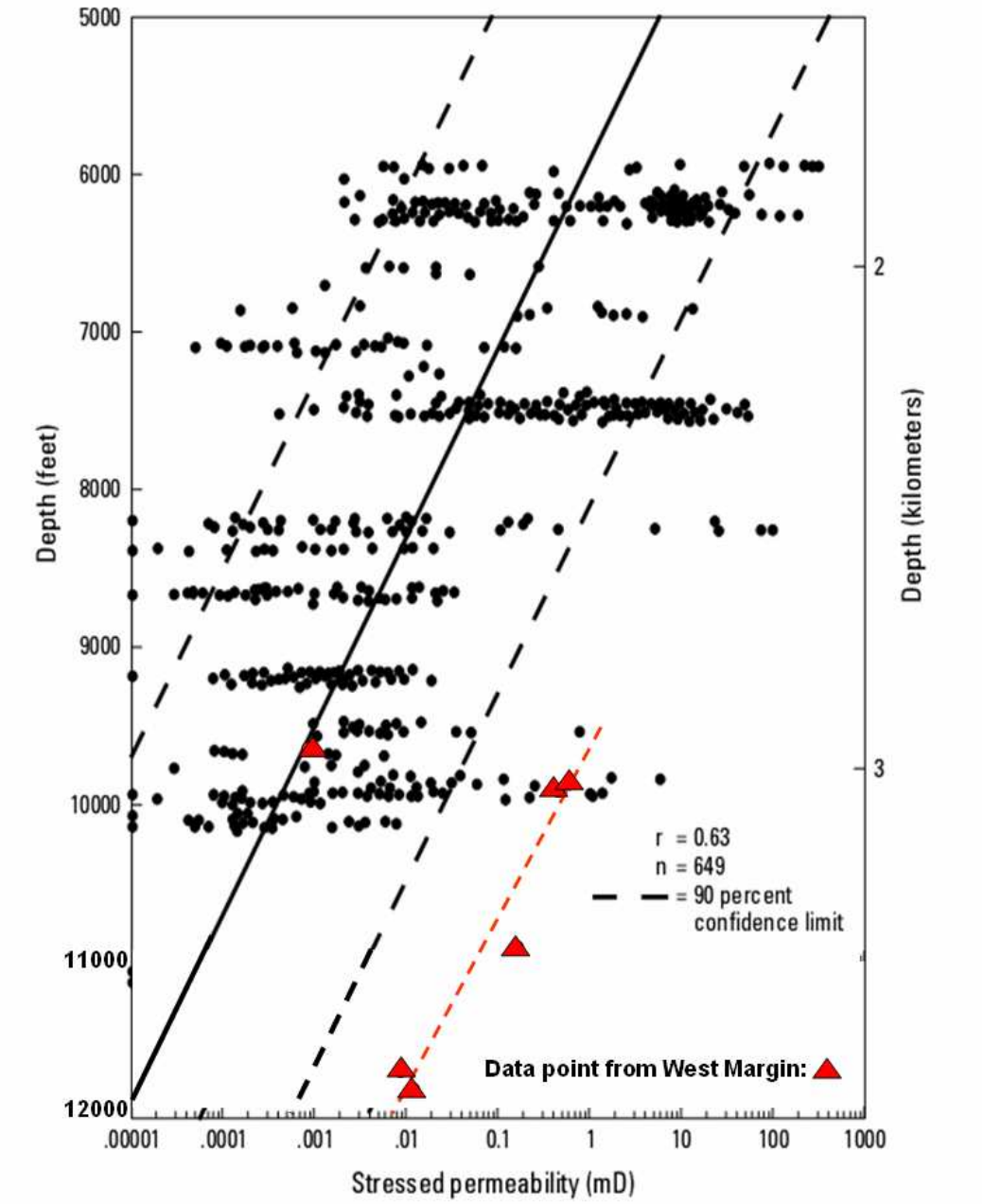

Figure 55. Semi-log plot of stressed permeability versus depth for Travis Peak sandstone samples from wells in east Texas (modified from Dutton, 1991), with overlay of permeability values of 6 Travis Peak samples from one well in Robertson Co. The Robertson Co. samples are "calculated" permeability, which may, in part, explain the why permeability of those sample is several orders of magnitude higher than the mean value of Dutton et al. (1991) samples at similar depths.

TRAVIS PEAK PETROLEUM SYSTEMS

Potential Hydrocarbon Source Rocks

It is improbable that TP shales are hydrocarbon source rocks. Shales interbedded with TP sandstone were deposited in floodplain and delta plain settings, where organic matter commonly was oxidized and was not preserved. Total organic carbon (TOC) measured in TP shales is generally less than 0.5 percent (Dutton, 1987) ref). Dutton (1987) concluded that oil and gas source rock in East Texas are probably prodelta and basinal marine shales of the Bossier formation and shales and carbonates of the Smackover formation (Fig. 1). Ridgely et al. (2006) concluded that kerogen types in the Bossier Shale in the ETB are uncertain owing to the overmature state of the strata, but most Type III, Type II, and Type IV kerogens appear to be most common. Total organic content (TOC) of the Bossier ranges between 1 and 5% in Limestone County (Newsham and Rushing, 2002).

Burial History and Hydrocarbon Generation

Dutton (1987) studied the burial history of the Travis Peak Formation in Nacogdoches County, Texas (south flank of Sabine Uplift; Figs. 4 and 56) and made a burial-history curve for the tops of the Travis Peak, Cotton Valley, Bossier, and Smackover formations, using the Ashland S.F.O.T. No. 1 well (Fig. 56). Maximum burial depth was approximately 11,000 ft for the Travis Peak and 13,000 ft for the Bossier Shale, a probable source rock for Travis Peak gas. The Bossier Shale reached thermal maturity for oil approximately 113 Ma and for gas approximately 105 Ma. There was a minor

period of uplift and erosion from approximately 102 Ma to 90 Ma. A second period of uplift and erosion extended from the middle Eocene (41 Ma) until the present. Today, the reservoir temperature of the top of the Travis Peak Formation in Ashland S.F.O.T. No. 1 well is approximately 129 °C (264 °F), which is in the oil generation window. The Bossier Shale top is 165°C (329 °F) and the Smackover formation top is 183 °C (361 °F). There is insufficient information to determine whether the Bossier and/or Smackover are still generating hydrocarbons and hydrocarbon overpressure, since uplift and cooling were initiated approximately 58 Ma (Fig. 56).

During Tertiary uplift between 58 and 46 Ma, approximately 1,500 ft of strata were removed across much of northeast Texas (Dutton, 1987; Laubach and Jackson, 1990; Jackson and Laubach, 1991). However, if the gas found in Travis Peak reservoirs was derived from Bossier Shale source rocks, migration of that gas into Travis Peak sandstones probably commenced between 65 Ma, and if the hydrocarbons migrated from Smackover, migration probably began 90 to 100 Ma. There may have been two stages of generation and migration of hydrocarbons into Travis Peak reservoirs. First, oil from Bossier or Smackover source rock may have migrated into Travis Peak sandstones traps. Later, with increased burial that caused Bossier and Smackover source rocks reached the gas window, a second hydrocarbon charge, this one gas, entered Travis Peak reservoir, and the earlier stage oil in the TP experienced deasphalting by the gas charge or/and, the oil was thermally cracked to gas upon deeper burial of the TP.

Hydrocarbon Migration and Trapping

Generally, Travis Peak sandstones reservoir are not overpressured. Bartberger et al. (2003) reasoned overpressure does not exist because the hydrocarbon charge was insufficient relative to volume of Travis Peak sandstone reservoirs available for storage. Other explanations may be the depletion of pressure caused by escape of hydrocarbon from the Travis Peak or cooling of strata, owing to Tertiary uplift and erosion.

The Bossier and Smackover formations are well within the gas generation window. Therefore, overpressure may exist in those formations.

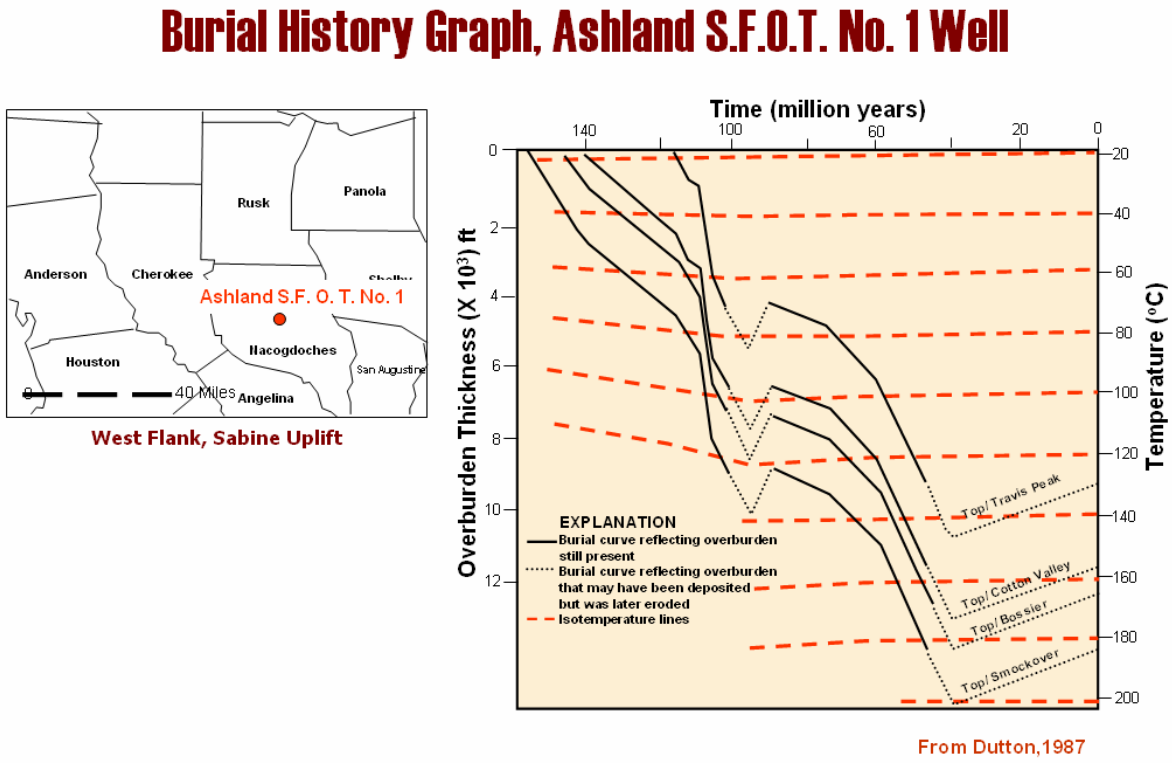

Figure 56. Burial-history curve, Ashland S.F.O.T. No. 1 well, in Nacogdoches County (south flank of the Sabine Uplift) (from Dutton, 1987)

HYDROCARBON TRAPS

Historic Travis Peak Traps

Common TP hydrocarbon traps in East Texas are structural, stratigraphic, and combination traps (Dutton, et al., 1991). Along the west margin of the basin, intermediate-amplitude salt structures are the primary element in forming traps. However, pinch-outs of permeable sandstones into impervious sandstones or shales are also important hydrocarbon trapping mechanisms (Seni and Kosters, 1989).

Tri-Cities field is a combination trap, as is shown by the structural map and production data. Average daily gas production is high in the middle and southwest parts of Tri-Cities field (Fig. 57). I contoured TP daily gas production and overlaid the production contours on the structure map of Travis Peak top (Fig. 58). This overlay map clearly shows a combination trap. Primary control on the field occurrence is the salt structure, and secondary control is the quality of the reservoir facies, where high daily gas production is inferred to coincide with high-quality reservoir facies.

Other TP fields, such as Reed field, demonstrate stratigraphic trapping. In that field, TP sandstone pinches out on the east flank of a local uplift (Fig. 6).

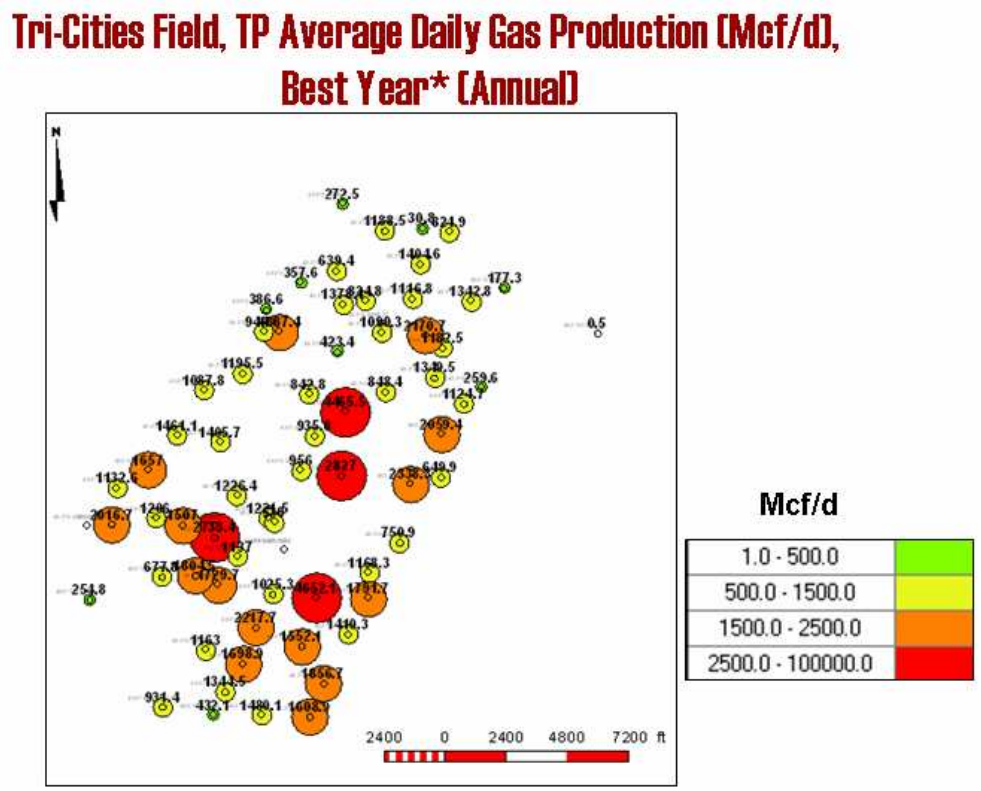

Figure 57. Bubble map of average daily gas production from the Travis Peak formation, Tri-Cities field (data from HPDI, 2005).

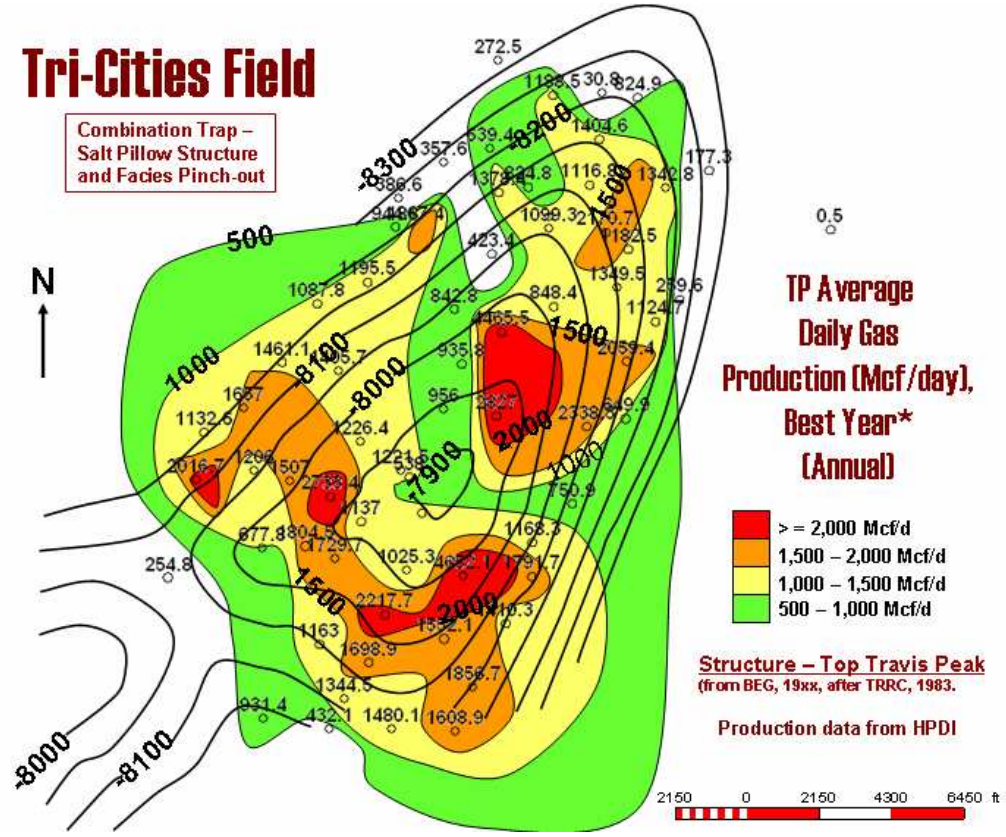

Figure 58. Overlay of gas production contour map with top of Travis Peak structure map, Tri-Cities field (structure map from Procter, 1951).

PRODUCTION ANALYSIS

Gas Production

For the study area along the west margin of the East Texas Basin, TP cumulative gas production from all (940) wells in the HPDI database was 1.43 Tcf from January 1, 1961 through December, 31, 2005 (Table 2). The production values in Table 2 are for all wells in the 6-county study area (Anderson, Freestone, Henderson, Limestone, Leon and Robertson Counties) (Fig. 13). For calendar year 2005, gas production from all TP wells was 24.4 Bcf (Table 2). Statistical analysis of cumulative gas production from individual TP wells is shown in Figure 59. The mean cumulative gas production is 1.46 Bcf/well from 1961-2005.

Table 2. Cumulative gas, oil, and water production from all TP wells, west margin of the East Texas Basin for the period from January 1, 1961- December 31, and for calendar year 2005 (data from HPDI, 2005).

TP Cumulative Production			
	Gas (Bcf)	**Oil (bbl)**	**Water (bbl)**
Jan, 01,1961- Dec, 31,2005	1,430.7	2,712,137	65,880,268
2005	24.4	48,208	2,633,186

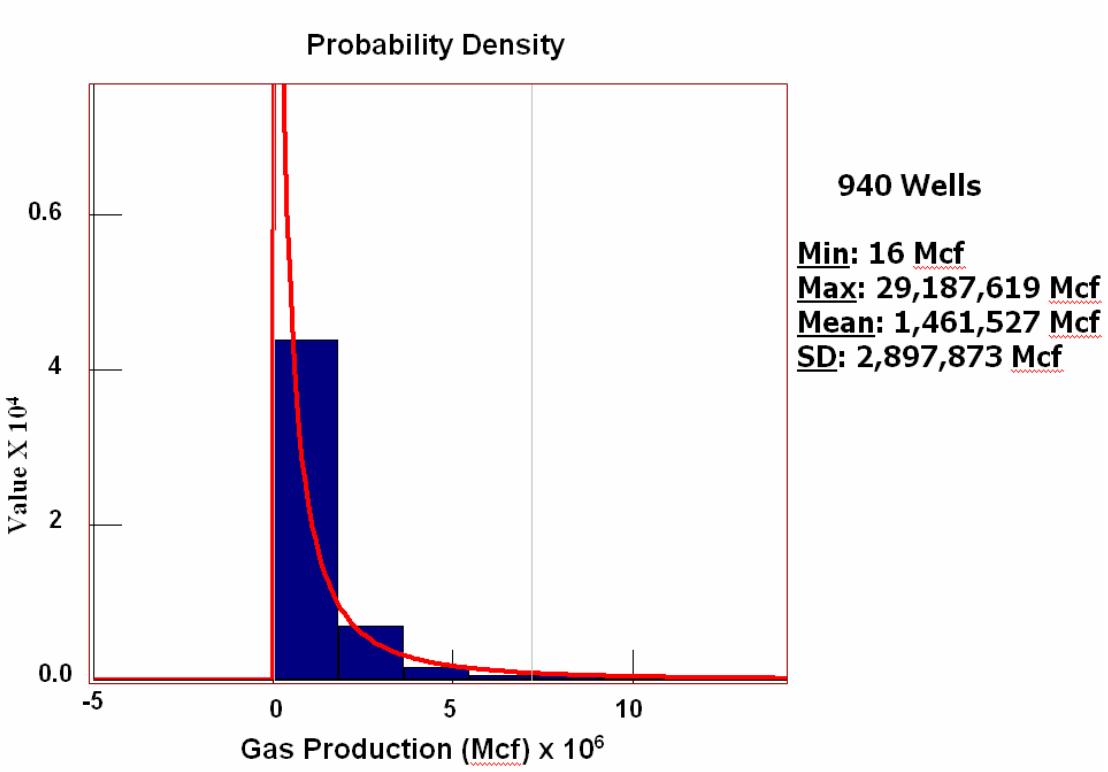

Figure 59. Statistical analysis of Travis Peak cumulative gas production from individual wells along the west margin of the East Texas Basin, 1961-2005 (from Li and Ayers, 2006) (data from HPDI, 2005).

In the late 1980s and early 1990s, the Travis Peak Formation in the Sabine Uplift was the focus of many research projects funded by the Gas Research Institute (now Gas Technology Institute), with the objective of developing technology for economic gas recovery from low permeability sandstones.

Moreover, for wells spudded during the 1980s and early 1990s, operators received an unconventional resources tax credit from the Federal government under Section 107 of the old Federal Natural Gas Policy Act (NGPA), for producing gas from low-permeability reservoirs. After the Federal tax credit expired, Texas (through the Railroad Commission of Texas, RRC, Statewide Rule 101) recognized the importance of

continued development of gas from low-permeability and other selected reservoirs by designating wells completed in those reservoirs as “high-cost” wells and making those wells eligible for a state severance tax reduction or exemption. The Texas Railroad Commission (RRC) defines high-cost gas wells as follows:

- Production is from a completion which is located at a depth of more than 15,000 feet;
- Produced from geopressured brine;
- Occluded natural gas produced from coal seams;
- Produced from Devonian shale; or
- Produced from designated tight formation or produced as a result of production enhancement work.

Along the west margin of the East Texas Basin, the Travis Peak formation produces gas from conventional and low-permeability (permeability ≤ 0.1 md) sands. To further evaluate TP production, I compared production from all wells to production from high-cost wells, by decade (Figs. 60 and 61). Also, I calculated the cumulative gas, oil and water production in high cost gas fields (Table 3). I identified high-cost gas fields in study area by searching the RRC database (REF). Importantly, I assumed that all wells drilled in what presently are designated “high-cost” fields are high-cost wells, although many of the wells were drilled prior to this designation and this assumption may be invalid. The high-cost gas fields in the study area are mostly in Freestone, Limestone, Robertson, and Leon counties (Fig. 62).

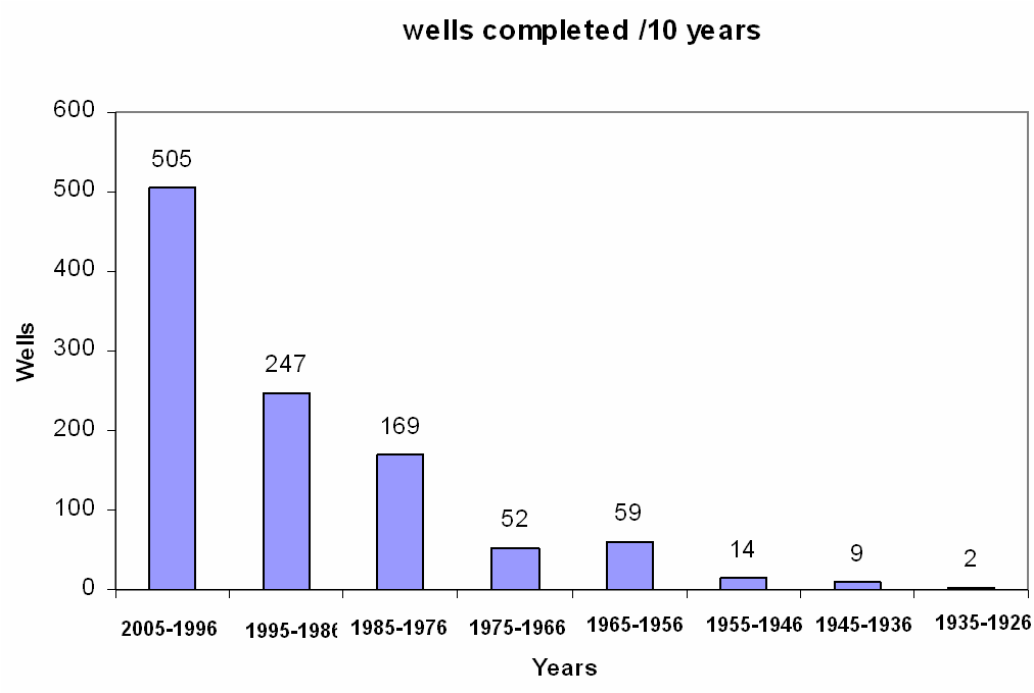

Figure 60. Total number of wells completed in the study area, by decade (from Li and Ayers, 2006) (data from HPDI, 2005).

For the period from January 1, 1961 through December 31, 2005, fields that today are classified high-cost fields accounted for 33.2% of the TP cumulative gas production in study area. However, in 2005, TP high-cost gas comprised 63.2% of the total TP gas production in study area, demonstrating that gas production from high-cost fields has markedly increased in importance in recently years. Moreover, in the decade 1996-2005, wells completed in high-cost fields comprised 66% of the total Travis Peak completions (333 of 505 completions (Figs. 60 and 61).

TP gas production averaged 925 Mcf/well/day during the best calendar year of production (Fig. 63). Many TP gas fields on the west flank of the ETB, especially those in Freestone and Limestone Counties (Figs. 62 and 63), are aligned parallel to the Mexia

Fault Zone, suggesting the importance of minor structural feature in the occurrence of the hydrocarbon traps. For fields further to the east, such as Opelika and Tri-Cites fields in Henderson County, hydrocarbon traps are associated with larger salt structures (Fig. 63) (Howard, 1951; Procter, 1951).

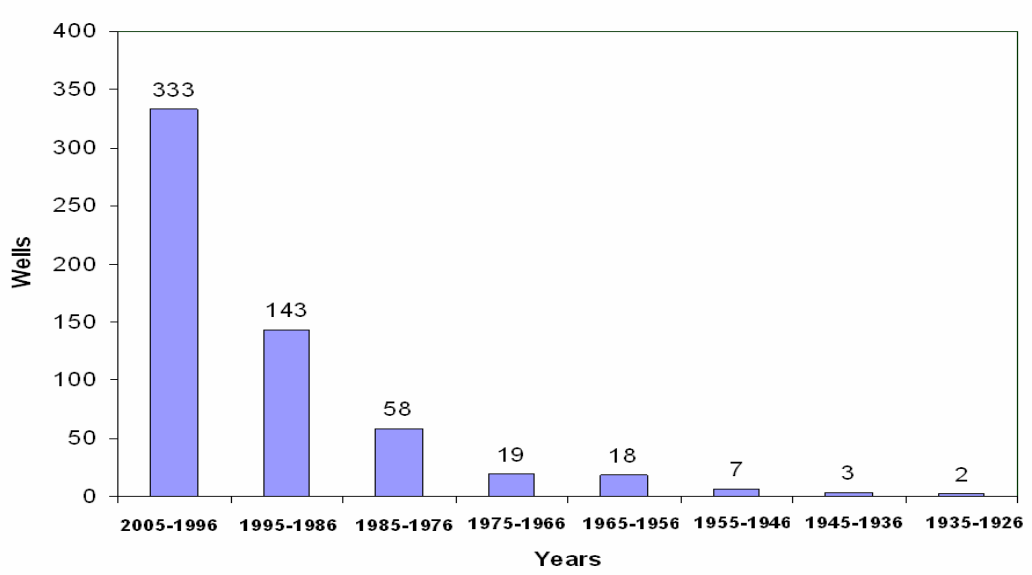

Figure 61 Total number of wells completed in high-cost fields in the study area, by decade. Data from RRC and HPDI, 2005.

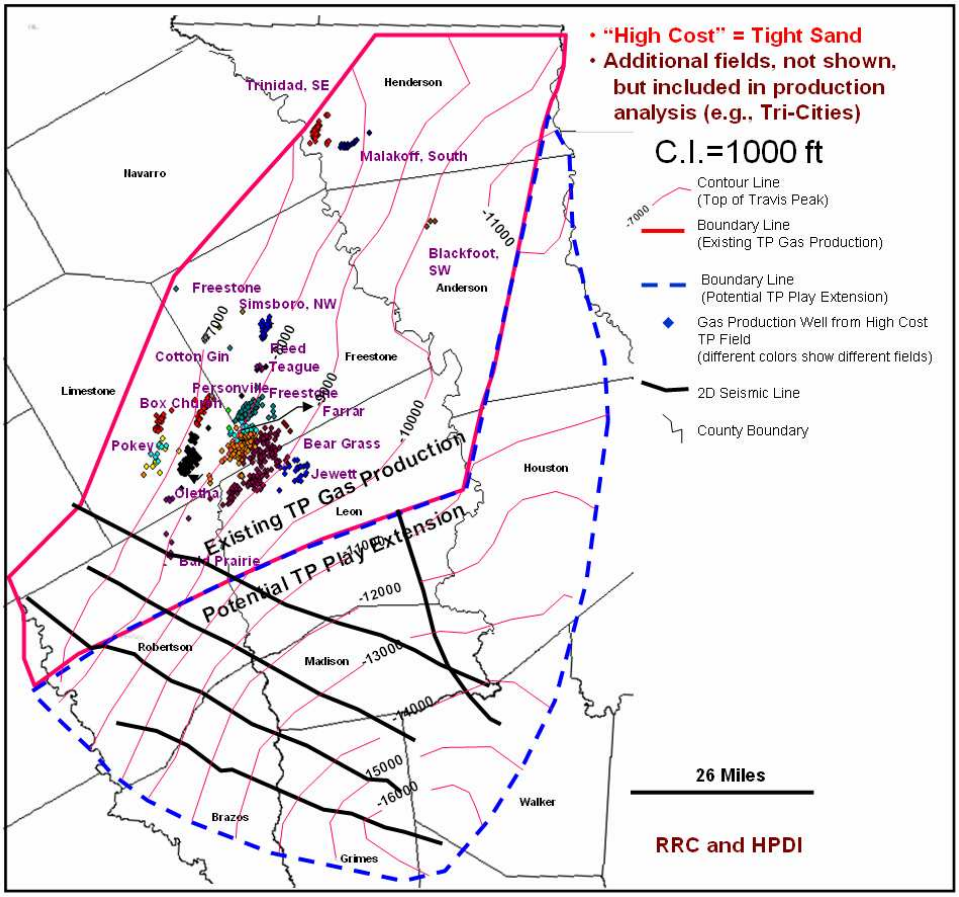

Figure 62. High-cost gas fields along the west margin of the East Texas Basin, color coded by field (data from RRC, 2005; HPDI, 2005).

Table 3. Cumulative production of Travis Peak gas from high-cost fields, west margin of the East Texas Basin, 1961-2005 and 2005, only (data from HPDI, 2005).

Travis Peak High-Cost Gas Production			
	Gas (Bcf)	**Oil (bbl)**	**Water (bbl)**
Jan, 01,1961- Dec, 31,2005	475.6	1,521,212	38,056,901
2005	15.4	33,670	2,340,761

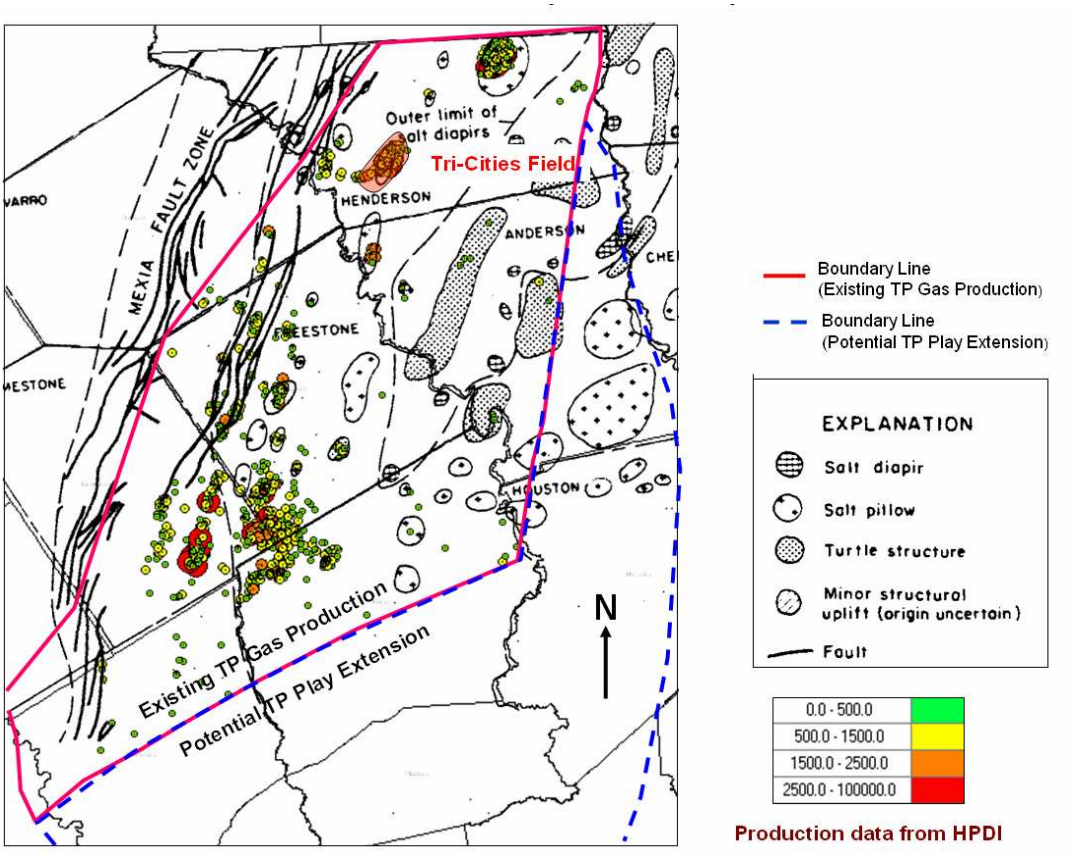

Figure 63. Bubble map of Travis Peak average daily gas production (Mcf/d) during the best calendar year of production (data from HPDI, 2005). The magnitude of average daily gas production of wells is related to the diameter of the bubbles. On the west, gas wells and fields are aligned parallel to the Mexia Fault Zone. Fields further east, such as Reed and Tri-Cities, are associated with individual salt structures.

Water Production

Travis Peak reservoirs have a lot water production (Fig. 64). The accumulate water production bubble map show the areas where water is produced from Travis Peak reservoirs. The highest water/gas rate is 2,656,820 bbl . TP fields along fault trends in Freestone and Limestone counties and fields related with salt structures in Henderson

counties significant water. Moreover, from reported trapping mechanism analysis, some those TP fields are combination traps. Therefore, Travis peak sandstone reservoirs in the productive area most likely are not basin-centered gas accumulations, because basin-centered gas accumulations should not have water production (Law, 2002).

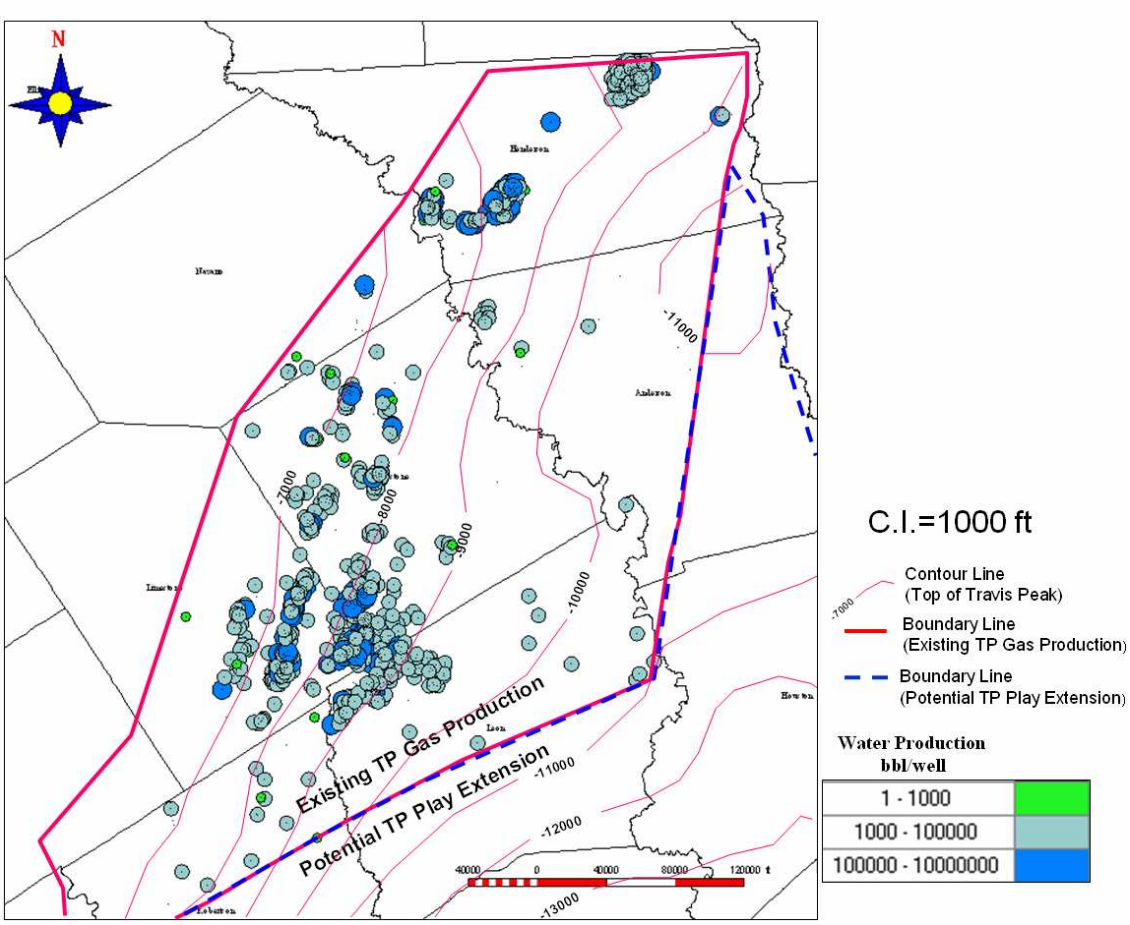

Figure 64. Cumulative water production bubble map (data from HPDI, 2005).

DISCUSSION

More than 940 gas wells produce from updip TP sandstones along the west margin of the ETB (Fig. 63). These reservoir sandstones are primarily fluvial, channel-fill sandstones that were deposited along the western margin of the ETB by the Ancestral Red River system. There is no production in the downdip, basinward (southeast) half of the study area (Fig. 63). Therefore, there may be opportunities to expand production to more distal TP fluvial, deltaic, shelf and deepwater depositional facies.

The presence of TP or other downdip plays depends on the: (1) burial history and diagenesis of source and reservoir rocks, which affect generation of hydrocarbons, pressure regime and modifications of reservoir quality; (2) sedimentary facies of reservoir rocks, which determine initial reservoir quality and occurrence of stratigraphy traps; and (3) structural setting, which determines migration pathways and the occurrence of structural and combination traps. Evaluation of the downdip play potential was based primarily on structural and stratigraphic interpretations of five 2D seismic lines and secondarily on TP lithofacies maps (Figs. 34 and 35). Since the data available to assess these parameters are limited, there is great uncertainty about the potential TP downdip hydrocarbon plays described below.

Burial History, Pressure Regime and Diagenesis

Potential source rocks of the Smackover and Bossier formations had a complex burial history (Fig. 56) (Dutton, 1987). In the updip, productive area, total organic content (TOC) of both formations is reported low (lean source rocks; TOC = 0.5-1.5%) and

organic materials are dominantly type III and IV with some type II kerogen (Ridgely et al., 2006). No source rock analyses are available from the downdip area. The burial history curve suggests that Smackover and Bossier source rocks would have generated oil and gas (130 ma – 50 ma) (Fig. 56) (Dutton, 1987), and Ridgely et al. (2006) report that the Bossier formation is overmature.

In the productive updip region of the study area, both conventional and tight sands are present (Figs. 60 and 61). Established production along the west margin of the ETB, the top of the Travis Peak Formation ranges from 5,000 to 17,000 ft deep, whereas in the downdip region of potential play extension, top of Travis Peak formation ranges from 9,000 to 17,000 ft. Limited data suggest that TP porosity and permeability will decrease markedly with depth, owing to diagenesis. Integrating the petrophysical results from a single well in Robertson County with the results of Dutton and Diggs' (1992) Sabine Uplift study shows systematic decrease in reservoir porosity and permeability with increasing of depth of TP strata (Figs. 54 and 55). Whereas some TP sandstones less than 7,100 ft deep adequate porosity and permeability to be classified as conventional reservoirs, deeper Travis Peak sandstones have experienced significant diagenesis and will most likely be classified as tight sands.

In the updip, productive area, most TP sandstones are normally pressured. Bartberger et al. (2003) reported that hydrocarbon/water contacts are common in Travis Peak gas fields, and they concluded that basin-centered gas is not present in the productive regions of the Travis Peak. However, in downdip potential area, TP sandstones and their associated source rocks are much deeper and hotter. It is possible that these deeper strata

are overpressured (Fig. 49), owing to relict hydrocarbon generation, and that basin-centered gas is present.

Travis Peak Sedimentary Facies and Potential Stratigraphic Traps, Downdip Study Area

TP sandstones in the downdip study area were deposited in fluvial and deltaic, as well as marine shelf, slope, and deepwater environments (Fig. 42). TP strata were deposited approximately 140-115 ma, and thus, potential TP stratigraphic traps were in place during most of the time that Smackover and Bossier potential source rocks would have generated oil and gas (130 ma – 50 ma) (Fig. 56). Net sandstone thickness maps of 2 TP intervals (Figs. 34 and 35) indicate the sandbody occurrences and dip-elongate (southeast) sandbody trends. Limited well log and seismic data hamper my ability to identify potential stratigraphic traps and plays, but I can point to several types of potential stratigraphic plays. These are listed below and are shown in Figures 65 and 66.

Downdip TP – Potential Stratigraphic Plays (Figs. 65 and 66)

- Updip pinch-outs of fluvial sands (Play 2)
- Updip pinch-outs of deltaic sands (Plays 3 and 4)
- Deltaic sand pinch-outs below TP unconformity (?) (Plays 3 and 4)
- Updip pinch-outs of slope sands (Play 7)
- Pinch-out of withdrawal-basin reservoir sandstones against salt features (Play 6)

Travis Peak Potential Structural Traps and Combination Traps, Updip Study Area

Faults are common in the downdip and updip study area. Most of the faults are associated Louann salt deformation that occurred during the Early Cretaceous, and they extend from the Smackover and Bossier into the TP. Thus, they may have served as migration pathway from the source rock to TP sands, or as possible traps. Some of the potential structural traps types occur on several of the seismic lines, suggesting the possibility of multiple, related prospects (plays). Potential TP structural or combination traps are listed below and are shown in Figures 65 and 66.

TP – Potential Structural and Combination Plays (Figs. 65 and 66)

- Shallow fault-related structures (Play 1)
- Domal traps above salt features (Play 5)

Potential for other Hydrocarbon Plays, Downdip Study Area

Hydrocarbon reservoirs may exist in the Cotton Valley and Bossier formations. However, exploration for these traps with widely space 2D seismic data is difficult, owing to the structural complexity that resulted from intense salt deformation. I infer that reservoir quality of these deep sands most likely would be very poor as result of advanced diagenesis. Depending on reservoir and seal quality, the Knowles reef trend may have the greatest potential below the Travis Peak formation.

Potential Bossier and Cotton Valley Plays (Figs. 65 and 66)

- Knowles Limestone (Play 9)
- Deepwater basinal sands (Play 8)
- Deep faults from salt or basement deformation (Play 7)

Limitations of the Studies

Uncertainty is great with regard to the potential for downdip hydrocarbon play extension. Only five 2D seismic lines were available for the study, and there were only 6 wells available in the downdip area that penetrated the top of the TP. This database is insufficient to allow confident identification or description of plays on the basis of stratigraphic, facies, or structural analysis.

Moreover, in the only well for which TP petrographic and petrophysical data were available (from Robertson County), the deepest TP sample was from 11,930 ft. But at even that depth, quartz overgrowths had greatly reduced porosity and permeability to approximately 7% and 0.01 md, respectively. Additionally, complex salt deformation made hydrocarbon play analysis difficult. Because the TP fluvial strata are sand-rich and lack extensive shale units, acoustic impedance contrast of these strata is poor, which made stratigraphic analysis difficult.

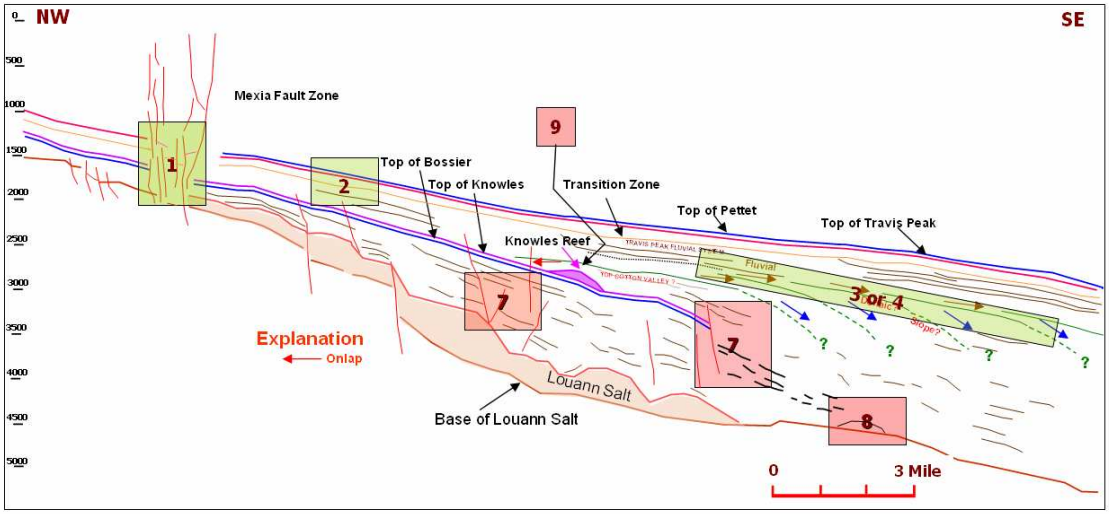

1. Shallow fault-related structures
2. Updip pinch-outs of fluvial sands
3. Updip pinch-outs of deltaic and slope sands
4. Deltaic and slope sand pinch-outs below Travis Peak unconformity
5. Domal traps above salt
6. Pinch-out of sandstones against salt domes or pillows
7. Deep faults from salt or basement deformation
8. Deep water sand
9. Knowles reef

Figure 65. Interpretation of Seismic Line 58A, showing potential Travis Peak and deeper Cotton Valley and Bossier hydrocarbon plays (See Fig. 39 for uninterpreted seismic line). Seismic data supplied by Seismic Exchange, Inc (SEI).

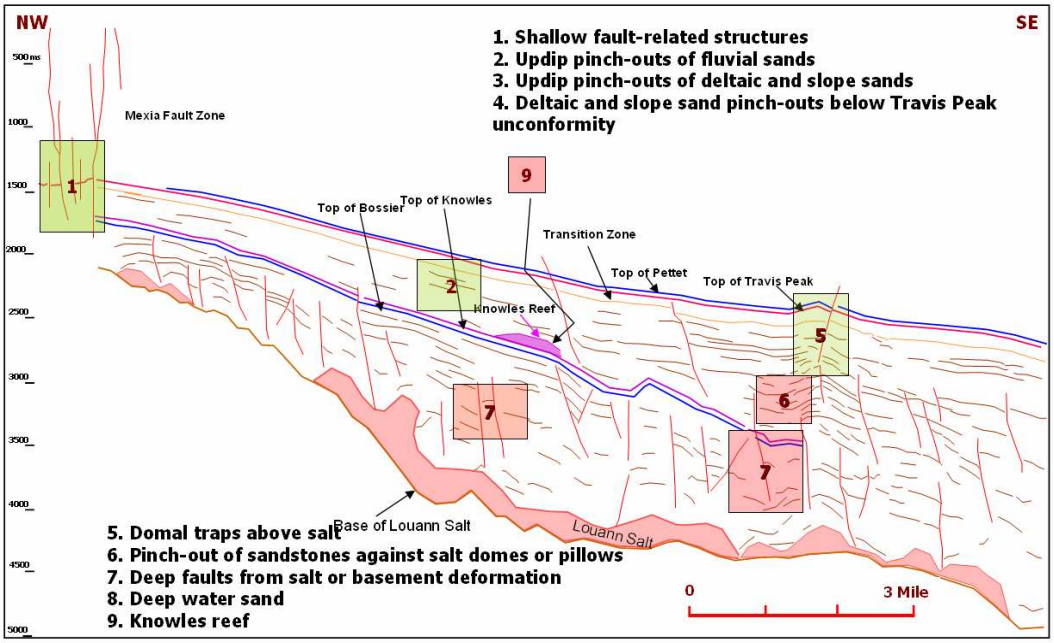

Figure 66. Interpretation of Seismic Line 57A, showing potential Travis Peak and deeper Cotton Valley and Bossier hydrocarbon plays. Seismic data supplied by Seismic Exchange, Inc (SEI).

CONCLUSIONS

1. TP sandstones along the west margin of the ETB occur in belts that are elongate and trend southeastward (basinward). These sandbody geometries and trends are consistent with basinward transport of sediment by the Ancestral Red River fluvial deltaic system. A limitation on the reliability of these maps was the paucity of well control; in the southeast half of the study, only 6 wells penetrated the mapped TP intervals.
2. For the upper 300 ft of the Travis Peak formation, the mean value of net sand thickness is 170 ft (57%), whereas, in the interval from 300 ft to 1,000 ft below top of Travis Peak, the mean value of net sand thickness is 488 ft (70%)
3. I infer that these TP fluvial systems supplied sediment to deltas and submarine fans further basinward, in Grimes, Walker, and Houston Counties.
4. TP sandstones are fine-grained (0.14 to 0.21 mm), moderately well sorted, subangular to subrounded, quartz arenites and subarkoses.
5. Petrophysical analysis of TP sandstone from only one well suggests the following.
    a. Some shallow TP sandstones (9,620 ft in this study) have poor reservoir quality, owing to euhedral dolomite that replaced micritic lime mud matrix that results in reservoir porosity of 2.7% and permeability of 0.001 md.
    b. Travis TP sandstones at intermediate depth (9,830 - 10,820 ft) have good reservoir quality. Porosity is 12.4 - 13.5% permeability is 0.19 - 0.55 md.

   c. Deeper TP sandstones (11,780 – 11,930 ft) are highly compacted and extensively quartz-cemented, which results in poor reservoir quality. Porosity is 5.2 – 6.7%, and permeability is 0.009 – 0.012 md.

6. TP sandstones from Robertson County along the west margin of the ETB are compositionally very similar to TP sandstones in the Sabine Uplift area, suggesting that they are from the same provenance and depositional system, the Ancestral Red River; TP knowledge learned from Sabine Uplift studies may be used for to make preliminary judgments concerning diagenesis and reservoir quality of TP sandstones along the west margin of the ETB.
7. Analysis of production data indicates that, along the west margin of the ETB, TP gas fields are aligned parallel to the Mexia Fault Zone, indicating the importance of structural features on occurrence of hydrocarbon traps.
8. Structural, stratigraphic, and combination traps are common TP hydrocarbon trap types in East Texas. Along the west margin of the basin, intermediate-amplitude salt structures are of primary element in forming traps. However, pinch-outs of permeable sandstones into impervious sandstones or shales are also important in hydrocarbon trapping.
9. TP mean daily gas production was 925 Mcf/well during the best calendar year of production. TP cumulative gas production for all wells in the 6-county study area was 1.43 Tcf from January 1, 1961 through December 31, 2005. Cumulative gas production from high cost fields account for 33.2% of this production. In 2005,

gas production from high cost fields was 63.2%, indicating that production from high-cost gas has increased markedly during the historic production period.

10. TP wells along the west margin of the ETB were completed in the updip or proximal clastic facies of the Ancestral Red River fluvial-deltaic system, in Limestone and Freestone Counties. Opportunities may exist to extend TP production downdip areas to the southeast and along strike to the southwest.
11. The geothermal gradient for the west margin of the ETB is 1.55 °F/100 ft. This gradient is slightly less than that reported for the same general area by previous workers, possibly because data were not available to correct BHT values.
12. The temperature gradient calculated for this area suggest that strata below 5,000 ft are mature for oil generation, and strata below 12,500 ft are well within the gas generation window.
13. Pressure gradient analysis indicates that strata deeper than 12,500 ft are overpressured.
14. It is probable that source rocks below 12,500 ft are in the gas generation window, which has resulted in hydrocarbon generation of overpressure in deeper strata, including the Bossier and Smackover formations.
15. The middle Jurassic Louann Salt played a distinct role in affecting deposition and structural deformation of younger strata and the formation of hydrocarbon traps in those younger strata.
16. Louann salt deformation caused several structural features that may provide hydrocarbon traps. These include the Mexia Fault Zone, folds associated with

salt pillows or domes, and minor faults that extend from Package 1 and 2 and which may be hydrocarbon migration pathways.

17. Paucity of data in the southeast half of the study area severely limited analysis of potential for TP plays extension.
18. Potential for extension of the Travis Peak hydrocarbon production downdip of basinward depends on the (1) burial history and diagenesis of source and reservoir rocks, (2) sedimentary facies of reservoir rocks, and (3) structural setting.
19. Potential Travis Peak hydrocarbon plays identified in seismic data in the downdip region of the study area include: (1) updip pinch-outs of fluvial, deltaic and slope sandstones; (2) pinch-outs of sandstones at the margins of salt-withdrawal basins; (3) possible domal traps above salt structures; and (4) possible deepwater sands.

FUTURE DIRECTIONS

Analysis of the well log and seismic data available for this study suggest that Travis Peak shoreline and deepwater sediment should exist basinward of the present study area. Paucity and poor quality of the available data greatly hindered assessment presence and hydrocarbon potential of those strata in this study. Further evaluation of the potential for TP hydrocarbon play extension, downdip and along strike to the southwest, will require availability of additional well log and seismic data. These data should be calibrated using core analyses and petrographic studies.

REFERENCES CITED

Bartberger, C. E., T. S. Dyman, and S. M. Condon, 2003, Potential for a basin-centered gas accumulation in the Travis Peak (Hosston) Formation, Gulf Coast Basin, U.S.A: U.S. Geological Survey, Bulletin 2184-E, 36 p.

Bebout, D. G., R. G. Loucks, and A. R. Gregory, 1978 Frio sandstone reservoirs in the deep subsurface along the Texas Gulf Coast; their potential for production of geopressured geothermal energy: The University of Texas at Austin, Bureau of Economic Geology, Report of Investigations 91, 92 p.

Bebout, D. G., White, W. A., Garrett, C. M., Jr., and Hentz, T. F., 1992, Atlas of major central and eastern Gulf Coast gas reservoirs: The University of Texas at Austin, Bureau of Economic Geology, 88 p.

Bushaw, D. J., 1968, Environmental synthesis of the East Texas Lower Cretaceous: Transactions - Gulf Coast Association of Geological Societies, v. XVIII, p. 416-438.

Davidoff, A. J., 1993, Deep basement structure and sedimentary fill, central East Texas: Texas A&M university, college station, Texas, Ph.D. Dissertation, 114 p.

Davies, D. K., B. J. Williams, and R. K. Vessel, 1991, Reservoir models for meandering and straight fluvial channels; examples from the Travis Peak Formation, East Texas: Transactions - Gulf Coast Association of Geological Societies, v. XLI, p. 152-174.

DeFord, R. K., Kehle, R. O., and Connolly, E. T., 1976, Geothermal gradient map of North America: American Association of Petroleum Geologists and U.S. Geological Survey, scale 1:5,000,000.

Dutton, S. P., 1987, Diagenesis and burial history of the Lower Cretaceous Travis Peak Formation, east Texas: The University of Texas at Austin, Bureau of Economic Geology, Report of Investigations No. 164, 58 p.

Dutton, S. P., Laubach, S. E., Tye, R. S., 1991, Depositional, diagenetic, and structural controls on reservoir properties of low-permeability Sandstone, Travis Peak Formation, East Texas: The University of Texas at Austin, Bureau of Economic Geology, v. 41, p. 209–220.

Dutton, S. P., and T. N. Diggs, 1992, Evolution of porosity and permeability in the Lower Cretaceous Travis Peak Formation, East Texas: AAPG Bulletin, v. 76, no. 2, p. 252 – 269.

Dutton, S. P., S. J. Clift, D. S. Hamilton, H.S. Hamlin, T. F. Hentz, W. E. Howard, M. S. Akhter, and S. E. Laubach, 1993, Major low-permeability sandstone gas reservoirs in the continental United States: The University of Texas, Bureau of Economic Geology, Report of Investigations No. 211, 221 p.

Finley, R. J., 1984, Geology and engineering characteristics of selected low-permeability gas sandstones: a national survey: The University of Texas at Austin, Bureau of Economic Geology, Report of Investigations 138, 220 p.

Fracasso, M. A., S. P. Dutton, and R. J. Finley, 1988, Depositional systems and diagenesis of Travis Peak tight-gas sandstone reservoirs, Sabine Uplift area, Texas: Society of Petroleum Engineers, Formation Evaluation, v. 3, p. 105–115.

GeoSystems, LLP, 2003, Reservoir quality and formation sensitivity analyses, Georgetown, Travis Peak, Cotton Valley, and Bossier formations, T Bar-X H. Cole No. 1. Robertson, Co., Texas, variously paginated.

Halliburton Energy Services, 2005, VSP, sonic calibration, synthetics and Q estimation report for Burlington Resources, Rainbolt Ranch # 1. Leon County, Texas, variously paginated.

Herald, F.A., ed., 1951, Occurrence of oil and gas in northeast Texas: The University of Texas, Bureau of Economic Geology, 449 p.

Hill, E. B., 1951, Reed Field, Freestone County, Texas: East Texas Geological Society, p. 327-330.

Howard, E. L., 1951, Tri-Cities Field Henderson County, Texas: Tyler, East Texas Geological Society, p. 389-394

HPDI, 2005, Oil and gas industry production data: http://www.hpdi.com/home.htm

Jackson, M. P. A., 1981, Tectonic environment during early infilling of the East Texas Basin, Geology and Geohydrology of the East Texas Basin, v.3, p. 7-11.

Jackson, M. P. A., 1982, Initiation of salt flow, East Texas Basin: AAPG Bulletin, v 66, no. 5, p. 584-585.

Jackson, M.L.W., and Laubach, S.E., 1991, Structural history and origin of the Sabine arch, east Texas and northwest Louisiana: The University of Texas, Bureau of Economic Geology, Geological Circular, v.91, no. 3, 47 p.

Kehle, R. O., 1971, Origin of the Gulf of Mexico: Unpaginated Manuscript on File at The University of Texas at Austin, Geology Library.

Kosters, E.C., Bebout, D.G., Seni, S.J., Garrett, C.M., Jr., Brown, L.F., Jr., Hamlin, H.S., Dutton, S.P., Ruppel, S.C., Finley, R.J., and Tyler, N., 1989, Atlas of major Texas gas reservoirs: The University of Texas at Austin: Bureau of Economic Geology, 161 p.

Kreitler, C.W. et al. 1981, Purpose and scope, geology and geohydrology of the East Texas Basin, Bureau of Economic Geology , v. 20, p. 3-11.

Laubach, S.E., and Jackson, M.L.W., 1990, Origin of arches in the northwestern Gulf of Mexico Basin: Geology, v. 18, p. 595–598.

Laudon, R. C., 1996, Principles of petroleum development geology: University of Missouri, Rolla, Missouri, Chapter 6, p. 85-101.

Law, B. E., 2002, Basin-centered gas systems, AAPG Bulletin, v. 86, no., p. 1891–1919.

Li, Y., and W. B. Ayers, 2006, Evaluation of Travis Peak gas reservoirs, west margin of the East Texas Basin: East Texas Geological Society, Proceedings of a Symposium on the Gulf Coast Mesozoic Sandstone Province, p. 14-1 – 14-17.

McGowen, M. K., and D. W. Harris, 1984, Cotton Valley (Upper Jurassic) and Hosston (Lower Cretaceous) depositional systems and their influence on salt tectonics in the East Texas Basin: *in* W. P. S. Ventress et al., eds., The Jurassic of the Gulf Rim; Gulf Coast Section SEPM Foundation, Third Annual Research Conference Proceedings, p. 213–253.

M.J. Systems, 2005, Well log raster images, UCL: http://www.mjlogs.com/index.html

Newsham, K. E., and J. A. Rushing, 2002, Laboratory and field observations of an apparent sub capillary-equilibrium water saturation distribution in a tight gas sand reservoir: Society of Petroleum Engineers, SPE Paper 75710, 11 p.

Procter, D. E., 1951, Opelika Field, Henderson and Van Zandt Counties, Texas: East Texas Geological Society, p. 287-293.

Railroad Commission of Texas (RRC), 2005, Well records, UCL: http://www.rrc.state.tx.us/divisions/og/notices-pubs-swr/notices/ogpn26.html

Ridgely, J. L., J. D. King, and M, J. Pawlewicz, 2006, Geochemistry of natural gas and condensates and source rock potential of the Jurassic Bossier formation and adjacent formations, East Texas Salt Basin: East Texas Geological Society Proceedings of a Symposium on the Gulf Coast Mesozoic Sandstone Province, p. 5-1 to 5-37.

Salvador, A., 1987, Late Triassic-Jurassic paleogeography and origin of Gulf of Mexico Basin: AAPG Bulletin, v. 71, no. 4, p. 419–451.

Sassen R. C. H. Moore,1978, Source rock study of smackover formation from East Texas to Florida, AAPG Bulletin, v.71, no. 5, p. 610 – 610.

Saucier, A. E., 1985, Geologic framework of the Travis Peak (Hosston) Formation of East Texas and Louisiana, *in* Finley, R. J., et al., The Travis Peak (Hosston) Formation: Geologic framework, core studies, and engineering field analysis: The University of Texas at Austin, Bureau of Economic Geology, contract report no. GRI-85/0044 prepared for the Gas Research Institute under contract no. 5082-211-0708, 233 p.

Seni, S. J. and Kreitler, C. W., 1981, Evolution of the east Texas Basin, Bureau of Economic Geology, *in* Kreitler, C. W. et al. eds., Geology and Hydrology of the East Texas Basin: The University of Texas at Austin, Geological Circular 81-7, p. 12-20.

Seni, S. J., and E. C. Kosters, 1989, Lower Cretaceous – Jurassic sandstone, Travis Peak Formation – cotton valley group – salt structures – western margin, East Texas Basin, Kosters, E. C., et al. eds., Atlas of Major Texas Gas Reservoirs: The University of Texas Bureau of Economic Geology, Chapter KJ-3, p. 71.

Shaker S., 2003, Geologically based pore pressure modeling: reconciling pressure vs. depth plots with mud weight equivalent vs. depth plots: Geopressure Analysis Services (G.A.S.), Houston Geological Society Bulletin, October 2003, p. 39-53.

Shoemaker, P. W., ed., 1989, Occurrence of oil and gas in northeast Texas: East Texas Geological Society, 210 p.

Shreveport Geological Society, 1946, Reference report on certain oil and gas fields of north Louisiana, south Arkansas, Mississippi, and Alabama: Shreveport Geological Society Reference Volume I, no. 2, 333 p.

Shreveport Geological Society, 1947, Reference report on certain oil and gas fields of north Louisiana, south Arkansas, Mississippi, and Alabama: Shreveport Geological Society Reference Volume II, no. 2, 503 p.

Shreveport Geological Society, 1951, Reference report on certain oil and gas fields of north Louisiana, south Arkansas, Mississippi, and Alabama: Shreveport Geological Society Reference Volume III, no. 1, 42 p.

Shreveport Geological Society, 1953, Reference report on certain oil and gas fields of north Louisiana, south Arkansas, Mississippi, and Alabama: Shreveport Geological Society Reference Volume III, no. 2, 109 p.

Shreveport Geological Society, 1958, Reference report on certain oil and gas fields of north Louisiana, south Arkansas, Mississippi, and Alabama: Shreveport Geological Society Reference Volume IV, no. 2, 204 p.

Shreveport Geological Society, 1963, Report on selected north Louisiana and south Arkansas oil and gas fields and regional geology: Shreveport Geological Society Reference Volume V, no. 2, 202 p.

Shreveport Geological Society, 1987, Report on selected oil and gas fields, Arkansas, Louisiana, Texas and Mississippi: Shreveport Geological Society Reference Volume VII, no. 2, 153 p.

Soeder, D. J., and P. Chowdiah, 1990, Pore geometry in high- and low-permeability sandstones, Travis Peak Formation, east Texas: Society of Petroleum Engineers Formation Evaluation, SPE Paper 17729, p. 421– 430.

Spencer, C.W., 1987, Hydrocarbon generation as a mechanism for overpressuring in Rocky Mountain region: AAPG Bulletin, v. 71, no. 4, p. 368–388.

Spencer, C. W. 1989, Review of characteristics of low-permeability gas reservoirs in Western United States: AAPG Bulletin v. 73, no. 5, p. 613-629.

Tye, R. S., 1989, Fluvial sandstone reservoirs of Travis Peak (Hosston) Formation, East Texas Basin (abs.): AAPG Bulletin, v. 73, p. 421.

Waples, D.W. & M. Ramly 2001. A statistical method for correcting log-derived temperatures. Petroleum Geoscience, v. 7, p. 231–240.

Waples, D, W., J. Pacheco, and A. Vera, 2004, A method for correcting log-derived temperatures in deep wells, calibrated in the Gulf of Mexico: Petroleum Geoscience, v. 10, no. 3, p. 239-245.

Wescott, W. A., 1985, Diagenesis of Cotton Valley sandstone (Upper Jurassic), East Texas: implications for tight gas formation pay recognition: AAPG Bulletin, v.69, no.5, p. 816–818.

Wood, D. H., 1981, Structural effects of salt movement in the East Texas Basin, Bureau of Economic Geology: The University of Texas at Austin, Austin, Texas

Worrall, D. M., and Snelson, S., 1989, Evolution of the northern Gulf of Mexico, with emphasis on Cenozoic growth faulting and the role of salt, *in* Bally, A. W., and A. R. Palmer, eds., The Geology of North America; An Overview: Geological Society of America, The Geology of North America Series, v. A, p. 97–138.

APPENDIX

Table A 1. Bottomhole temperature and mud weight recorded from 106 well headers, west margin of the ETB.

Well ID	Measure Depth (ft)	Bottomhole Temperature (oF)	Mud Weight (LB/G)	Geothermal Gradient (oF/100ft)
420013036800	10628	218	10.3	1.430
420013087100	11347	236	10	1.498
420013092400	12384	246	11.5	1.453
420013108400	10656	238	10.3	1.614
420013225500	10750	247	9.7	1.684
420013237300	12957	280	11	1.652
421609673300	12100	268	10.2	1.669
421610078100	11460	230	10.8	1.431
421613004300	8308	196	9.9	1.565
421613010900	8600	212	9.6	1.698
421613056100	10950	228	10.4	1.479
421613058500	15785	355	10.5	1.831
421613064800	13100	256	12.7	1.450
421613072500	12800	259	12.3	1.508
421613076100	12266	253	11.1	1.525
421613086200	9312	268	10	2.169
421613090900	12300	256	11.4	1.545
421613095800	13040	284	13.4	1.672
421613115200	11039	254	10	1.703
421613115500	11500	241	10.2	1.522

421613122100	11035	247	9.7	1.640
421613136200	10346	239	9.6	1.672
421613138900	10700	250	10.2	1.720
421613142600	9570	218	9.5	1.588
421613144900	9810	221	9	1.580
421613154100	13100	285	10.9	1.672
421613155800	11160	242	11	1.577
421613179400	13085	266	9.3	1.528
421613191900	11180	259	9.95	1.726
422130098100	11700	270	10.5	1.744
422133003300	12767	250	10.9	1.441
422133028400	12324	244	9.6	1.444
422133030400	17600	342	17.8	1.568
422133063200	12103	254	9.3	1.553
422133066600	13645	285	11.9	1.605
422133067100	11995	255	9.6	1.576
422133068300	12100	260	9.4	1.603
422133071000	11600	240	10.2	1.500
422133082000	9300	214	9.5	1.591
422253043800	17990	293	12.4	1.262
422253045500	18300	359	17	1.601
422253052900	19540	388	16.9	1.648
422253065300	13005	274	11.2	1.599
422893006200	10182	222	10.1	1.532
422893031700	16500	332	17.6	1.612
422893034800	12204	248	10.5	1.491

422893036700	10007	205	10.4	1.389
422893040300	11517	210	10.6	1.250
422893041500	10300	232	10.3	1.612
422893042400	11500	220	11	1.339
422893043200	17500	338	13.3	1.554
422893045400	10884	233	11	1.534
422893046900	11320	229	11	1.440
422893050200	11925	228	12.6	1.358
422893051000	12526	260	10.1	1.549
422893053200	12360	250	13.4	1.489
422893055300	12338	245	11	1.451
422893055400	13600	264	11.2	1.456
422893056000	11500	249	10.4	1.591
422893086900	9600	210	10.6	1.500
422893087200	9812	215	10.7	1.519
422893109600	11000	245	10.7	1.627
422893132500	9700	227		1.660
422933091300	10785	263	10.8	1.827
422933128400	10960	248	9.8	1.661
422933131400	11300	253	10.6	1.655
423133039500	12076	218	10	1.259
423133072000	10500	196		1.238
423133076900	13052	226	9	1.226
423490143000	7343	160	10.1	1.280
423493031000	10704	222	10	1.457
423493112400	10200	210	9.4	1.412

423493132200	9750	215	10.1	1.528
423493142600	9801	218	9.8	1.551
423493145200	9850	210	9.4	1.462
423493178100	12500	246	11.6	1.440
423493321700	9850	196	9.2	1.320
423953020200	13750	310	13.8	1.775
423953021800	15050	340	15.3	1.821
423953025300	7991	190	10.3	1.552
423953025500	13250	295	12.4	1.728
423953031900	9948	238	10	1.729
423953038500	13200	281	11.4	1.629
423953039200	12950	268	11.3	1.560
423953042500	11597	201	9.3	1.164
423953043300	11649	222		1.339
423953060300	15900	355	17.5	1.818
423953061800	10800	248	10.2	1.685

VITA

Name: Yamin Li

Address: 3116 TAMU, College Station, TX 77843-3116

Email Address: amyyamin@hotmail.com

Education: M.S., Texas A&M University, Petroleum Engineering

B.S., University of Petroleum (China)